REFERENCE ONLY

UNCLASSIFIED

[redacted]

JPL
SPS 37-15, VOL. 2
Cy 797
M Berdahl
125-138

Classification Changed to
UNCLASSIFIED
Authority
E.O. 11652
Date
12/21/72 E. Talamantes

Space Programs Summary No. 37-15, Volume II

for the period March 1, 1962 to May 1, 1962

The Planetary – Interplanetary Program

(Title Unclassified)

[redacted]

[redacted]
Downgr[redacted]year
int[redacted]clas[redacted]
12 years

[redacted]

jpl [redacted]

JET PROPULSION LABORATORY
CALIFORNIA INSTITUTE OF TECHNOLOGY
PASADENA, CALIFORNIA

May 31, 1962

"This copy for JPL use only"

[redacted]contains information affecting [redacted] the defense [redacted] the Espionage Laws, Title [redacted] and 794, the transmission of which [redacted]ion of which in any manner to an unauthorized person is prohibited by law.

[redacted]

UNCLASSIFIED

LAB B03041

[redacted] UNCLASSIFIED

[redacted]

Classification Changed to
UNCLASSIFIED
Authority
E.O. 11652
Date
12/21/72
By
L Tallamantes

NATIONAL AERONAUTICS AND SPACE ADMINISTRATION
CONTRACT NO. NAS 7-100

[redacted]
...document contains information ...
... Defense of the ... Laws,
within ... and 794. Its
Title 18, U.S. ... contents
transmis... ... an unauthori... is
... by law.

Space Programs Summary No. 37-15, Volume II

for the period March 1, 1962 to May 1, 1962

The Planetary — Interplanetary Program

(Title Unclassified)

[redacted]
GROUP 4
Down... ...dar
inter... ...l
...12 years

[redacted]

Copy No. 00797

JET PROPULSION LABORATORY
CALIFORNIA INSTITUTE OF TECHNOLOGY
PASADENA, CALIFORNIA

May 31, 1962

"This copy for JPL use only"

[redacted]

[redacted] UNCLASSIFIED

LAB B03041

UNCLASSIFIED

Preface

The *Space Programs Summary* is a bimonthly publication designed to report on JPL space exploration programs and related supporting research and advanced development projects conducted under the sponsorship of the National Aeronautics and Space Administration.

Beginning with this issue the *Space Programs Summary* is divided into six volumes. All information formerly documented in the JPL *Research Summary,* together with reports on advanced development projects, will in the future be reported in Volumes IV and V of the *Space Programs Summary*. The subtitles of all volumes of the reorganized *Space Programs Summary* are:

Vol. I, The Lunar Program (Confidential)
Vol. II, The Planetary-Interplanetary Program (Confidential)
Vol. III, The Deep Space Instrumentation Facility (Unclassified)
Vol. IV, Supporting Research and Advanced Development (Unclassified)
Vol. V, Supporting Research and Advanced Development (Confidential)
Vol. VI, Space Exploration Programs and Space Sciences (Unclassified)

The *Space Programs Summary,* Volume VI is an unclassified digest of appropriate material from Volumes I through V, plus the reports of the JPL Space Sciences Division.

W. H. Pickering, *Director*
Jet Propulsion Laboratory

UNCLASSIFIED

Space Programs Summary No. 37-15
Volume II

Copyright © 1962
Jet Propulsion Laboratory
California Institute of Technology

UNCLASSIFIED

LAB B030-41

[redacted] UNCLASSIFIED

Contents

I. **Program Objectives** 1

II. ***Mariner* R Project** 3

A. Systems Test and Operations 3
B. Spacecraft Design 7
C. Guidance and Control 15
D. Telecommunications 26
E. Propulsion 27
F. Supporting Activities 28

III. ***Mariner* B Project** 31

A. Systems 31
B. Spacecraft Design 32
C. Guidance and Control 40
D. Space Sciences 54
E. Propulsion 60

IV. ***Voyager* Project** 65

UNCLASSIFIED

I. Program Objectives

The primary long range objective of the NASA Planetary–Interplanetary Program is the development of automatic, unmanned, interplanetary spacecraft technology and the use of this technology in the form of space probes to gather fundamental scientific knowledge concerning the planetary and interplanetary environments, the planets themselves, and solar phenomena, both out of and within the plane of the ecliptic.

The secondary long-range objective of the program is the development of technology and the collection of scientific data which will contribute to the successful manned exploration of the planets and interplanetary space.

The primary objective of the program by 1970 is to have rather completely demonstrated and, to some reasonable extent, exploited (in terms of acquired scientific data) spacecraft capable of (1) being put into orbit around and (2) landing on the surface of Mars and Venus.

A secondary objective during this period will be the initial effort toward extending the above capability toward the planets Mercury and Jupiter and space shots out of the plane of the ecliptic and in toward the Sun. The immediate objective of the program is the initial probing of Mars and Venus.

The Planetary–Interplanetary Program at present consists of three projects: *Mariner* R using the *Atlas–Agena* B vehicle, *Mariner* B using the *Atlas–Centaur* vehicle, and the *Voyager*, using the *Saturn* vehicle. The missions planned for these projects are obviously subject to change because of such influences as new scientific discoveries or unexpected developments in vehicle availabilities.

II. *Mariner* R Project

The intent of the *Mariner* R Project is to perform flyby missions to Venus in 1962 using the *Atlas–Agena* B vehicle. These missions are a replacement for the *Mariner* A project which was cancelled during September 1961 due to unavailability of *Centaur* launch vehicle.

The primary objective of the *Mariner* R Project is to develop and launch two spacecraft to the near vicinity of the planet Venus in 1962, to receive communications from the spacecraft while in the vicinity of Venus, and to perform a radiometric temperature measurement of the planet. A secondary objective is to make interplanetary field and/or particle measurements on the way to Venus and in the vicinity of Venus.

A follow-on to the *Mariner* R 1962 missions is planned involving two concurrent launchings to Venus in 1964 from separate pads.

The mission objectives in 1964 are identical to those in 1962. The 1964 spacecraft will differ from those in 1962 only for the following reasons:

(1) Any equipment items which fail in the 1962 missions or which are of such marginal quality that they jeopardized the mission shall be improved for reasons of reliability.

(2) Modest failure-mode modifications may be permitted.

(3) Any science experiments which are successful in 1962 and which, if repeated in 1964, would be of negligible scientific value, may be replaced by experiments that have only insignificant interface effects on the data conditioning system and the rest of the spacecraft.

Completely assembled flight spacecraft, *Mariner* MR-1 and *Mariner* MR-2, were subjected to system tests and environmental tests during March and April. Incompatibilities between subsystems were uncovered and corrective actions were taken during, and subsequent to, these tests. The environmental tests included a space simulation test series, and a composite shake test series involving the *Agena* spacecraft adapter and the spacecraft. Testing during this period has proceeded essentially on schedule.

A project status review meeting held at JPL was attended by launch vehicle system, spacecraft, and AMR operations people.

A. Systems Test and Operations

The *Mariner* MR-1 and -2 spacecraft preparations are presently on schedule (Table 1). The original schedule was changed to incorporate a required spacecraft cable harness exchange, and further to reflect the use of the small vacuum chamber in place of the formerly designated 25-ft chamber. The shipping dates did not change.

1. Mariner MR-1

a. Scope of operations. Testing operations for *Mariner* MR-1 included subsystem evaluations, integrated system testing, match-mates, RF coupler tests, space simulation testing, vibration tests, and weight and center-of-gravity measurements.

Table 1. Spacecraft assembly and operations schedule

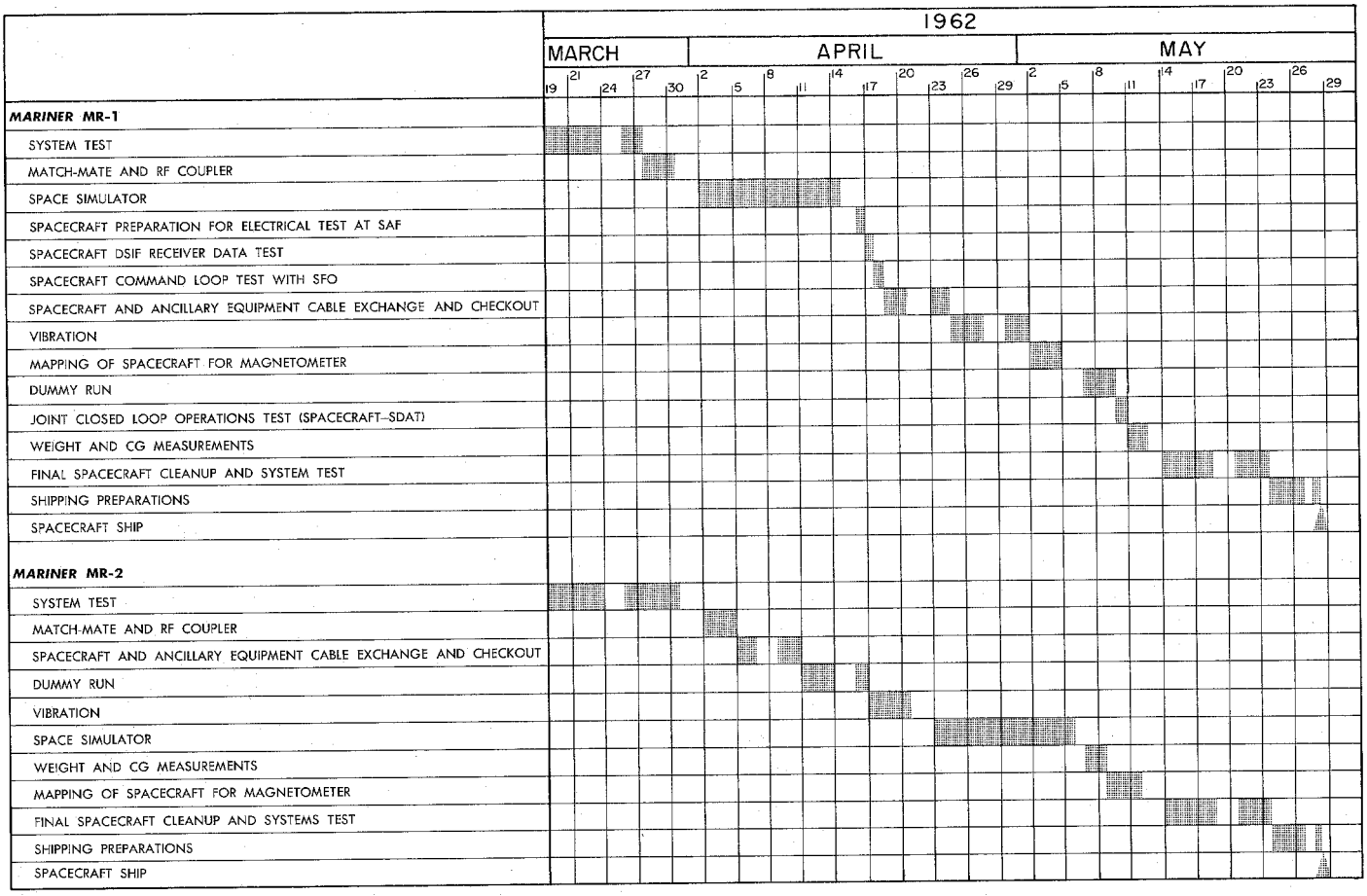
1962
MARCH
APRIL
MAY
19 21 24 27 30 2 5 8 11 14 17 20 23 26 29 2 5 8 11 14 17 20 23 26 29
MARINER MR-1
SYSTEM TEST
MATCH-MATE AND RF COUPLER
SPACE SIMULATOR
SPACECRAFT PREPARATION FOR ELECTRICAL TEST AT SAF
SPACECRAFT DSIF RECEIVER DATA TEST
SPACECRAFT COMMAND LOOP TEST WITH SFO
SPACECRAFT AND ANCILLARY EQUIPMENT CABLE EXCHANGE AND CHECKOUT
VIBRATION
MAPPING OF SPACECRAFT FOR MAGNETOMETER
DUMMY RUN
JOINT CLOSED LOOP OPERATIONS TEST (SPACECRAFT–SDAT)
WEIGHT AND CG MEASUREMENTS
FINAL SPACECRAFT CLEANUP AND SYSTEM TEST
SHIPPING PREPARATIONS
SPACECRAFT SHIP
MARINER MR-2
SYSTEM TEST
MATCH-MATE AND RF COUPLER
SPACECRAFT AND ANCILLARY EQUIPMENT CABLE EXCHANGE AND CHECKOUT
DUMMY RUN
VIBRATION
SPACE SIMULATOR
WEIGHT AND CG MEASUREMENTS
MAPPING OF SPACECRAFT FOR MAGNETOMETER
FINAL SPACECRAFT CLEANUP AND SYSTEMS TEST
SHIPPING PREPARATIONS
SPACECRAFT SHIP

b. Test results. Test results indicated that further investigations were required in the areas of solar power capabilities, booster–regulator and ac inverter long-term operating characteristics, and Case IV temperature control. Modifications are being incorporated to reduce the effects of switching transients during operation of the attitude control and scientific subsystems in a normal flight sequence.

c. Test schedule. The test efforts remaining to be accomplished at JPL are:

(1) Magnetometer mapping.

(2) Dummy run.

(3) Joint closed-loop operations.

(4) Final spacecraft assembly.

(5) Pre-shipment system evaluation test.

d. Subsystem testing. Each subsystem was evaluated on an individual basis, and its signal and control interfaces verified with other subsystems.

Operation of the available scientific instruments were checked through the scientific data conditioning system and the telemetry data encoder.

As soon as proper operating conditions were established, the engineering information outputs were calibrated with the data encoder system in preparation for system testing.

These subsystem efforts resulted in logic, component, and wiring changes designed to reduce the effects of system noise, switch transients, and intermittent electrical connector problems.

The flight shroud, adapter, and spacecraft were mechanically and electrically assembled to verify proper interface (Fig. 1). An area of interference was noted near the spacecraft antenna gear box. RF measurements through the antenna coupler showed a greater loss than expected at the command receiver frequency. Modification of the shroud was requested.

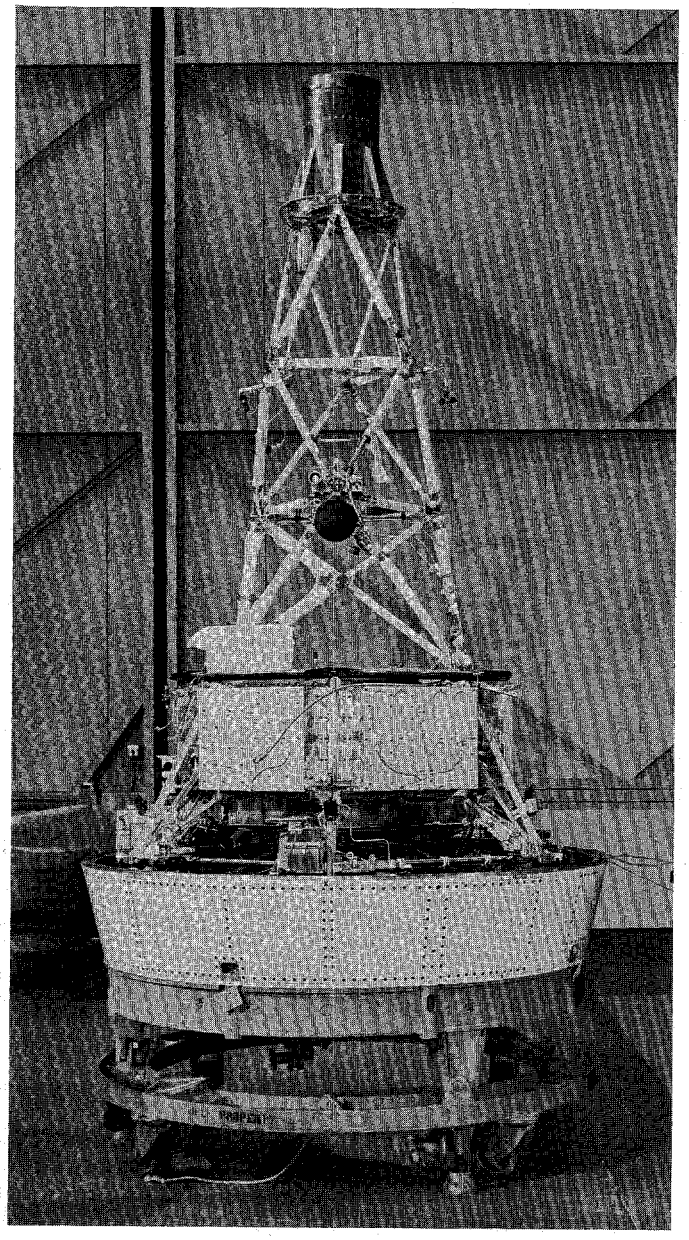

Fig. 1. MR-1 match-mate and RF coupler test

e. Space simulation testing. The MR-1 was subjected to a space simulation test during the period from April 4 to April 12, 1962 (Fig. 2).

During the test period, the spacecraft was tested at three temperature levels and a mean vacuum of 7.7×10^{-5} mm of Hg. The temperature levels were established by applying heat to solar dependent areas with locally controlled contact heating pads. Cold vacuum chamber walls operating at -330 to -100°F provided a heat sink to dissipate spacecraft thermal energy.

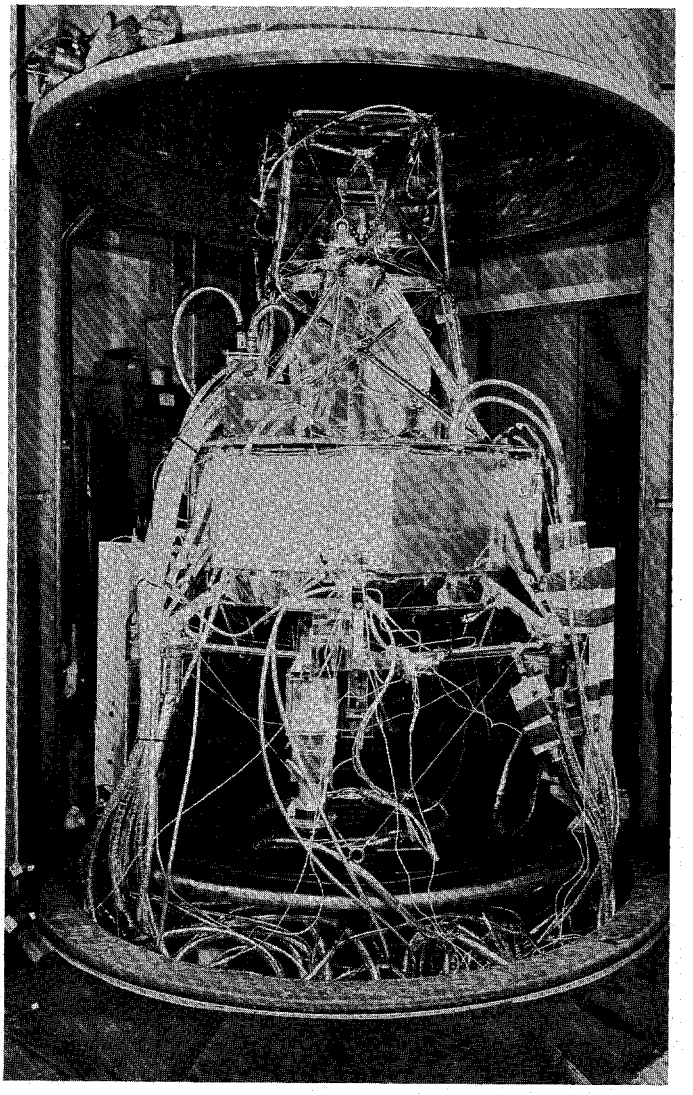

Fig. 2. MR-1 space simulation testing

The remaining problems under investigation as the result of the space simulation test period are:

(1) The 400-cps power inverter indicated an overload while operating under single-phase conditions.

(2) The roll gyro offset was near full scale (positive) for approximately 20 min when temperatures on Case IV were between 42 and 47°F. Further investigation is required to determine if the low extremes noted in testing are probable in flight.

f. System testing. MR-1 has completed three systems tests:

(1) System test No. 1 provided information for updating the systems test procedure and, in addition, pointed out several areas for subsystem investigation.

(2) System test No. 2 appears as the first *valid* system test conducted on MR-1. Additional system noise-to-transient phenomena were noted during the normal flight sequence operation. These problems were defined in post-system test investigations, and changes were incorporated to minimize system operation problems.

It was noted that the solar panel simulators did not establish the operating conditions predicted by the design of the flight solar panels. An investigation was requested to determine if the flight conditions being simulated were realistic and consistent with spacecraft power requirements.

(3) System test No. 3 was delayed to allow a scheduled replacement of the ring and case harness connectors. Results showed a minor wiring error between the command and attitude control systems; several minor calibration problems were detected between spacecraft subsystems. These problems were scheduled for investigation and resolution before the next formal system test.

System test No. 3 was also used as an evaluation test prior to vibration testing.

g. Vibration testing. The assembled MR-1 spacecraft, in full flight configuration, was vibration tested while mounted to an *Agena* adapter fastened to the vibration fixture (Fig. 3).

Spacecraft operation in the launch mode was monitored during vibration, utilizing the in-flight telemetry and communications systems.

Test results. Measurements taken during the test indicated normal system operation throughout the vibration sequence. Following vibration along each axis, the complete spacecraft system was evaluated by performing a modified system test. Immediately following vibration in the *z*-axis, the spacecraft battery voltage was observed to be out of tolerance. The output voltage on cell 6 had dropped to zero. A review of the records showed only that the failed cell had a history of low voltage as compared with other cells in the battery. Two other problems were detected following spacecraft vibration:

(1) A momentary out-of-regulation indication in the DCS power supply.

(2) A transient short circuit of the plasma scientific experiment deflection plates.

Each of these problems is currently under investigation.

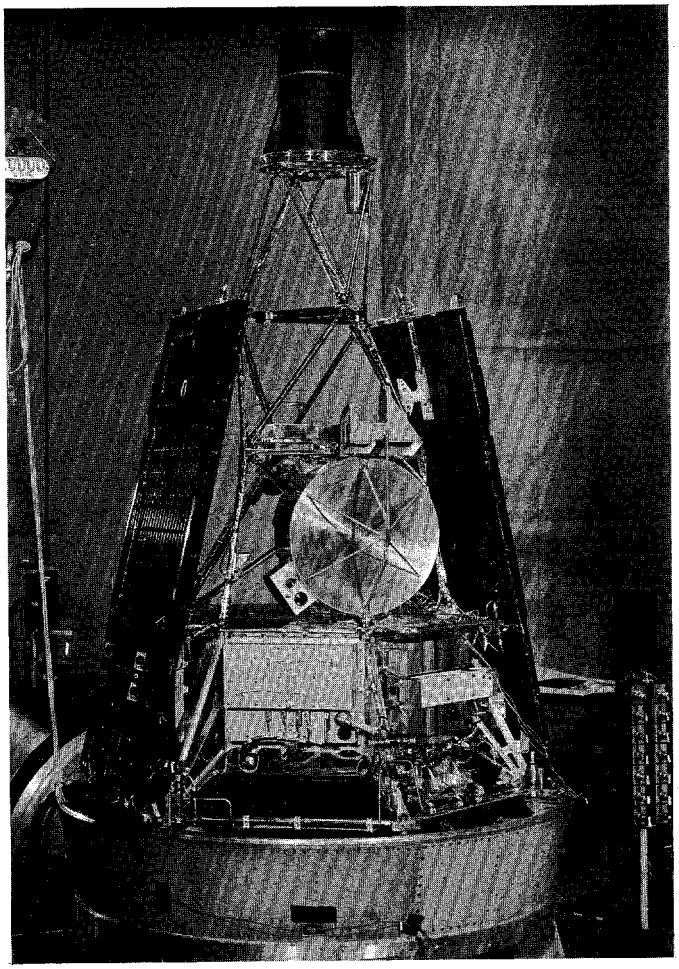

Fig. 3. MR-1 vibration testing

h. Weight and center-of-gravity measurements. With the spacecraft in full flight configuration, weight and center-of-gravity measurements, originally scheduled to follow the dummy run operations, were performed following the vibration tests. Preliminary calculations show the weight to be approximately 440 lb.

2. Mariner MR-2

a. Scope of operations. This report summarizes *Mariner* MR-2 activities during the period from March 15 to April 23, 1962, including systems and vibration testing.

b. Test schedule. System test No. 1 on MR-2 spacecraft was performed on March 16, 1962. System test No. 2 was performed on March 27. Other tests were performed in the system test configuration for trouble-shooting purposes during this period. Systems test operations were interrupted to change the complete ring harness and case harness from Deutsch connectors to Bendix connectors, which was completed without diffi-

culty on March 30. RF coupler and match-mate tests were conducted from April 2 through April 3. The system test of MR-2 was concluded on April 10.

Dummy run tests, using blockhouse GSE equipment, were conducted from April 11 through April 13.

MR-2 was moved to the ETL on April 16 to verify the design by shake in three planes and to perform a flight acceptance test of both the cable and ring harnesses.

On April 23, MR-2 was placed in the space simulation chamber to start a simulated space flight.

c. Match-mate and RF coupler testing. During the week of April 2, match-mate and RF coupler testing was conducted in the SAF. Test results proved that the mechanical and electrical interface compatibility between *Mariner–Ranger* spacecraft and LMSC's spacecraft support structure, nose cone, and *Agena* forward equipment rack was inadequate for flight. The two major unsatisfactory areas were the metal-to-metal contact of the LMSC shroud line with the spacecraft high-gain antenna gear box, and the unstable RF operation in the command antenna coupler system at 890-mc frequency. Modifications to correct these conditions have been initiated.

d. Dummy run operations. The objective of the first dummy run on April 12, with actual blockhouse GSE equipment, was to refine the procedure and to check out equipment.

The second dummy run was conducted as a formal countdown on April 12.

RF interference tests were successfully completed the morning of April 13 with live squibs installed, followed by squib activation during simulated flight sequence.

The final dummy run was performed April 13 in the SAF with the spacecraft in flight configuration.

e. Vibration testing. MR-2 was moved to the ETL on April 16, 1962 and set up for vibration testing. A pre-shake disclosed no serious problems.

On April 19, the z-axis post-shake test was conducted with the system on the motor loading stand and cabled to the system test complex equipment. Results were as follows:

(1) Mixed signal playback showed a frequency shift in the 2400-cycle power supply, causing loss of sync in data encoder and data display.

(2) Relay failure discovered during z-axis shake affecting science turnoff; investigation pending.

(3) Recycling of data encoder corrected erroneous event channel readouts due to transients.

The following discrepancies were revealed during the x- and y-axis post-shake systems tests:

(1) Defective primary pitch Sun sensor was replaced.

(2) Loss of data encoder sync; investigation underway.

(3) Arc-over caused high-voltage step failure in plasma experiment. Experiment returned for investigation.

(4) Pyrotechnic control GSE did not show proper PVA function. GSE problem found and corrected.

f. Space simulation testing. On April 23, 1962, MR-2 was placed in the small space chamber and an abridged space flight sequence initiated. This test is scheduled for completion May 4.

g. Test data reduction. All systems tests were supported by a 7090 data reduction program. Teletype tapes of the tests were generated for data reduction. This program has been refined and the results of these tests are being processed as tab runs in engineering units, and as analog plots in graphic form.

B. Spacecraft Design

The reporting period was primarily spent performing miscellaneous qualification tests of prototype and flight spacecraft. A brief review of the significant tests follows.

Vibration testing of the flight spacecraft has been completed successfully and extensive testing (reported in *SPS 37-13* and *-14*) has been accomplished on the structural test model, coupled with corrective action where necessary.

Temperature–vacuum tests of the flight spacecraft have been completed, uncovering only minor problems. No attempt was made to measure a heat balance during these tests, since all of the direct-access cables significantly altered the thermal configuration. Liquid nitrogen cold walls on the vacuum chamber were used to provide a simulation of the infinite heat sink of space. Heaters were placed on critical areas to insure that no components would be damaged by excessive cold.

Match-mate tests between both flight spacecraft and also spacecraft-to-*Agena* adapters have been completed successfully. Only minor problems were encountered,

many others having been uncovered and solved during preliminary match-mates of prototype hardware. A determination of the spring constant of the spacecraft and adapters together was determined at this time. This is necessary in order to get the proper pre-load between spacecraft and adapter so there is no separation between them during vibration.

Weight and CG measurements have been made of the flight spacecraft, using a new fixture designed to speed the operation. The spacecraft is placed on three load cells on the fixture and measurements taken at each cell. To ensure that no lateral forces induce erroneous readings in the load cells, ball thrust bearings were placed between load cell and stand. By rotating the spacecraft relative to the load cells and taking three sets of measurements 120 deg apart, any nonlinearities in the load cells can be detected. To determine the axial CG location, the spacecraft is tilted 15 deg to the vertical and the above procedure repeated.

A series of separation tests has been completed, verifying that the long range Earth sensor damper fix reported in *SPS 37-14* did not jeopardize separation of the spacecraft from the *Agena*. No changes to either the spacecraft or *Agena* resulted from these tests.

Assembly of a third *Mariner* spacecraft has begun. This spacecraft is to be used as an ex-post-facto proof test model, and will verify flight situations or simulate anomalies. Assembly is proceeding on a noninterference basis.

The *Mariner* R spacecraft configuration (Figs. 4 and 5) has changed little from that described in *SPS 37-12*. Among the changes are:

The ion chamber and particle flux detector experiments have been relocated on the superstructure. They have been moved from the top solar panel tie frame to the top radiometer support frame to reduce their magnetic effect on the magnetometer.

Removable 0.016-in. polished aluminum thermal shields have been installed on the faces of several hex electronic boxes and on the sides of the cable trough. The cable trough side shields must be removed to enable the hex electronic box harnesses to be disconnected from the cable trough. The bottom thermal shield must be installed after the motor is inserted in the spacecraft.

Three vibration dampers have been added (*SPS 37-14*). A spring-loaded damper between the spacecraft frame and the Earth sensor is intended to damp vertical Earth sensor excursions. A second damper damps Earth sensor lateral excursions. The third damper is bolted between the antenna yoke and the rim of the high-gain antenna. During the mid-course maneuver, it is intended to damp out torsional antenna motions that may couple with the autopilot, making it unstable.

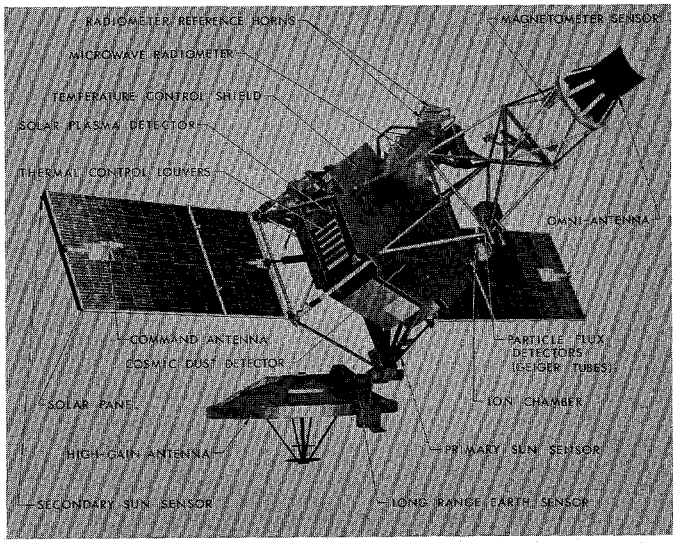

Fig. 4. *Mariner* R spacecraft

A light baffle box has been added to the antenna yoke. The box extends from the Earth sensor mirror past the rim of the high-gain antenna. The purposes of the baffles are to prevent stray light from the antenna dish, antenna feed and spacecraft from entering the Earth sensor.

1. Packaging

a. Electronic equipment arrangement. Location of the electronic subassemblies in the hex compartment and a detailed description of the assembly arrangement was given in *SPS 37-12* together with the *Mariner* R packaging assembly. Detailed packaging considerations will be described for each assembly.

b. Assembly I, scientific equipment. Figure 6 shows this assembly on the spacecraft. The power switching and logic subassembly is bolted to the outside surface. The unusual shape of this subassembly is explained by the fact that it was originally designed for the *Mariner* A spacecraft and was to be located on the intercostals. On the *Mariner* R spacecraft this subassembly was located on the face of Assembly I so that short cables from the power switching and logic subassembly to the battery and solar panels could be used. In addition, this location allowed some 15 w of heat dissipated in the power switching and logic to be utilized to keep the scientific instruments, located inside the hex, warm.

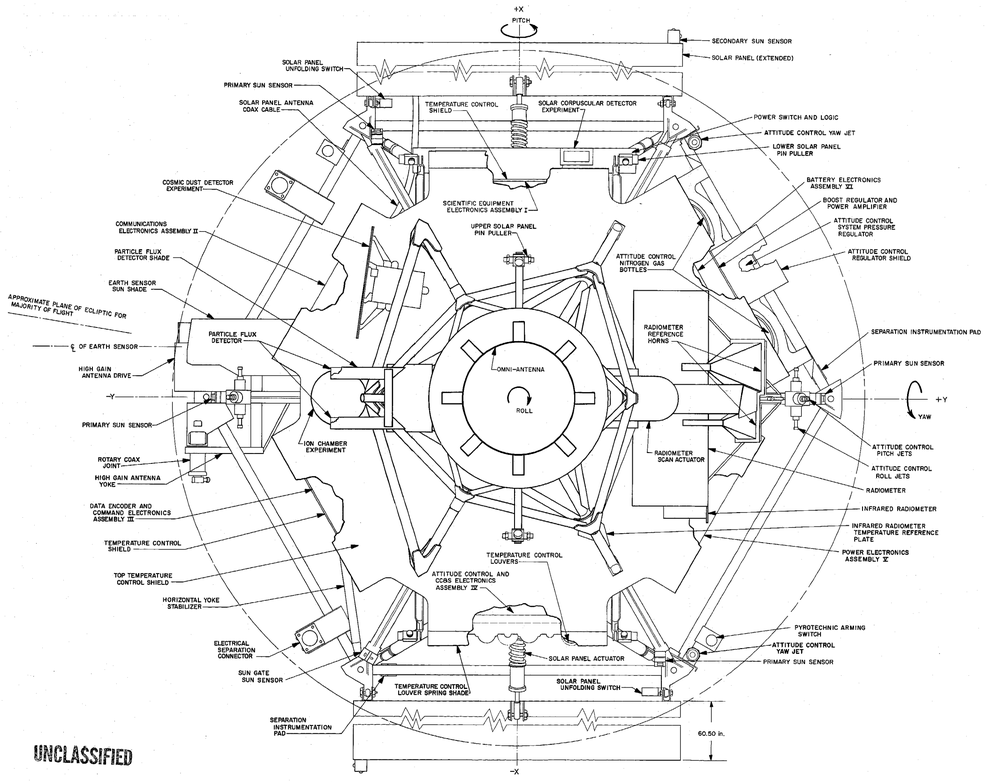

UNCLASSIFIED

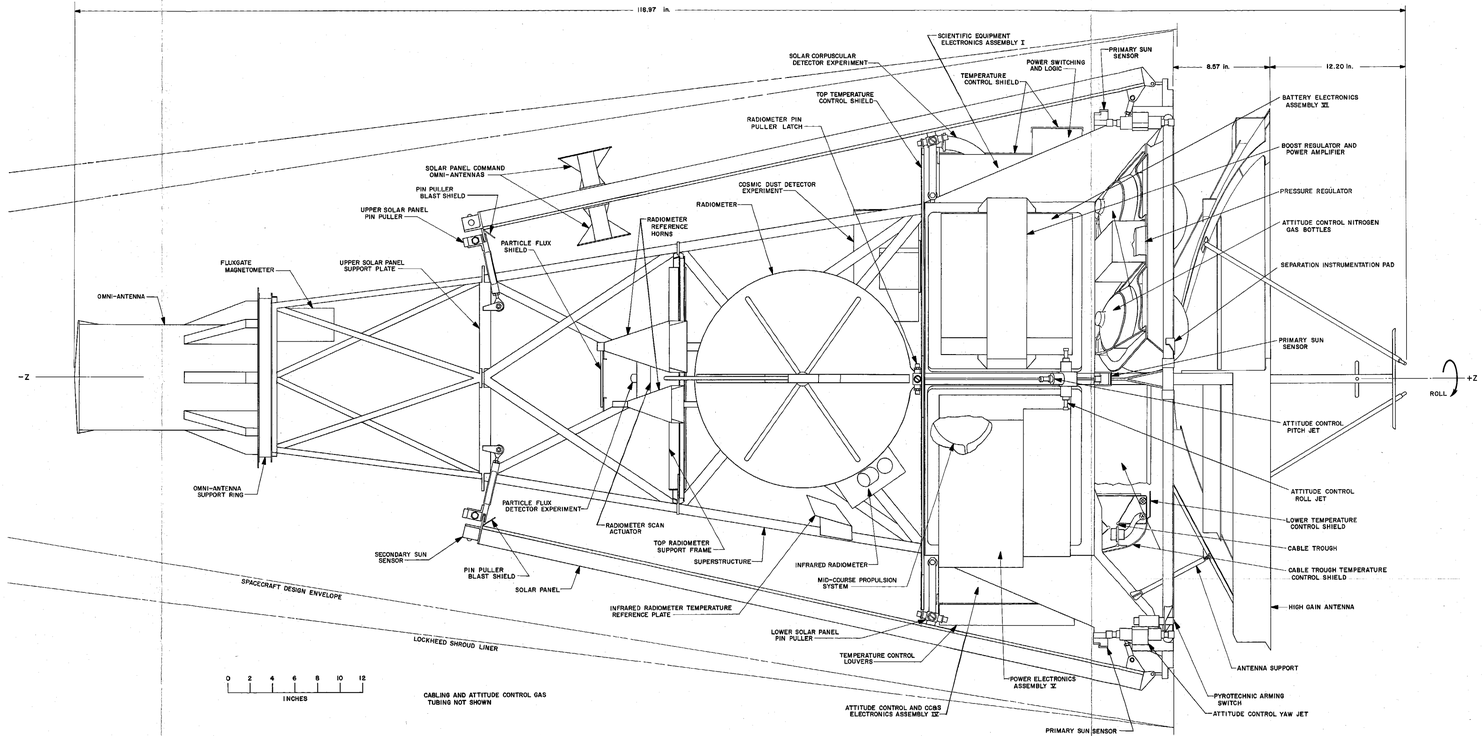

Fig. 5. *Mariner R* spacecraft configuration

Deflection plates for the solar plasma instrument are shown on Fig. 6 in the upper left corner of the assembly. In this location, the deflector orientation to the Sun was satisfied, and the electronics inside the assembly could be packaged on subassemblies of the standard shape. Thus, compactness and better weight efficiency could be obtained for other electronic subassemblies in the same chassis: magnetometer, data conditioning, and scientific power switching.

c. Assembly II, communications. Figure 7 shows the communications assembly in a handling fixture which was provided to protect the thermal coatings, transducers, and louvers on the chassis from damage during electrical assembly and checkout. Such fixtures were provided for all of the electronic assemblies.

A significant packaging improvement in this assembly can be noted in the transponder and RF amplifier areas. Figure 8 shows a *Ranger* 1 communications assembly. The transponder was packaged in a large, heavy case bolted across the chassis, while the three amplifiers were located on the bottom surface. This type of communications packaging was defined prior to the establishment of modular packaging techniques for *Ranger* 1. For the *Mariner* spacecraft, more compatible packaging was obtained by mounting the same transponder modules in a standard configuration (Fig. 9). In this form, the transponder subchassis was used as an assembly chassis stiffener, in a manner similar to other standard electronic subassemblies. These transponder subassemblies occupied less than half the volume of the assembly.

Similarly, the three cavity amplifiers were combined into a single unit (Fig. 10) in a shape compatible with the standard configuration.

Both the transponder and cavity amplifier packages used the same inside parts previously developed for *Ranger*. With this new communications package, an appreciable weight reduction was effected by packaging the complete subsystem in one standard chassis: transponder, transponder amplifiers, filter, circulator and power monitor, T-R unit, and the junction box.

d. Assembly III, data encoder and command. This assembly contains densely packaged electronics on standard shape subassemblies. The chassis for Assembly III is shown in Fig. 11. This chassis, as well as chassis for Assemblies I, II and III, was made from a *Mariner* A standard magnesium chassis. Low-emissivity surfaces were obtained by riveting 0.016-in. thick polished aluminum shields to the chassis. The figure shows temperature transducers mounted on the front surface and special

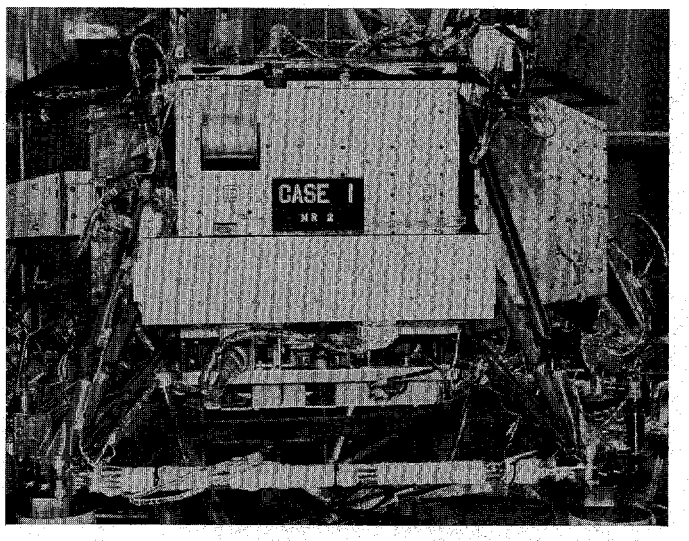

Fig. 6. Assembly I on spacecraft

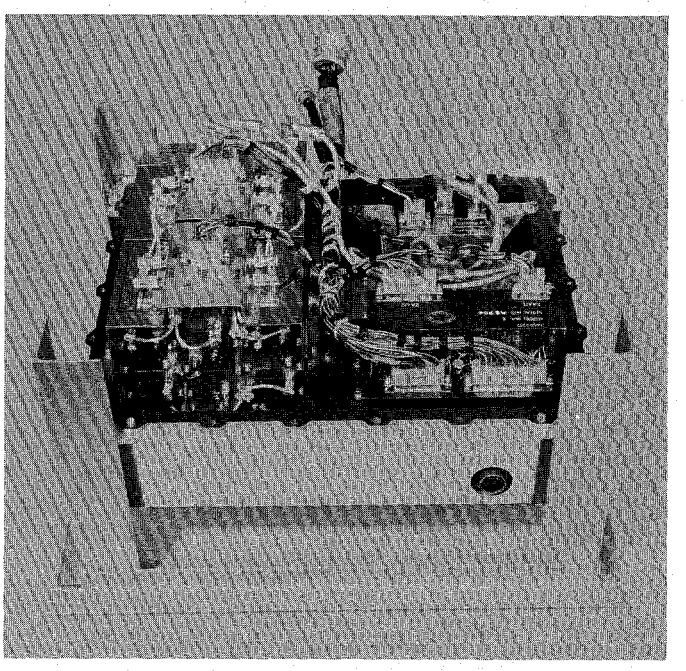

Fig. 7. Assembly II in handling fixture

hinges, which were added to ease service handling problems after the assemblies are attached to the spacecraft.

e. Assembly IV, attitude control and CC&S. The equipment is packaged on standard shaped subassemblies. Attitude control electronics were adapted from *Mariner* A, while the CC&S required only one new subassembly. This chassis required temperature control louvers to accommodate large power dissipation changes occurring during spacecraft acquisition and maneuver. Figure 8 is a standard chassis with louvers attached.

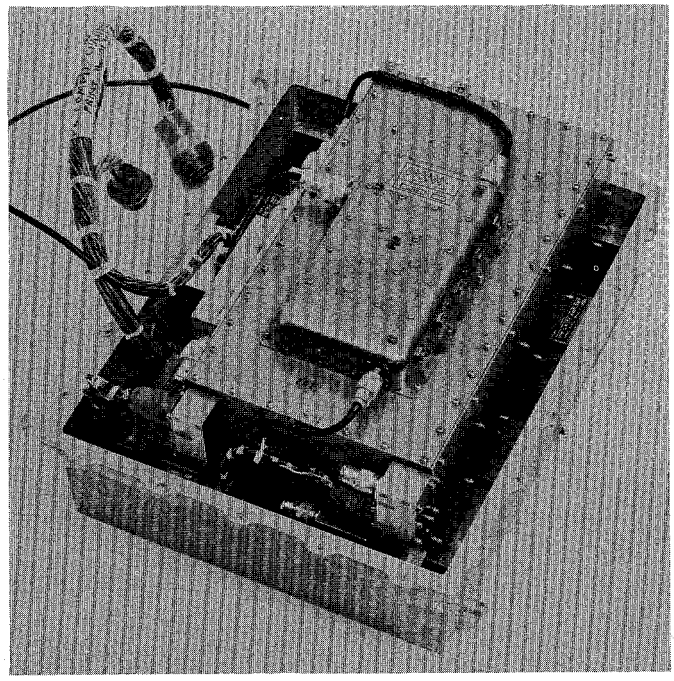

Fig. 8. *Ranger* 1 communications assembly

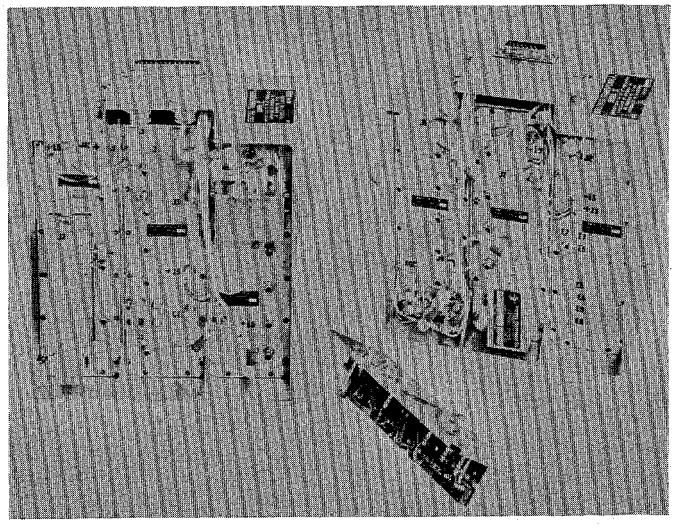

Fig. 9. Transponder

f. Assembly V, power. This assembly was packaged to contain the *Mariner* A secondary hex power subassemblies which were in an L shape for *Mariner* A, and therefore required a new chassis to accommodate them on the *Mariner* R hex. Figure 13 shows the chassis which was developed to accommodate these subassemblies. The cutouts are for connectors, since the power cabling is external.

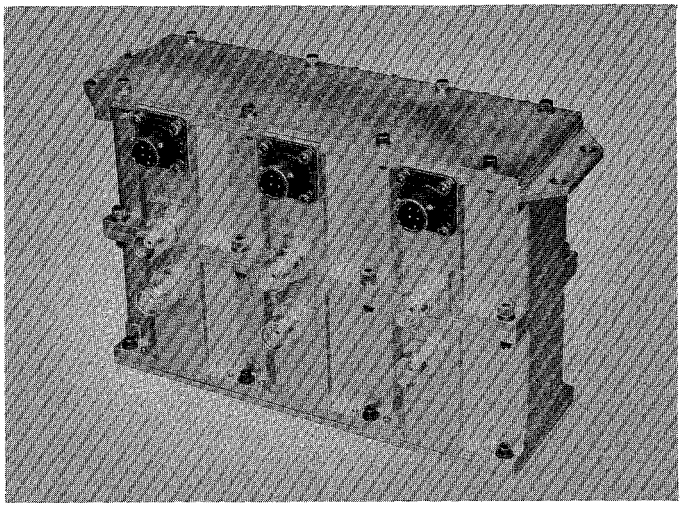

Fig. 10. Cavity amplifiers

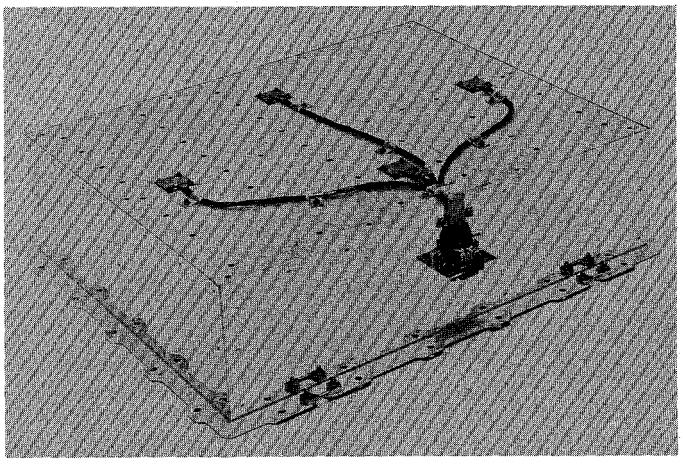

Fig. 11. Assembly III chassis

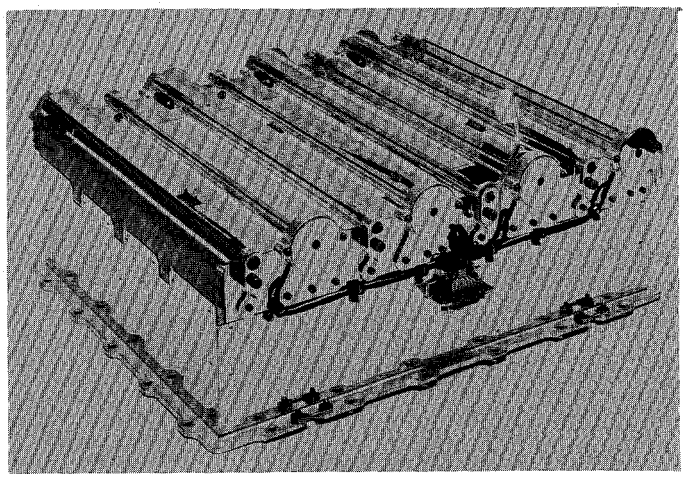

Fig. 12. Assembly IV chassis

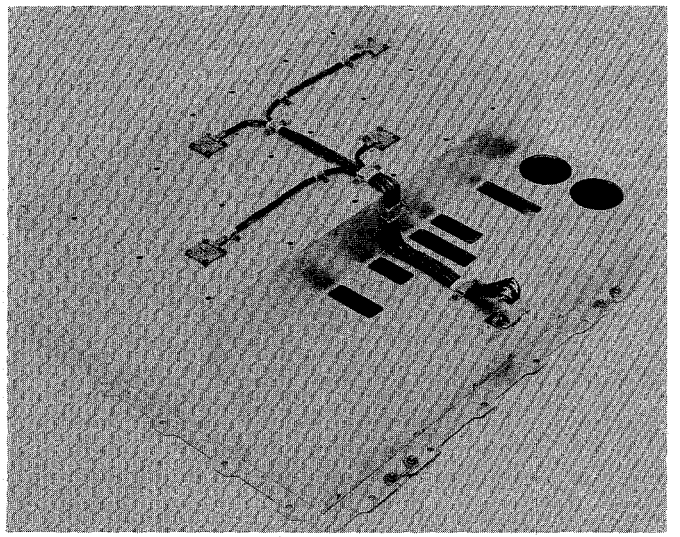

Fig. 13. Assembly V chassis

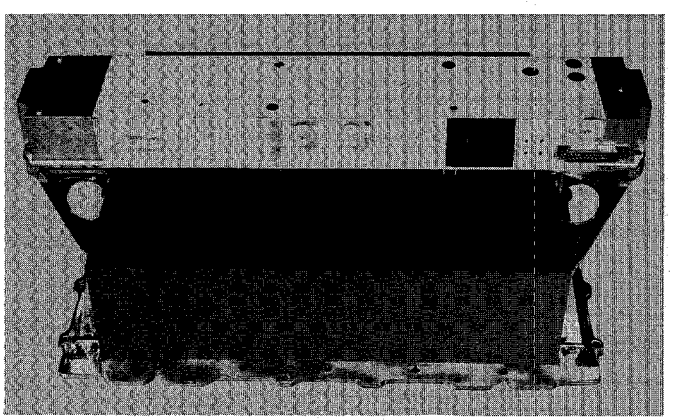

Fig. 14. Assembly VI

g. Assembly VI, battery. Figure 14 shows the battery chassis which utilized *Mariner* A battery cells. Location of this assembly on the hex was primarily governed by cabling requirements and spacecraft CG location.

The power amplifier subassembly is on the outside of the battery assembly developed for the *Mariner* A. This location was chosen to provide heat to the battery from the power amplifier.

h. Radiometer. For *Mariner* R, a new microwave radiometer was packaged using much of the electronics and RF components from a three-dish *Mariner* A radiometer. Figure 15 shows the instrument complete with thermal shield as installed on the spacecraft.

The generally parabolic shape of the dish was machined in steps, to avoid focusing solar energy at the feed of the instrument.

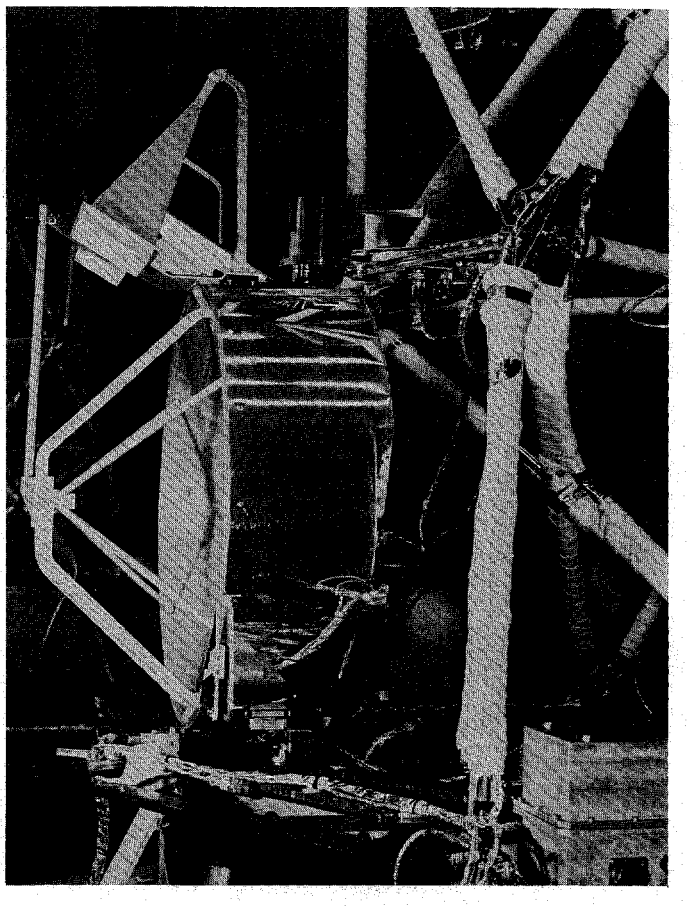

Fig. 15. Radiometer on spacecraft

To conserve weight, the back side of the instrument also utilized stepped machining which was coordinated with that on the face of the dish (Fig. 16).

A one-piece machined chassis can be noted; this was done to obtain a more efficient and stiffer structure by utilizing the dish while the stiffening ribs were used for mounting electronic components. The center channel, while serving as a stiffener, is also used for attaching the thermal shield over the instrument. The two ribs on the lower right corner are included to provide attachment to the infra-red radiometer.

i. Particle flux detector. Figure 17 shows the instrument with the thermal control cover removed. The chassis is shaped around the power supply underneath and the three Geiger tubes, leaving the top surfaces for the electronics.

2. Temperature Control

In previous issues of this summary the general design approach to the temperature control of the *Mariner* R components was discussed. Also, analytical techniques

UNCLASSIFIED

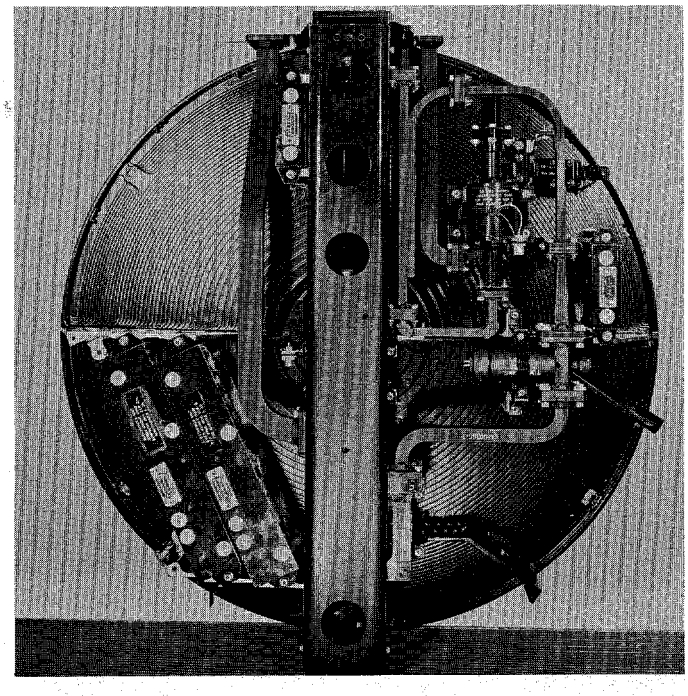

Fig. 16. Radiometer back view

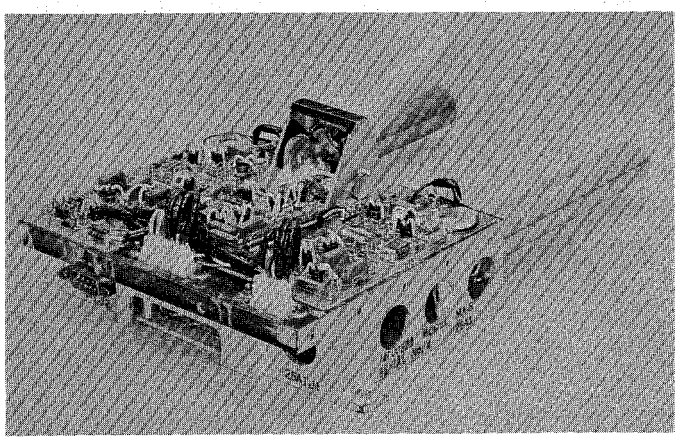

Fig. 17. Particle flux detector electronics

which were semi-empirical in nature were treated. The purpose and nature of the experimental tests which were conducted on a full-size thermal model of the spacecraft, will be discussed in this issue.

It was originally intended to verify the temperature-control system operation and calibration in a space simulator. This simulator would approximate, within acceptable limits, the vacuum, infinite heat sink and solar radiation properties of space. The tests were to be conducted first on a temperature control model (TCM) and then on each flight unit. It is recognized that the assumptions required to analytically state the thermal problem severely limit the accuracy to which temperature predictions can be made.

Unfortunately, the construction and checkout of the space simulator could not maintain pace with the *Mariner* development schedule and it became necessary to cancel those tests which used simulated sunlight. It was possible to complete a vacuum and cold-wall chamber of adequate size so that an essentially complete spacecraft could be tested as a unit.

The TCM used in these tests was identical to the flight models in every respect except that resistance heating elements were substituted for the electronic circuits. The solar heat input was also simulated with specially designed heater pads, shaped to cover the areas which would be illuminated during the Sun-oriented modes of the flight. Electrical input to them was determined by calculating the product of the solar intensity (S), the surface solar absorptance (α), and the illuminated area. The exterior of the heater pad was surfaced to have the same emissivity (ε) as that of the surface to which it was bonded. Thus, it was possible to measure the temperature of the assemblies and imply relative importance of the conduction and radiation effects. Temperatures of the spacecraft assemblies were allowed to reach a steady state for the various distributions of power which exist during the flight. The solar heat input was also varied from that experienced in the orbit of Earth to that of Venus.

Surface coatings were changed where required to adjust the temperatures to the desired levels. It became necessary to repeat these tests because the power distribution in the spacecraft was revised after measurements were made on the flight spacecraft. This clearly demonstrated how dependent the temperature control is on the power profile.

The flight spacecraft will not be tested in the manner of the TCM because it is felt that uncertainties caused from the lack of solar illumination are great enough to make testing of the flight units unwarranted. These uncertainties probably tend to make the spacecraft colder in test than in flight because of the lack of reflected energy and difficulties in actually heating all illuminated areas.

3. Pyrotechnics

The *Mariner* R pyrotechnic subsystem has been modified since reported in *SPS 37-12*. The telemetry indication of squib current was changed to a firing switch

closure. This modification was necessary to eliminate multiple pulses which reduced the intelligibility of telemetered data. All flight and spare pyrotechnic subsystems were modified and requalified by flight acceptance testing. The two modified units in the *Mariner* spacecraft have functioned properly in all system tests to date.

The microswitch indication of pin puller actuation has been routed on a ground line to the launch complex equipment and is not telemetered as previously reported. This was done to insure the reliability of the indicating system, since the actuation during countdown of any pin puller is of vital importance.

Live pyrotechnics were energized as a part of the MR-2 dummy run and functioned properly. A similar test, utilizing live pyrotechnics will be conducted on the MR-1 spacecraft.

4. Cable Insulation Materials

Vacuum–thermal tests of *Ranger* 4 gamma-ray spectrometer cable materials showed that the outer jacket of the coax cable contained an external plasticizer which, when volatilized in a space simulator test, resulted in stiffening of the cable and the formation of a yellow-brown spot on the thermal control coating of the instrument.

The assumption that cable stiffening was due to loss of plasticizer from the coating material may be only partly valid in light of further experience with *Mariner* R cables. After exposure to heat sterilization conditions, cables consisting of 100-wire bundles tied intermittently with nylon cord became very stiff. Examination showed definite fusion and bonding between adjacent wires resulting in numerous shear ties. Manufacturers' literature states that irradiated polyolefin, because of its cross-linked nature, has no fusion point and should easily withstand the heat sterilization temperature. Obviously, a sufficient percentage of the polyolefin has remained thermoplastic and will fuse at relatively low temperature–pressure conditions.

Irradiated polyolefin coated wire must be used with caution. Where flexibility is required (e.g., with an articulating boom), coating materials such as Teflon, other fluorocarbons, or silastic should be considered. Although special techniques may initially circumvent the problem (e.g., heat sterilization followed by sterile assembly), the cable will still stiffen if subsequently exposed to temperatures around 100°C, and then cooled.

As a consequence, all *Mariner* R cables required to flex during flight have been changed from irradiated polyolefin to Teflon insulation.

C. Guidance and Control

1. Spacecraft Power Subsystem

Activities on the *Mariner* R power subsystem during this reporting period have been related primarily to subsystem testing, type approval or proof testing, and flight equipment delivery. *Mariner* R flight equipment has been delivered to the SAF in support of the system and environmental testing. Systematic problems which required limited design modifications were uncovered in the electrical conversion area. The most serious problem in the spacecraft power subsystem is a potential shortage of power which is now anticipated based on a review of the *Ranger* 3 flight data. *Ranger* 3 solar panels operated at approximately 60°C, which was 15°C higher than anticipated. Consequently the voltage, and hence power, was approximately 8% low. This did not present a problem on *Ranger* since there is adequate contingency for this magnitude decrease. The implications of the *Ranger* 3 temperature data, however, when applied to the *Mariner* R solar panels indicate that there would be a 13% power shortage. This problem is under consideration and recommended modifications will be determined.

a. Electrical converters. System testing of the spacecraft has indicated power system problems, most of which were encountered in the 400-cps three-phase supply, requiring rework of these modules. During evaluation tests on the *Mariner* MR-1 spacecraft, the 400-cps three-phase supply appeared to develop abnormal voltages when the unit was switched from single-phase to three-phase operation. The problem was traced to high current arcing of approximately 8 amp through a relay contact. To correct the arcing condition a high power relay which is capable of switching 10 amp per contact has been selected. Parallel contacts have been utilized with a total capability of 20 amp. In addition, a current limiting resistor has been introduced to limit the maximum current discharge to approximately 5 amp. All 400-cps amplifiers have been modified to incorporate the new relay and have been flight acceptance tested again prior to delivery to the SAF.

A second failure in the 400-cps three-phase supply occurred during evaluation tests of *Mariner* MR-2 spacecraft. An indication of abnormally low voltages appeared

on all three phases when the spacecraft power was turned on. The problem was traced to an abnormal breakdown characteristic of a 2N1015C transistor in one of the three-phase preamplifier stages. The transistor (manufactured by Westinghouse) has these specifications:

Characteristic	Value
Power dissipation	150 w
V_{ceo} breakdown	150 v
Leakage current at 150 v, V_{cex} and V_{be}	1.5 v
Junction temperature of 150°C	20 ma, max.

In the preamplifier stage the transistor has a power dissipation of 0.2 w, V_{cer} of 104 v with an "R" of 3.9K. From this specification, the transistor seems to be operating within its limits. Investigation of breakdown characteristics of 20 2N1015C and 20 2N1016C transistors available in the laboratory showed normal leakage current at V_{ces} of 150 v, but readings of high leakage on some transistors were measured at a V_{ceo} of 150 v. Westinghouse was requested to analyze this circuit application and to examine the failed transistor. This effort is still in progress.

An additional problem with the operation of the 400-cps three-phase supply was uncovered on MR-1 when the spacecraft was subjected to environmental tests. The module operated normally on the three-phase mode, but intermittently indicated abnormally low voltage when the unit was operated in the single-phase mode. The voltage observed was lower than could be accounted for by a failure of the mode switching relay. Neither analysis nor testing has explained the condition.

A test has been performed, operating the unit in the chamber in both a hot and cold environment and switching the unit manually in order to force it to repeat this low voltage output. Test results showed that the unit was operating normally during both modes of operation; there was no evidence of a malfunction. Because of the inconclusive test results and the fact that the failure was observed only in the single-phase mode of operation, it is planned to replace the relay involved with the capacitor switching, retest the repaired unit, and return it to the SAF.

b. Solar panels. The *Mariner* R sample solar panel (1050 flat mounted cells) has successfully completed all type approval tests; i.e., the Table Mountain sunlight performance before and after the tests was unchanged. Type approval testing of the solar panel (identical to flight panels) has also been completed. Electrical performance of the panel was 59.8 w/Langley at 34°C measured in sunlight at Table Mountain, and the voltage at maximum power was 43.0 v. This is approximately 5% less power than the required 63 w/Langley at 34°C, and the voltage at maximum power is 3.0 v below the nominal design value. The performance at 127°C was 33.2 w/Langley, compared to a required 34 w/Langley. Failure of the *Mariner* R solar panels to satisfy the power and voltage design requirements and the implications of the *Ranger* 3 solar panel temperature data have resulted in a power source which has an 18% power deficiency. Several power subsystem and spacecraft modifications are under consideration.

As of April 25, 1962 JPL had four flight solar panels which have been fully flight acceptance tested. Two of these have been flight vibration tested on one of the *Mariner* R spacecraft and the other two will be vibration tested on a second spacecraft shortly. Flight panels 5 and 6 are near completion.

c. Battery. The battery design (type approval) testing program described in *SPS 37-14* is continuing. Status of the three battery charger systems being tested is:

TA-1 (50°F) has successfully completed the launch and mid-course maneuver power and is now in the 5th month of simulated flight (cruise mode). This unit is scheduled for completion of testing on May 21, 1962.

TA-2 (100°F) was removed from the vacuum–temperature test chamber after 9 weeks of simulated space flight. At this time in the test sequence two cells developed shorts and a small quantity of electrolyte was discharged into the vacuum chamber. This failure cannot be specifically related to the test environmental conditions because this unit (TA-2) had experienced two extended periods at temperatures above 100°F earlier in the test sequence. These two high temperature periods were the result of malfunctions of the control systems operating the environmental chambers. The battery developed an electrolyte leak after the first control system failure, and an attempt was made to reseal the battery. This unit is now being disassembled to permit an examination of all critical components to determine the cause of this latest leakage and all shorting.

TA-3 (80°F) is now in the 4th month of simulated flight (cruise mode) and present performance is acceptable. This unit is scheduled for completion of testing July 10, 1962.

2. Central Computer and Sequencer

The *Mariner* R central computer and sequencer (CC&S) is responsible for all spacecraft time sequenced events (excluding the science experiment sequence). In performing this function, the CC&S must keep track of

spacecraft time after launch, and execute commands at pre-determined times during the *Mariner* R mission. Briefly, the CC&S provides:

(1) A 38.4-kc sync frequency used as a spacecraft time reference.

(2) Commands, shortly after launch, to extend solar panels and turn on attitude control power.

(3) An Earth-acquire command 7 days after launch.

(4) Decoding and duration storage capability for the three mid-course maneuvers: roll, pitch, and velocity correction.

(5) Sequenced commands to the attitude control system for spacecraft positioning, and start and stop commands to the pyrotechnics for motor burn during the mid-course maneuver.

(6) On-pad adjustment of the planetary encounter start and stop commands normally sent to the science subsystem in the vicinity of the planet.

(7) A continuous 16.7-hr periodic command to the attitude control system to update the position of the high gain antenna during flight.

The *Mariner* R CC&S block diagram is shown in Fig. 18.

The 38.4-kc sync signal is a square wave obtained by frequency division from the central 307.2-kc oscillator in the CC&S. This oscillator is crystal controlled with a frequency stability of $\pm 0.01\%$ over the temperature range of 0 to 65°C. This 38.4-kc signal is used by the power subsystem as a stable frequency sync for the spacecraft primary 2.4-kc ac power.

Further frequency division of the crystal oscillator derived frequency yields frequencies of one pulse per sec (1 pps), one pulse per min (1 ppm), one pulse every 3.3 hr, and one pulse overy 16.7 hr. The 1-pps signal is used as the time reference during countdown of the roll and pitch mid-course maneuvers. The 1-ppm signal serves as the basic count frequency for the launch events: solar panel extension at $L + 44$ min and attitude control power on at $L + 60$ min. The 1-ppm signal is also used at the basic count input to the mid-course counter during the mid-course maneuver to provide roll, pitch, and velocity correction start commands at 60, 72, and 94 min, respectively, after the start of the mid-course maneuver. The 3.3-hr pulses (50) are counted to obtain the Earth-acquire command at 167 hr after launch. The 3.3-hr pulses are also used as the basic input to the pulse counter associated with the planetary encounter start and stop commands. The 16.7-hr signal is used to command the high gain antenna position update directly.

In addition to the basic 3.3-hr input, the encounter pulse counter mentioned above can be advanced by update pulses from the CC&S blockhouse panel prior to launch. These update pulses are used to adjust the time after launch at which the encounter start command is given. With this blockhouse signal, the encounter start command can be adjusted to occur at any 3.3-hr increment between $L + 3.3$ hr and $L + 277$ days. The encounter stop command is actuated a fixed 66.7 hr after encounter start.

Since all commands are referenced to launch, or a short time before, the CC&S must be inhibited until the proper time is reached in the countdown. The *Mariner* R CC&S is normally inhibited before spacecraft power is turned on, and is released at $L - 3$ min. The inhibit is located at the 1-pps point in the counter chain, and thus prevents all frequencies or repetition rates beyond 1 pps from functioning.

In addition to the blockhouse inhibit and update functions described above, there is also a clear command to enable the CC&S counters to be cleared to zero before the inhibit is released. The relay hold function which is initiated prior to spacecraft power on, commands all relays to the reset position and holds them there until it is released. This prevents any command relay from being actuated erroneously on the launch pad prior to launch. If any relay is not in the reset condition the relay position indicator (RPI) lamp will glow red.

After the inhibit is released at $L - 3$ min the CC&S will begin counting, and after 2 min will send a "clear release" command to the blockhouse to extinguish a lamp on the panel. At the time the inhibit is released, a 2-min timer in the blockhouse panel is started and if the clear release coincided with the 2-min timer the *go, no-go* lamp on the panel will remain white (*go*). If the two signals do not coincide the lamp will glow red (*no-go*). This provides a cursory check of the CC&S's ability to count correctly.

All CC&S commands, with the exception of the 38.4-kc sync and the event blip output, are relay contact closures which either apply or remove spacecraft battery power on the signal lines from CC&S to the other spacecraft subsystems affected. Each command relay, upon actuation, generates an event blip which is sent to the data encoder for subsequent transmission to Earth. The 38.4-kc sync signal and the event blip output are transformer-coupled to the user.

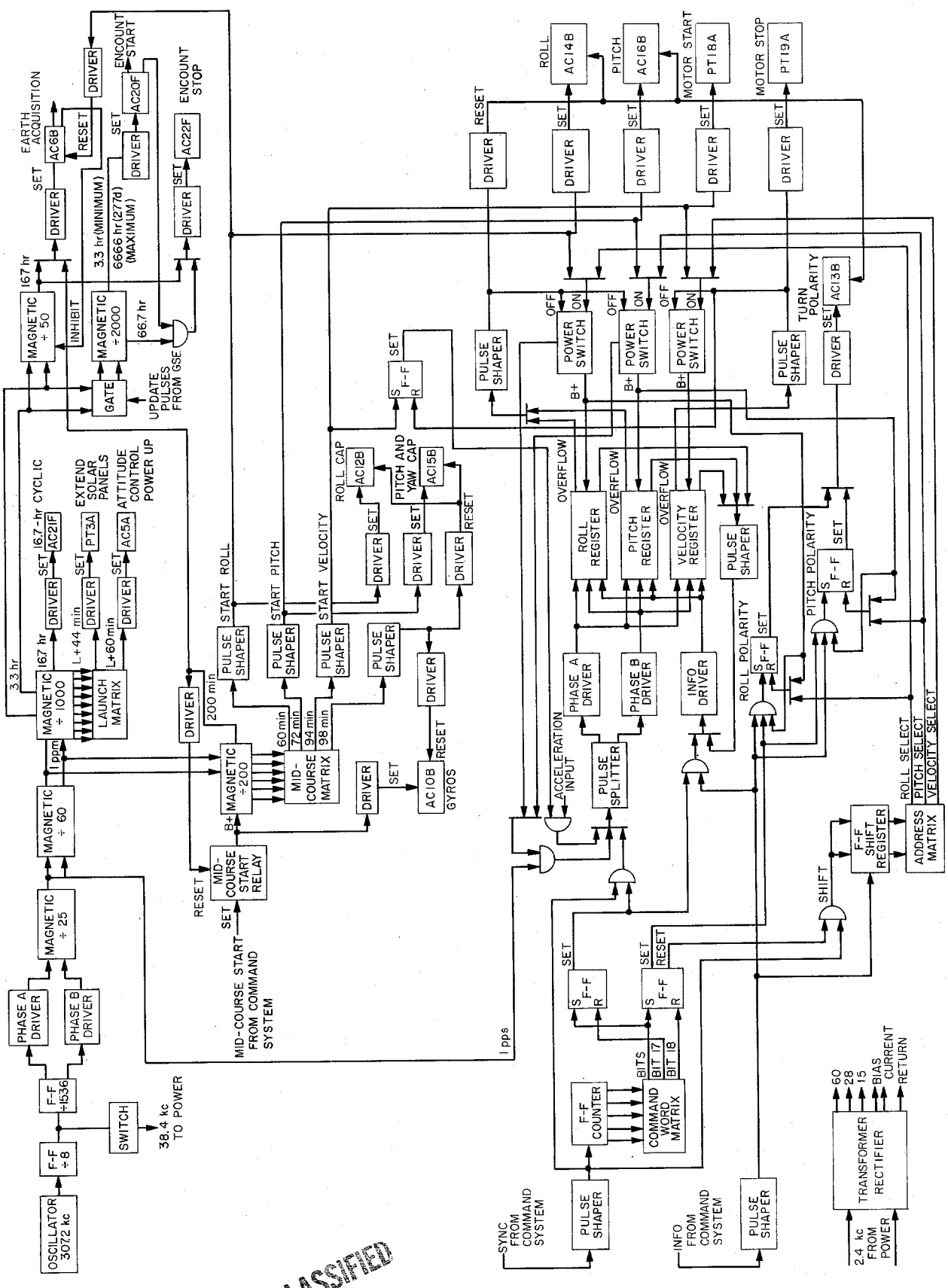

Fig. 18. *Mariner R* CC&S block diagram

UNCLASSIFIED

The CC&S subsystem consists of eight 6- × 6- × 1-in. modules which weigh a total of 12 lb and occupy approximately 330 $in.^3$ They are located in spacecraft Case IV along with the attitude control subsystem. Figure 19 shows an assembled *Mariner* R CC&S before encapsulation. The CC&S subsystem dissipates approximately 4.75 w of 2.4-kc power.

A brief description of each module follows.

a. Central clock (5A1). The central clock contains the stable, transistorized 307.2-kc crystal controlled oscillator from which all CC&S basic frequencies or repetition rates are obtained. The 38.4-kc sync signal is an output of this module obtained from a transistorized flip-flop divide-by-eight frequency divider chain from the 307.2-kc oscillator. The 38.4-kc signal is further flip-flop divided to obtain a 25-cps square wave. This signal is converted from a low level square wave to a high current level pulse train of the same frequency (repetition rate). This high current pulse train is fed as an input to a two-core-per-bit magnetic divider chain which has a 1-pps output. This pulse train, though high current, has a short pulse duration (2 to 3 μsec), and therefore low average power for repetition rates of 25 pps or less. The low average power magnetic core divider principle is used to obtain all basic repetition rates from this point on in the CC&S.

b. Launch counter (5A2). The launch counter receives the 1-pps output from the central clock and converts it, by a magnetic divide-by-sixty, to the 1-ppm repetition rate used as a basic frequency input for the maneuver counter as well as the remainder of the launch counter. The launch counter is used to provide, from a diode matrix, any duration from 1 to 999 min. Matrixed outputs furnish the 44- and 60-min commands for solar panel extension and attitude control power on, respectively. The overflow of this counter yields 1 pulse every 1000 min (16.7 hr) which is used to command the high gain antenna update.

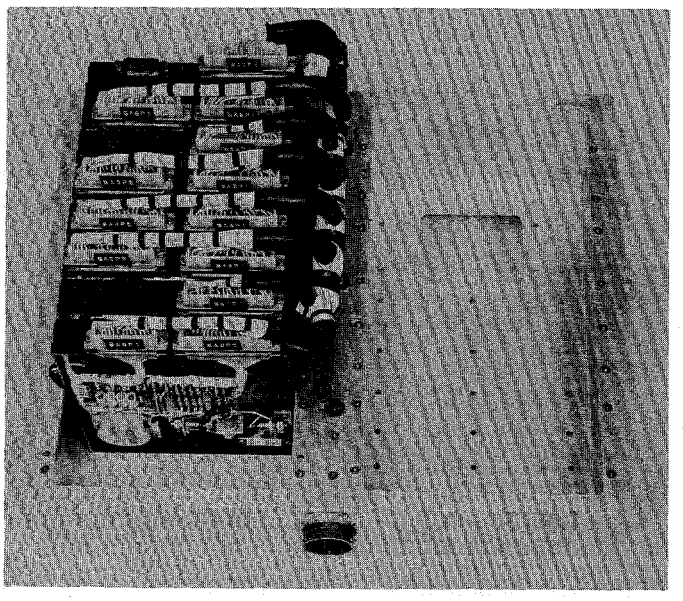

Fig. 19. *Mariner* R CC&S before encapsulation

The 2-min interval which tests the CC&S timing in the blockhouse is also obtained from this counter/matrix. This signal is designed to extinguish the clear light prior to the normal 2-min time after inhibit removal if the counter has not been completely cleared.

This subassembly also contains the transistorized relay drivers and the relays associated with the clear test, solar panel extension, attitude control power on, antenna update, and end counter update verify signals to the blockhouse (explained in the following discussion of the end counter). An additional output, obtained from within the launch counter, is the basic 3.3-hr signal used for Earth acquisition and encounter start and stop commands.

c. End counter (5A3). This module is similar to the launch counter in that it contains magnetic counters, relay drivers, and relays. There are two magnetic counter chains driven in parallel by the 3.3-hr input from the launch counter. One counter divides by fifty to obtain the 167-hr Earth acquisition command. The other is the updatable counter mentioned above used for the encounter commands.

Because the time of flight between Earth and planetary encounter will vary from launch date to launch date, the contents of the counter associated with the encounter commands must be variable. This variability is obtained with a counter whose normal overflow is greater than the longest flight time expected but which can be shortened for any particular flight time anticipated by pre-setting it with an appropriate number of counts from the blockhouse. The variability of this counter is between $L + 3.3$ hr and $L + 6600$ hr (277 days) in 3.3-hr increments. The encounter stop command is obtained from a point within this counter which yields a pulse every 66.7 hr. This pulse is normally inhibited from actuating the encounter stop relay until after the encounter start command has been delivered.

In the process of accepting the normal 3.3-hr input or the update pulses from the blockhouse, the count-by-twenty point in the counter will be activated once for every 20 pulses received at the counter input. This once-every-20 pulse is sent to the blockhouse equipment by

UNCLASSIFIED

way of the driver and relay in the launch counter (mentioned previously) and serves as a verify signal for the encounter update command.

In addition to the drivers and relays associated with Earth acquisition and the encounter commands, three of the drivers and relays associated with the mid-course maneuver are located in this subassembly to utilize the existing space.

d. Input decoder (5A7). The input decoder receives the radio-transmitted command words from the command subsystem, separates the information bits from the address bits, and routes this information to the appropriate storage register in the maneuver duration module. To perform this operation, the input decoder contains a five-bit transistorized flip-flop counter with a matrix output to provide signals at the end of the fifth bit (end of address), the end of the 17th bit (end of command information), and the end of the 18th bit (end of word). This binary counter counts sync pulses received from the command subsystem in order to perform its function.

Because logic levels are needed, two logic flip-flops are used to convert the pulses from the matrix into voltage levels. These levels gate the information associated with the first five bits into the address register, the next 12 bits into the appropriate storage register, and the last bit into the appropriate polarity storage flip-flop.

e. Address register and maneuver duration output (5A6). Part of this module contains the two-bit flip-flop address shift register which decodes, by diode matrix, the last two bits of the five-bit address. The input decoder provides shift pulses and the address information bits, derived from the command subsystem outputs, to the flip-flop register. The address contains the binary information to select a particular storage register (roll, pitch, or velocity) in the maneuver duration subassembly (to be further discussed). The polarity storage flip-flops, for roll and pitch, are also located in this subassembly. The rest of this unit contains the mid-course maneuver command relays not located in the end counter.

f. Maneuver clock (5A4). The maneuver clock contains a magnetic divider and diode matrix similar to the launch counter. It receives the 1-ppm signal from the launch counter as its basic frequency input. This counter is normally gated off until the mid-course start command is received from the command system. At receipt of this command, the counter begins counting and a command signal is sent to the driver and relay associated with turning on the gyros and accelerometer. During the operation of the mid-course counter, the diode matrix provides outputs at 60, 72, 94, and 98 min after start, which correspond to the roll, pitch, velocity correction start, and gyros and accelerometer off commands, respectively. The overflow of the mid-course counter occurs 199 min after start and is used to recommand Earth acquisition.

g. Maneuver duration (5A5). The maneuver duration module contains the storage shift registers which are used to store the mid-course turn durations transmitted by radio prior to the actual maneuver. At the start of each maneuver, commanded by the maneuver clock as described above, the shift register associated with a particular maneuver is turned on and shifted to "overflow" to obtain the stop command for that maneuver.

Each register consists of an 11-bit magnetic core shift register with "exclusive or" feedback which enables a particular "all ones" condition to exist once every 2047 shift pulses (if shift pulses are applied continuously). Because definite patterns of ones and zeros are produced in shifting from 1 to 2047, it is therefore possible to "pre-set" the shift register to some pre-determined count in order to have the overflow (all ones) occur sooner than 2047. Thus, the radio-transmitted mid-course data supplies the "pre-set" ones and zeros to allow each register to count to overflow in the desired length of time.

The roll and pitch maneuver registers are counted to overflow by the 1-pps signal from the central clock. The velocity register is driven directly by the output of the accelerometer.

h. Transformer-rectifier (5A8). All dc voltages used by the CC&S are provided by the transformer-rectifier (T-R). The input to this module is the 100-v peak-to-peak 2.4-kc square wave generated as primary power by the power subsystem. Rectified dc voltages available as outputs are −3, 15, 28, and 60 v. The 15- and 28-v outputs are zener-regulated to maintain a more constant voltage for the transistor circuitry they service.

i. Design and fabrication. Because of the short design time between the cancellation of the *Mariner* A project and the date on which a completely tested spacecraft had to be available for launch, all design effort put forward on *Mariner* A and the *Ranger* program was utilized, where possible, for the *Mariner* R CC&S. The launch and mid-course requirements for *Mariner* R are essentially the same as for the *Ranger* program. This was true of *Mariner* A also, and the major portion of the design effort on the *Mariner* A CC&S was on repackaging the *Ranger* design to accommodate more reliable, but often larger, *Minuteman* components. Thus, the basic circuitry for *Mariner* R was taken from *Ranger* and the high reliability component layout from *Mariner* A. Six of the eight subassemblies were built, with minor modifications, to the

UNCLASSIFIED

equivalent *Mariner* A specifications. A seventh module was built directly from *Ranger* specifications and the last subassembly is the one unit that required a new design. This subassembly, the end counter, is concerned primarily with the planetary encounter commands, which had no counterpart in *Ranger* or *Mariner* A.

The *Mariner* R design effort began in September 1961 with the first flight system delivered to the SAF on January 15, 1962. Fabrication, inspection, and testing of the *Mariner* R CC&S were all performed at JPL.

Since delivery to SAF, two *Mariner* R CC&S subsystems have been operating as part of the complete spacecraft.

3. Central Computer and Sequencer GSE

The ground support equipment (GSE) for the central computer and sequencer (CC&S) flight equipment has these capabilities:

(1) Automatic checkout of the CC&S with a coded printout record of test results.

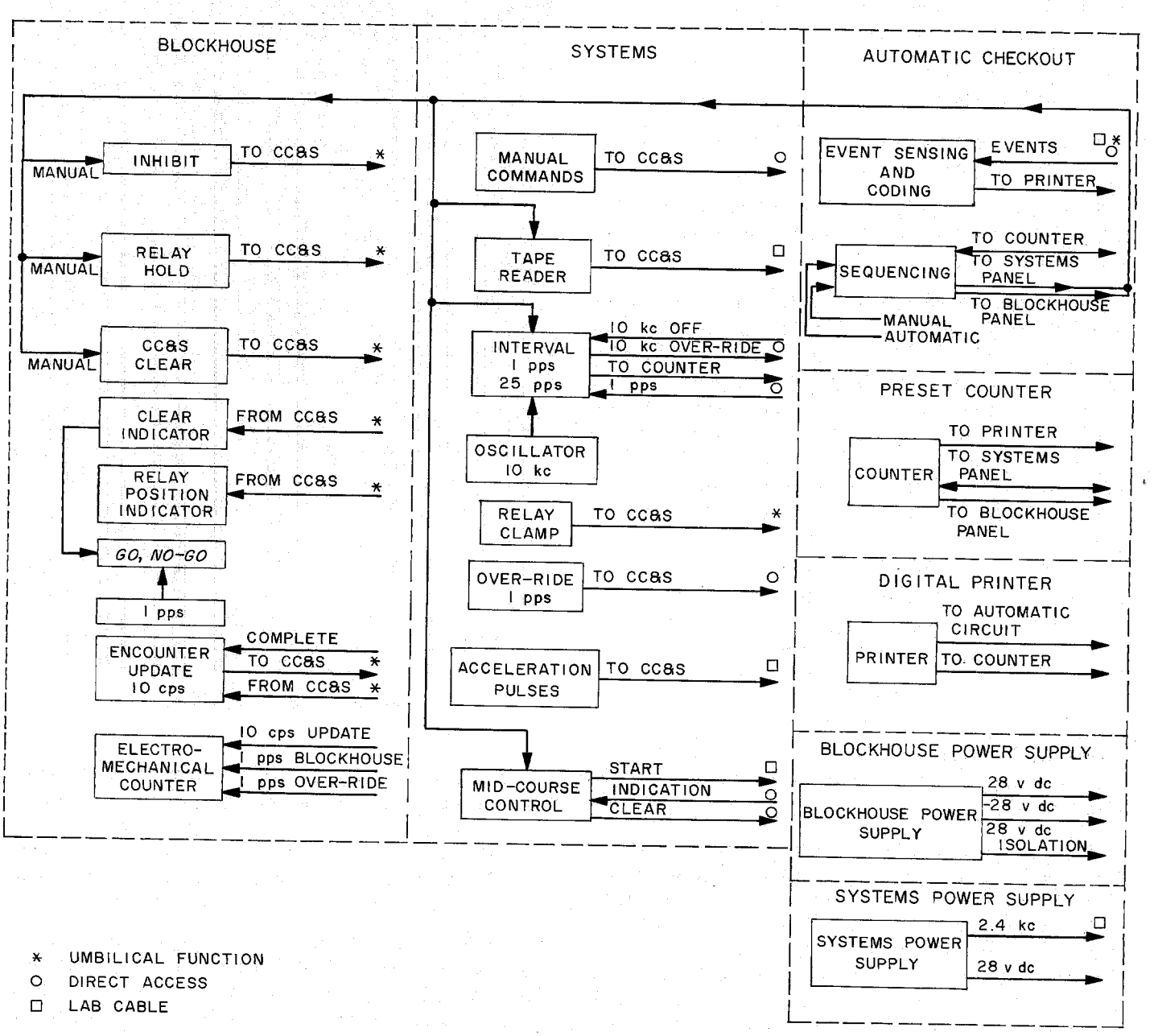

Fig. 20. CC&S GSE simplified block diagram

UNCLASSIFIED

(2) Manual control of all required CC&S functions for spacecraft system testing.

(3) Pre-flight monitoring and preparation of the CC&S in the launch complex area.

Capabilities (1) and (2) use identical equipment; (1) is used in the laboratory and in certain instances, with proper cabling, while the CC&S is installed in the spacecraft. GSE used in the laboratory and systems test complex is referred to as "Systems GSE." The GSE panel assemblies used in the blockhouse are identical and interchangeable with panels found in systems GSE. This accomplishes two important things:

(1) Operators using systems equipment are also familiar with blockhouse equipment.

(2) Spare equipment is provided for the blockhouse by the systems equipment.

Figure 20 is a simplified block diagram illustrating the three modes of operation between the CC&S and its GSE. Figure 21 is a photo of the systems GSE.

a. Automatic checkout panel. This panel automatically sequences and monitors the CC&S through its entire flight sequence. Interfaces with other subsystems on the spacecraft are simulated by this panel. Sequencing of the CC&S is accomplished by remotely controlling the manual functions found on the systems and blockhouse panels. A coded printout cycle is initiated by this panel whenever any CC&S output event occurs, such as inhibit release, CC&S relay command, etc. A typical printout cycle is:

	000121	40004
	000120	30003
	000120	20013
(red)	000120	10000
	CC&S coded time information, sec	

Events that occurred or have occurred are: telemetry blip, 39.4-kc pulse train, update complete, update verify, clear and start.

The CC&S time is taken from the pre-set counter and the coded outputs from the automatic checkout panel. Coded functions are assigned a particular location in the coded matrix, such as Row 2, Column 1. Three functions may be indicated by one location by assigning weighting factors to each; 1, 2, or 4. The coded printout may be any one of these numbers or the sum of the numbers. By referring to a master chart, the state of any function may be determined.

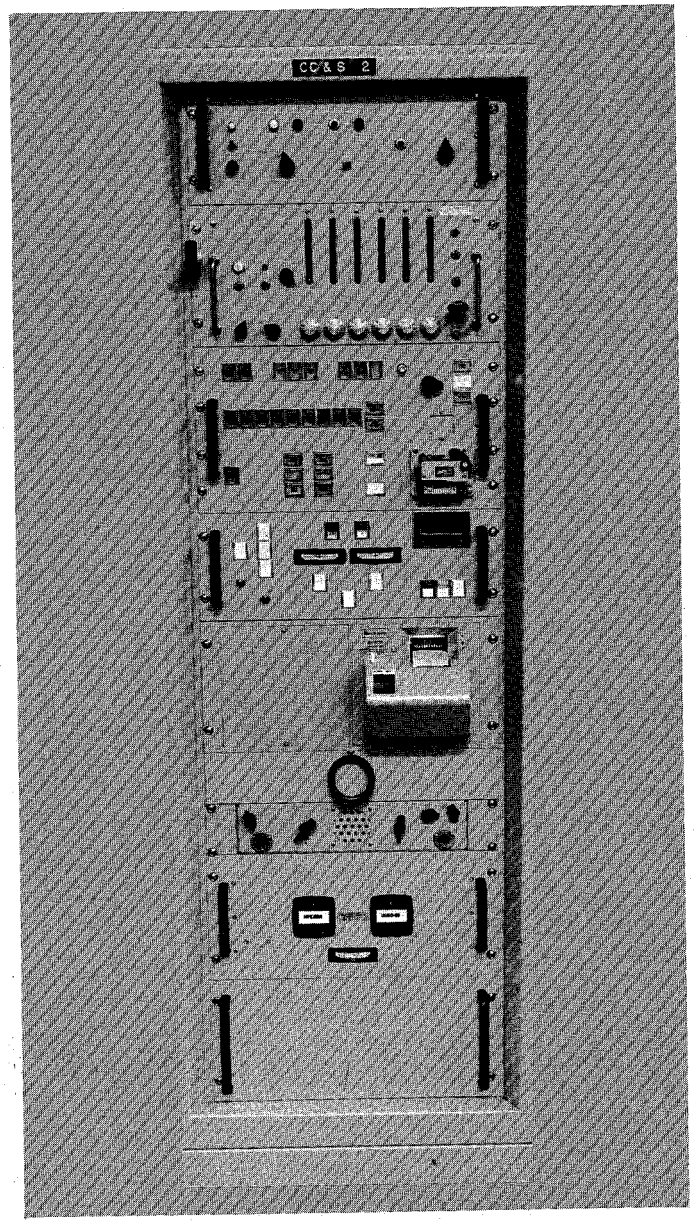

Fig. 21. CC&S systems GSE

The monitoring and printout capability of the automatic checkout panel may be used in a manual rather than an automatic mode. This allows monitoring of the CC&S during any short checks which may be run on the CC&S. It also allows monitoring of the CC&S events which occur during a spacecraft systems test.

b. Pre-set counter. The primary purpose of the pre-set counter is to keep track of CC&S counts. To shorten time between CC&S output events, a speedup capability is provided by the GSE. By over-riding the CC&S at its 400-pps point with a 10-kc signal, the sequence rate is

UNCLASSIFIED

increased to 25 times normal. The pre-set feature is used to stop this over-ride just prior to an event so that the event may be observed at the normal rate. Remote presetting of the counter is utilized when performing an automatic checkout of the CC&S.

c. Systems panel. The primary purpose of the systems panel is to operate and monitor the CC&S during systems testing of the spacecraft. Most of the functions come from the CC&S direct access cable to the GSE. Other functions on this panel are simulated spacecraft subsystem inputs which are not available during laboratory testing. These functions are energized by a special cable. Following are the direct access functions:

(1) Manual commands: Each relay in the CC&S may be manually set or reset from this panel. A light indication is provided when a relay is set.

(2) 25 pps: In this mode the CC&S operation is speeded up by a factor of 25. This is accomplished by injecting a 10-kc signal into the CC&S at the 400-to-1 divider. Therefore, instead of the normal 1-pps output to the counter, 25 pps is obtained. The 25-pps over-ride may automatically be stopped at a pre-set count using the pre-set capability of the counter. This is used in both laboratory and system testing.

(3) Interval check: Within the systems panel is a 0.01% 10-kc crystal oscillator. By gating this 10-kc reference signal with the CC&S 1 pps into the pre-set counter, a very precise check on the CC&S clock is obtained.

(4) 1-pps over-ride: This signal is used to facilitate overflow of the CC&S magnetic divide-by-50 counter (which gives the Earth-acquisition command) and the final overflow of the CC&S magnetic divide-by-2000 (which starts and stops science experiments at Venus). Ordinarily, these counters are counted down at a 1 pulse per 3.3-hr rate. Even at the $\times 25$ rate this would require excessive test time, thus the need for a 1-pps over-ride. The small digit counter on the blockhouse panel counts the number of pulses and the printer prints when this is started and stopped.

(5) Mid-course start and clear: The indication that the mid-course sequence has started, resetting of the mid-course relay, and clearing of the divide-by-200 CC&S magnetic counter are functions found on this panel. During laboratory testing the ability to start mid-course may also be accomplished via the laboratory cable.

These functions are found in the laboratory cable and are used to simulate other spacecraft subsystems:

(1) Tape reader: This is used to load the CC&S shift registers associated with roll, pitch and mid-course motor burn durations as ordinarily accomplished by the RF command system.

(2) Accelerometer pulse control: The velocity register for mid-course motor burn duration is ordinarily counted down by the output of a digital accelerometer. During lab tests, the 1 pps from the CC&S is shaped and fed back to the CC&S to simulate the accelerometer pulses.

(3) 2.4-kc power: Input power to the CC&S is 2.4 kc, 100 v peak-to-peak. In the absence of spacecraft power, this is supplied by the GSE and controlled by a button on the systems panel.

The following function is supplied through the umbilical cable:

Relay clamp: This provides a ground on the set driver of the first CC&S relay which, in turn, grounds the rest of the drivers. During flight the ground is supplied by the *Agena* adapter through one of the electrical separation connectors. This is to insure that no CC&S commands occur prior to separation. Since there is no adapter used in system testing, this function must be simulated on the systems panel.

d. Blockhouse panel. This is the most important panel in the console because it is used to monitor and control launch countdown functions. Each function will be discussed individually.

(1) Inhibit: A ½-amp dc current continuously supplied to the CC&S to prevent its counting while spacecraft power is on. This is redundantly indicated by a meter and a light which goes out if the current is too low.

(2) Relay hold: As a precaution against accidental CC&S output relay closures due to some unforeseen transient, a holding current is passed through the coils of each relay. Sufficient current is used so that a set relay driver being triggered, or a manual set command being given, will not operate any relay. 200 ma are used, indicated by a meter and a light as with the inhibit.

(3) Clear: This function resets the CC&S and GSE back to a zero time state. To clear the CC&S counters, a 1-amp 100-msec pulse is passed through all the magnetic counters, thereby setting all the magnetic cores to their zero state. This also sets

the clear relay which controls the clear light on the panel. If a proper clearing has been achieved, the light will go out at 120 counts from the CC&S. For safety reasons, an interlock makes it necessary to have the inhibit and relay hold on in order to initiate a clear pulse.

(4) Relay position indicator: This indicates when any relay in the CC&S has been set. A red indication here during the launch countdown would be cause for a hold.

(5) *Go, no-go* indication: In the launch configuration, the 1 pps from the CC&S is not brought out to the GSE. Therefore, a real time check on the 120-sec interval from inhibit-release to clear-light-out is made. The tolerance is 120 ±5 sec. A 1-pps 1% multivibrator in the panel is counted on the digit counter; if the tolerance is correct, the *go, no-go* remains green.

(6) Update sequence: Transit time to Venus will depend on the particular time of launch. The science sequence at Venus is initiated by the overflow of the divide-by-2000 magnetic counter in the CC&S. Normal pulse rate is 1 pulse per 3.3 hr which would take 277 days to overflow. A 10-pps generator within the panel is gated into the divide-by-2000 counter to adjust counter overflow to equal the transit time to Venus. These pulses are redundantly counted by two devices: the pre-set counter and a small electromechanical counter on the panel. A verify signal is received from the CC&S for every 20 pulses inserted. An update sequence would be:

(a) Set the pre-set counter to the number of pulses necessary to adjust overflow to the transient time.

(b) Activate first update. At 20 pulses, the first signal from CC&S occurs, stopping the update pulses. Both counters should read 20 and the green verify light will be on.

(c) If first update is normal, then activate second update which continues until the pre-set number is reached. The second update then indicates green and both counters should have the same count registered.

e. Digital printer. This operates in conjunction with the automatic checkout panel and the pre-set counter to give a printed record during laboratory and systems test.

f. MOIS. This is used for voice communication during system tests.

g. Blockhouse power supply. This power supply contains the dc voltages used in the launch complex.

h. System power supply. This supply contains the 2.4-kc supply and a dc power supply used in laboratory testing.

A signal conditioning module is used to stretch the 1-pps signal from the CC&S from 3 μsec to 1 ms. A one-shot, gated from the GSE and fed by the 1 pps from the CC&S is used for the 1-pps over-ride and is located here also. Three manual commands are also remotely controlled from this module. It is located 10 ft from the CC&S and 124 ft from the GSE in the system test area.

4. Attitude Control GSE

The system test attitude control (A/C) ground support equipment (GSE) for *Mariner* R incorporates all the monitoring capabilities required to demonstrate the flight readiness of the A/C subsystem during a spacecraft system test. The monitoring of A/C functions is done on a *go, no-go* basis. This allows a minimum of complexity in the GSE, coupled with a high state of GSE reliability. Scale factor and parameter checks of each flight subassembly are made in the laboratory and are rechecked at intervals. All system test area tests are made using spacecraft power, CC&S commands, and communications commands; therefore, no provision is made for the GSE to supply these functions.

Figure 22 shows a front panel view of the A/C GSE as installed in the spacecraft facility. The system test A/C GSE consists of the following assemblies:

a. Sensor and valve panel. Optical sensors on the spacecraft are excited by lamps mounted in light-tight hoods which are installed on the sensors during a systems test. These lamps are controlled by switches mounted on the sensor and valve panel. Switch operation is indicated by lamps on the panel. Each of the cold gas valves on the spacecraft are fitted with pressure sensitive switches which control monitoring lamps. The spacecraft antenna hinge position is monitored by a meter and antenna hinge movement is noted by lamps. The Sun-gate-blip and Earth-lock are monitored through the direct access plug on the A/C case.

b. Mid-course panel assembly. Since the same panels used in laboratory subsystem tests are used in the system test console, there are some functions on these panels that are not used in the systems test area. The mid-course panel has such features. The jet vanes are each monitored through wires from the direct access plug. These signals are summed and read on meters as movements in pitch, roll, yaw and drag. The drag component is error caused by malfunction.

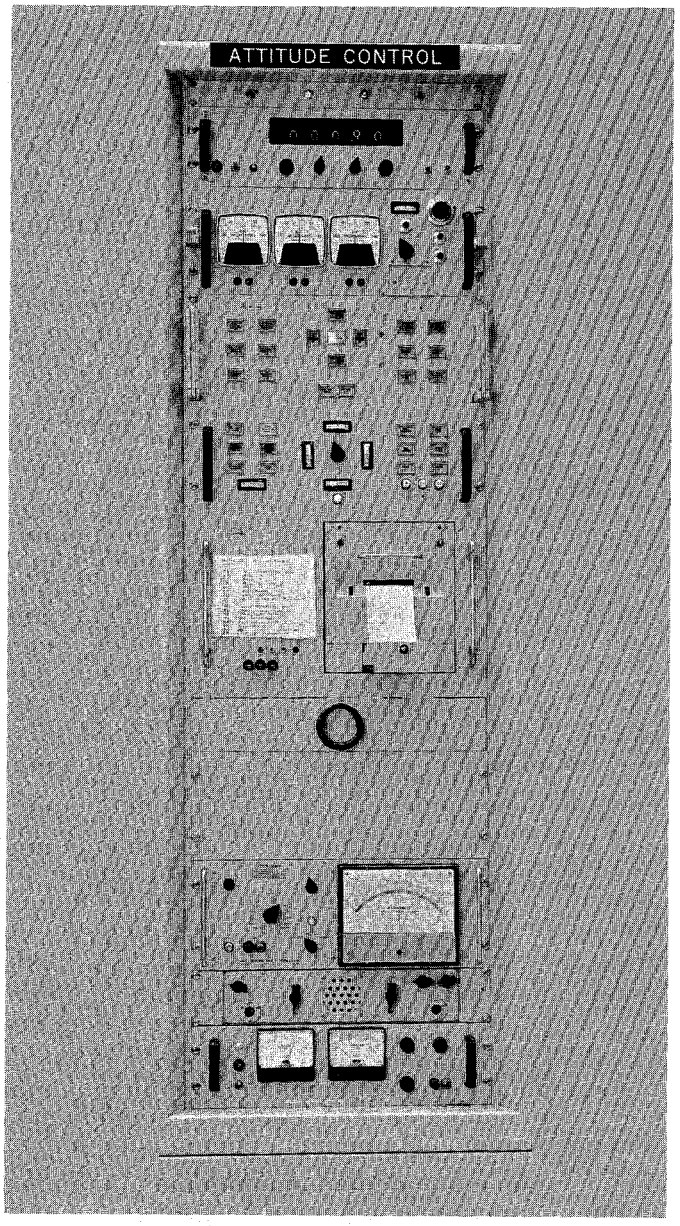

Fig. 22. Attitude control GSE

The gyro command and Earth inhibit functions are read as *on* or *off* indications by lamps on the panel.

The capacitor charge indicator is a panel-mounted lamp.

c. Gyro monitor and parameter insertion panel. This panel is the only A/C panel that connects to the spacecraft umbilical plug. The three A/C gyros are monitored by a panel-mounted meter for each gyro. A single switch selects one of the following scale factors for the meters: ±30 v, 3 v and 0.3 v, full scale. The monitoring point in the gyro control loop is set at the output of the gyro stabilization amplifier and is not affected by any switching that takes place during mid-course maneuver. The monitored scale factor will always be 60 v/deg/sec for a total ±1800 deg/hr.

Parameter insertion of the pre-set antenna hinge angle is accomplished by two switches, a ten-turn potentiometer with Deca-dial, and a null meter.

A Deca-dial calibration chart is included on each panel so that the proper pre-set angle may be selected. Then the plus or minus switch is depressed to return the meter to a null. This parameter insertion is possible only after spacecraft power is turned on and prior to A/C power turn-on.

d. Erie counter assembly. The flight accelerometer is turned on and off with the gyro control. Therefore, any time the gyros are turned on the accelerometer output is monitored with the Erie counter. In a 1-*g* field, the count is approximately 330/sec. If the spacecraft is positioned 6 deg above the horizontal, the count is approximately 35/sec.

e. Data display printer. Data display furnishes a printer for each A/C systems test console. There is a total of 18 telemetered functions monitored for A/C in this manner.

f. Perkins dc power supply. In order to reduce electrical noise caused by the GSE, all panel lamps and sensor exciting lamps are powered by dc. The only exception is the Sun gate lamp; due to the high current required, a transformer operated on 60-cycle, 110 v ac, is mounted near the Sun gate.

g. Launch complex. The A/C blockhouse equipment consists of a single panel. The gyro monitor and parameter insertion panel satisfies all launch complex needs. Until after separation in flight, only the A/C gyros and their associated loops are operating.

h. Laboratory test console. All panels used in the systems test console, with the exception of the data display printer, are used in the laboratory test console. In addition, a J-box simulating the ring harness, a gas manifold with valves simulating the gas system, spare jet vanes, antenna hinge actuator, Earth, Sun and Sun gate sensors complete the spacecraft simulation to make laboratory testing as identical as possible to actual system testing.

D. Telecommunications

1. Antennas and RF Components

a. RF couplers. Mariner R RF match-mate tests were conducted at JPL during the period from March 29 through April 4, using the MR-1 and MR-2 spacecraft and their associated flight adapters and shrouds. The test procedure used was identical to those used during the RF coupler tests reported in *SPS 37-14.*

The coupling loss at 960 mc from the communications pan through the omni-antenna and coupler to the quick disconnect was 12.3 db on MR-1, and 11.2 db on MR-2. This does not compare too favorably with the 9.3-db coupling loss through this system using the *Mariner* R structural model and the *Ranger* shroud. However, it is comparable to the losses obtained through this system on *Rangers* 1 and 2, and is therefore considered acceptable.

The coupling loss at 960 mc from the communication pan through the flight cables, rotary joint, high gain antenna, coupler, and *Agena* cable, to the umbilical quick disconnect connector was 9.3 db for MR-1, and 10.0 db for MR-2. This also does not compare favorably with the test results obtained from the structural model. However, it is still equal to or less than the 10.0-db design goal for this system.

The coupling losses at 890 mc through the command antenna omni-coupler system were excessive and highly unstable. The losses measured on MR-1 varied from 38 to 43 db and on MR-2 from 40 to 60 db. This excessive loss is very frequency sensitive with the highest losses occuring within a megacycle of 890 mc. The losses decreased to 27 to 32 db, 2 to 4 mc either side of 890 mc, and are much more stable.

When the high and unstable loss was first measured on the MR-1 coupling test, it was suspected that certain physical differences between the MR-1 flight configuration and the structural model previously used in these tests had caused the trouble. However, the coupling loss did not respond favorably to any adjustments of the configuration. Because the MR-1 flight spacecraft shroud and adapter were scheduled for other tests, the solar panels with the MR-1 flight command antennas, directional coupler, and cables were installed on the structure previously used. This combination, along with the *Ranger* shroud was then used to simulate the original test conditions. With this setup, the command and omni-antenna coupler losses reverted back to within ½ db of the original measured losses of 27.6 and 9.3 db, respectively.

In order to isolate the major cause of this excessive coupler loss between the spacecraft and the shroud, the *Ranger* shroud was then replaced with the MR-2 flight shroud. With this setup, the command coupler loss was 47 db and the omni-coupler loss was 11.9 db. The following table of coupler loss vs frequency for the omni- and command-coupler systems shows the frequency sensitivity of these losses:

Frequency, mc	Omni-coupler system losses, db	Command-coupler system losses, db
960	11.8	30.1
930	6.8	27.7
900	5.1	26.2
895	6.1	26.7
891	—	27.7
890	5.8	42.5
889	—	30.7
885	7.0	31.6

The results indicate that the problem was in the flight shroud configuration. There were two obvious physical differences between the flight shroud and the *Ranger* prototype shroud. First, the high temperature cable running from the coupler to the quick disconnect makes a double loop in the *Mariner* shroud before entering the cable trough between the shroud skin and inner liner. The mid-point of the cable loop is attached to the coupler support frame with a metal stand-off. On the *Ranger* shroud, the high temperature cable curves into the cable trough without looping and is not attached to the support frame. The second obvious difference was that neither flight shroud that arrived at JPL was equipped with a nose cone. To prove whether or not the absence of the nose cone had a detrimental effect on the command coupler system loss, the gap between the heat shield and the outside of the shroud, which the nose cone normally closed, was closed with metallic tape. Command antenna coupler losses at 891, 890, and 889 mc indicated that this modification had shifted the null point about 1 mc higher and had lowered the Q of the null slightly. It was concluded that, although this is not the prime source of the problem, in future RF match-mate tests it will be required that the shroud have the nose cone installed.

It is impossible to duplicate the high temperature cable configuration of the *Ranger* shroud since the high temperature cable is semi-rigid and should be bent only once. For this reason it could not be proved that this difference between the two shrouds was the prime cause for the high loss at 890 mc. However, by detaching the loop from the stand-off and by placing an absorber

through the high temperature cable loop, it was shown that this loop does have an effect on the shroud cavity field. However, it is not feasible for this loop to be straightened out for mechanical reasons. This cable routing appears superior to that in the *Ranger* shroud from a mechanical reliability standpoint. In order to determine if a foreshortened reflector surface in the nose of the shroud would have an appreciable effect, Reynolds Wrap was placed over the triangular coupler support structure and extended out to the shroud liner skin. A frequency vs command coupler loss measurement was then run. The results were:

Frequency, mc	Losses, db
895	24.3
891	30.0
890	27.8
889	29.5
887	25.8
885	40.0
880	31.6

It was concluded from these tests that the physical configuration of the area in the nose of the shroud above the omni-antenna coupler does indeed have a critical effect on the command system coupling. At this point tests were suspended using the structural model since the MR-2 was ready for match-mate tests.

During MR-2 match-mate tests, the command antenna system coupler system loss was found to be very erratic at 890 mc and a frequency run on this system showed the following:

Frequency, mc	Losses, db
900	29.4
895	32.9
891	40.9
890	40 to 60
889	38.0
885	33.0

It was then decided to try the aluminum foil technique over the omni-coupler triangular support section only. The command system coupling losses with this configuration were:

Frequency, mc	Losses, db
895	28.5
891	27.6
890	29.0
880	31.0
885	48 to 55

The omni-coupler system loss improved about 0.5 db; the final coupler loss amounted to 10.1 db.

Placing an RF reflecting sheet over the triangular coupler support effects a shift of the null of about 5 mc and brings about stable operation at 890 mc. It was recommended that LMSC provide such a device. The attachment will be made so that the sheet can be removed in the field, since this technique was not tried on the MR-1 shroud. At least two RF match-mate tests will be accomplished at Cape Canaveral prior to launch. One of these will be at the regular match-mate test; the other will be accomplished prior to this time.

b. Antenna patterns. A full-scale *Mariner* R is presently being assembled on the Mesa Antenna Range Facility. Upon completion, this mockup will be used to obtain no-vehicle radiation patterns of the omnidirectional antenna, the two command antennas, and the high gain antenna. Patterns will be taken in the same manner as for previous vehicles as described in *SPS 37-12*. The radiation patterns will be used in analysis of the communication link for various vehicle aspects.

E. Propulsion

The function of the *Mariner* R mid-course propulsion system is to remove or reduce *Agena* B injection dispersion errors so that a Venus flyby with a sufficiently small miss distance can be reasonably assured. This function is performed during the single spacecraft mid-course maneuver (executed approximately 8 days after launch) during which time the spacecraft turns to a prescribed position in space and imparts a corrective impulse by means of the mid-course propulsion system.

A description of the *Mariner* R mid-course propulsion system was presented in *SPS 37-12*.

The development program to date has been covered in *SPS 37-12*, *-13*, and *-14*. Since the last reporting period, the *Mariner* MR-3 flight propulsion system buildup had been completed and the system placed in storage as a spare system.

New trigger assemblies for the fuel start and shutoff valve have been received and have successfully undergone testing. The new assemblies have a thicker cross section than the earlier models. It appears that the additional wall thickness in the pressure vessel cavity of the trigger assembly has solved the problem reported in *SPS 37-14* wherein local yielding and, in some cases, rupturing of the trigger assembly was witnessed when the dual bridgewire squibs were used in the fuel valve trigger assemblies.

Because of the relatively long period between *Mariner* R launch and mid-course correction (approximately 8 days), during which the propulsion system will see a "hard" vacuum, it has been decided to replace the MR-1 and MR-2 regulators, which were lubricated upon assembly with Hercules Lube No. 2031, with regulators utilizing essentially no lubricant. Satisfactory regulation has been realized with regulators whose moving and critical surfaces are silver plated and utilize no additional lubrication. It is expected that the aforementioned "dry" regulators and their regulation characteristics will be relatively unaffected by the 8-day "hard" vacuum storage from launch to mid-course correction whereas the original lubricated regulators would undergo friction changes, and therefore regulation changes, due to lubricant boiloff. A "dry" regulator has successfully undergone flight acceptance testing and has been installed on the MR-2 flight propulsion system. The MR-1 replacement regulator is currently undergoing flight acceptance testing.

F. Supporting Activities

1. Planetary Environmental Test Program

During March and April, 220 experimental, type approval, and flight acceptance environmental tests associated with the *Mariner* R Project were handled by the JPL environmental test laboratory (Table 2).

a. Vibration testing. The *Mariner* MR-1 and MR-2 spacecraft were successfully flight acceptance vibration tested during April. The high frequency complex wave portion of the test was run, using the Calidyne L-249 shake table and Ling 175/240 power amplifier. By taking full advantage of the L-249's 1.0-in. displacement capability, the low frequency portion of the specified test (6 to 20 cps at 1.0 *g* rms) was also run using the Calidyne machine. Many hours of test setup time were saved by utilizing the same shake table for both frequency ranges.

During the vibration test the spacecraft operation was monitored with appropriate GSE located in the users area of the control room adjacent to the vibration bay. A typical vibration test setup is shown in Fig. 23.

To reduce the test time required for vibration testing of a component or subassembly in the three axes, a vacuum mounting system has been designed for use with two 5000-lb exciters used in the environmental laboratory. It is being evaluated at the present time.

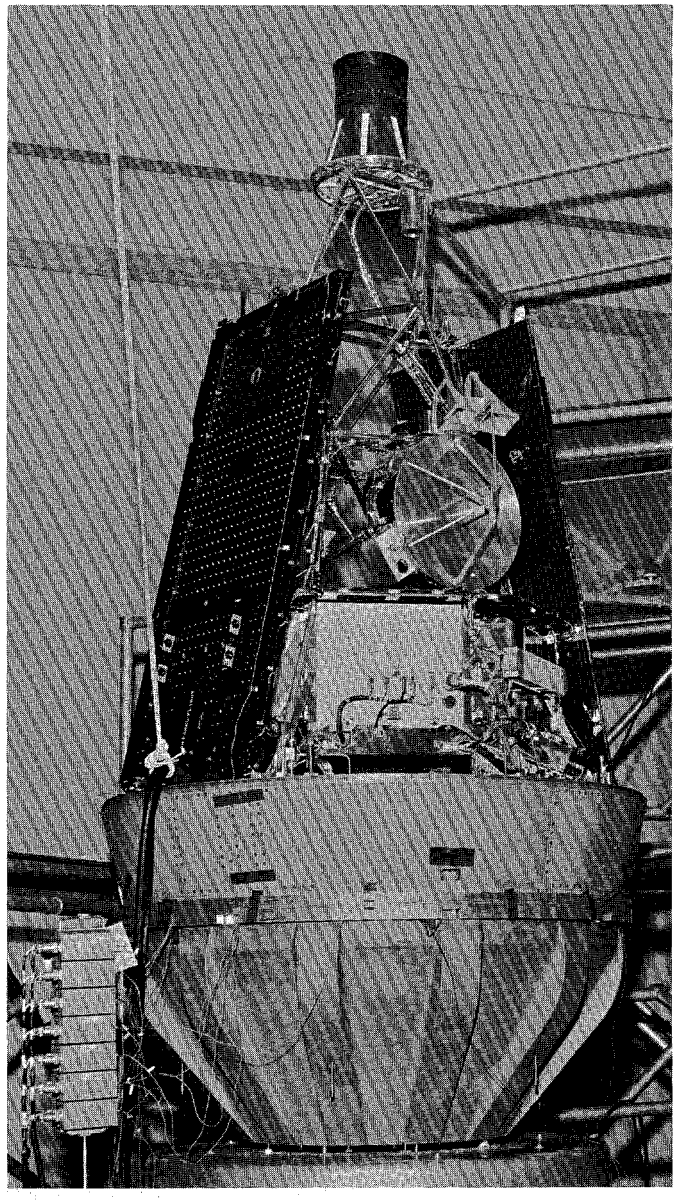

Fig. 23. *Mariner* R vibration test

By using a vacuum mounting system, the time required to bolt and unbolt the fixture from the shaker and the component to the fixture is saved.

The vacuum sub-plate (Fig. 24) is used with the C-25HB, which is operated in a vertical orientation. This plate bolts to the shaker head. Stat-O Seals are used under the bolt heads to insure a vacuum-tight seal at those points. On the top (mounting) surface of the plate is a semidovetail O-ring groove and a pumping port.

Table 2. *Mariner* R usage of ETL test facilities during March and April

Facility	No. of tests
Space simulator, 6-ft	5
Space simulator, 25-ft	4
Vacuum	14
Vacuum–temperature	55
Vibration	112
Low frequency vibration	4
Centrifuge	5
Shock	7
Temperature	9
Temperature–humidity	3
Explosive atmosphere	2

Volume of testing in each phase of the *Mariner* R Project during March and April			
Experimental	Type approval	Flight acceptance	Total tests
50	24	146	220

A small capacity mechanical vacuum pump is used to pull a vacuum between the vacuum plate and the fixture.

When a test is to be run, the fixture is placed on the vacuum sub-plate, and the vacuum pump is turned on. After the fixture has compressed the O-ring sufficiently to contact the sub-plate, the test can be run. As soon as the test is completed and the pump is shut off, air is bled into the system to free the fixture.

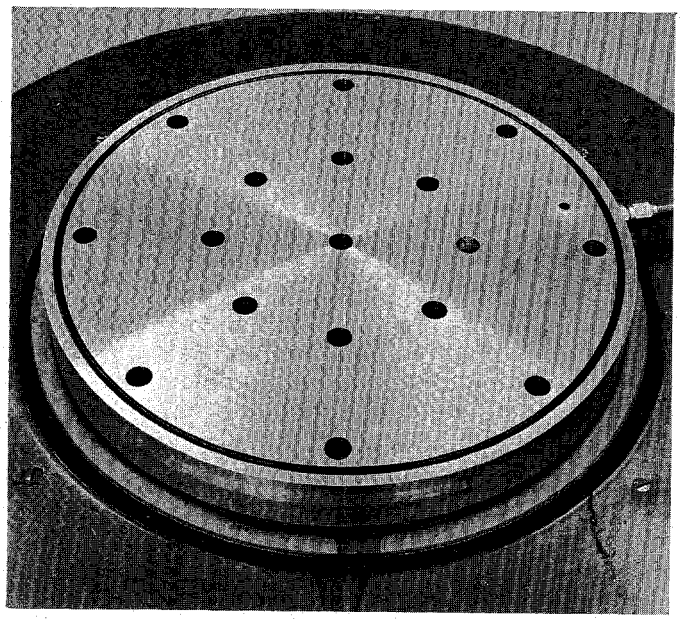

Fig. 24. Vacuum sub-plate vibration fixture

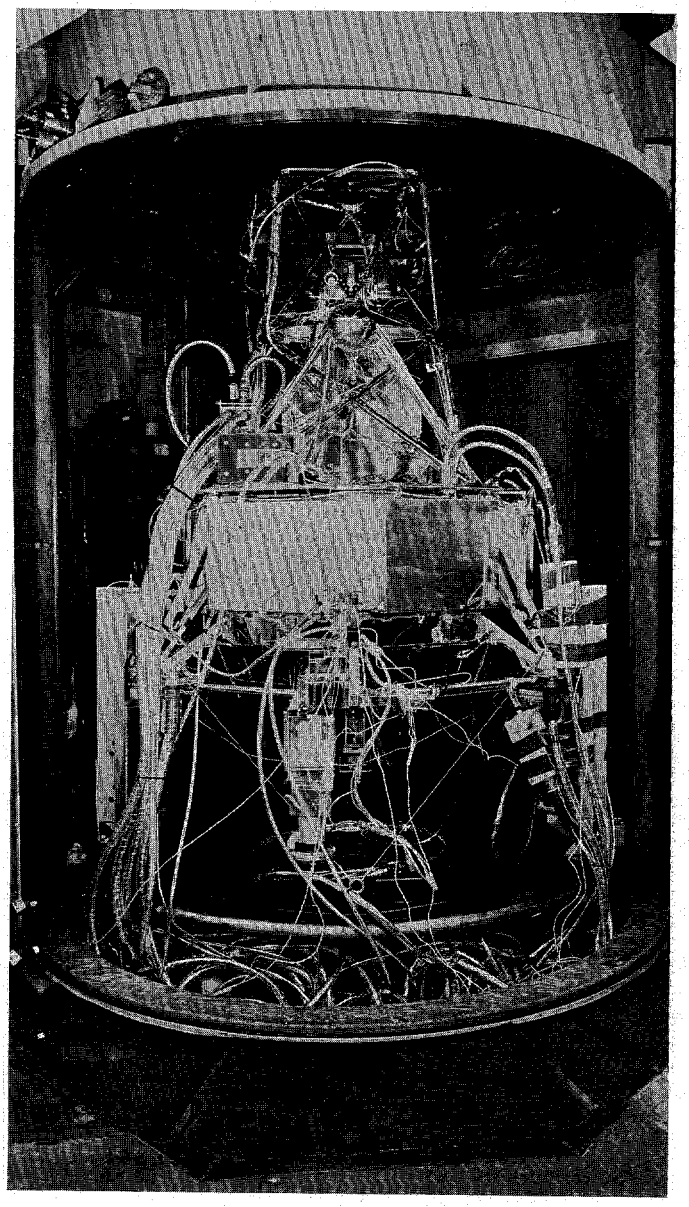

Fig. 25. *Mariner* R in 6-ft space simulator

From the data compiled so far, there is no indication of any separation between the sub-plate and the fixture within the force output range of the exciter.

At the present time, a series of preliminary tests is being run using this vacuum sub-plate setup for tests run in the horizontal axes. If this proves to perform satisfactorily, the vacuum mounting setup will be used for all vibration testing of component sized packages.

b. Vacuum testing. During the early part of April the *Mariner* MR-1 flight spacecraft was tested in a vacuum–temperature environment in the 6-ft space simulator.

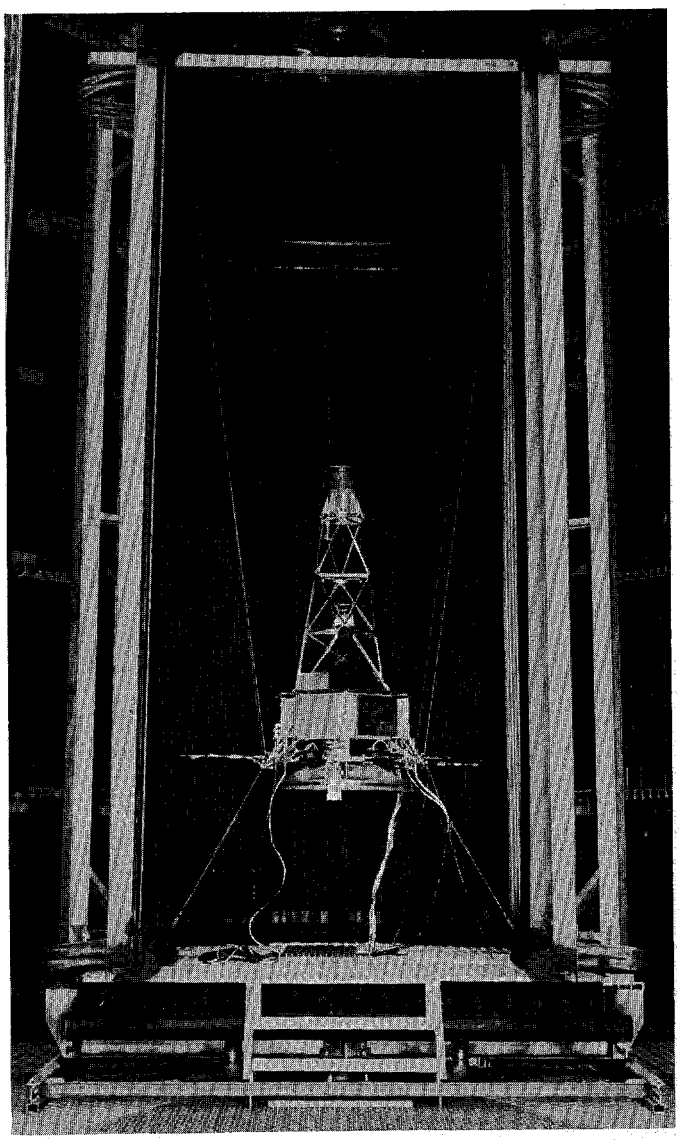

Fig. 26. *Mariner* R TCM in 25-ft space simulator

The environment during steady state conditions was: vacuum 5×10^{-6} mm Hg, wall temperature $-300°$F. Spacecraft temperature was controlled by resistance heaters mounted on the spacecraft structure. This test required 2 days of setup and pre-test operation, followed by 10 days of testing with the environment established. The spacecraft is shown mounted in the simulator in Fig. 25.

Objectives of the test were: (1) life test of spacecraft at predicted flight temperatures in a vacuum–temperature environment; (2) calibration of the spacecraft telemetry as a complete system at different temperatures while in a vacuum–temperature environment.

Setup and operation of the 6-ft space simulator for this test required 12 days of 24-hr operation (three shifts).

During the last week of April and the first week of May, *Mariner* MR-2 flight spacecraft will be installed and operated in the 6-ft space simulator with the same objectives as the previous *Mariner* MR-1 test. Space simulator operation will be the same.

In addition to complete system tests, four separate tests were run on *Mariner* R solar panels in the 6-ft space simulator. These tests were performed on both PTM and flight items to obtain thermal data on the solar panel zener diode heat sinks.

c. Space simulation. Four tests were conducted on the *Mariner* temperature control model (TCM) in the 25-ft space simulator to determine temperature distribution throughout the spacecraft, verify the passive temperature control design, and determine the effectiveness of the temperature control paint pattern under simulated space thermal and vacuum environments and at various internal power profiles. Results were:

Test No.	Start of test occupancy	Duration of test occupancy under vacuum, hr	Modes of operation[a]
1	2-26-62	33	Three modes (before and after Earth acquisition; vicinity of Venus)
2	3-9-62	34	Three modes (Test 1 repeated with new paint pattern)
3	3-15-62	54	Five modes (Test 2 repeated plus two additional modes)
4	4-9-62	33	Two modes (Earth and Venus

[a]Modes of operation as used in this table refer to a particular combination of operating conditions of internal electronic equipment and external heat inputs to the spacecraft.

The TCM in the *Mariner* mount within the space chamber is shown in Fig. 26. During testing, the chamber vacuum was below 10^{-4} mm Hg and the *Mariner* mount shroud was cooled to $-320°$F by liquid nitrogen. Solar thermal inputs were simulated by placing heating pads at regions of the model that would be exposed to solar radiation.

III. *Mariner* B Project

The primary purpose of the *Mariner* B Project is to permit scientific investigations of the planet Venus during the periods of availability in 1965 through 1967 and of Mars during the periods of availability in 1964 through 1967. Secondary purposes in order of priority are to (a) make interplanetary scientific investigations in the regions between Earth and Mars, (b) develop experience in the design of a spacecraft that has considerable flexibility with regard to the specific missions it is basically capable of covering, (c) provide experience and knowledge which will permit a quality and efficient design of the later *Voyager* spacecraft. To these ends, the spacecraft will be designed for a precision flyby mission and will incorporate the capability of either carrying or not carrying a small landing capsule. The *Mariner* spacecraft will be injected by the *Centaur* launch vehicle; it is expected to launch two identical probes at each of the planet launching opportunities. Deep space probes, to be launched in between periods of Mars and Venus availability, are included in the *Mariner* B Project.

Due to a revised launch vehicle schedule, the *Mariner* B Project has been revised as follows:

(1) The October 1963 test flight has been eliminated.

(2) The two flights for the Venus 1964 opportunities have been eliminated.

(3) A test/interplanetary flight of the Mars configuration will be conducted during May 1964.

The remainder of the *Mariner* B Project remains unchanged.

The preliminary design phase of *Mariner* B has been completed. Mission objectives, design characteristics and restraints, and functional specifications are currently being finalized and readied for publication. Comments on the pre-released Project Development Plan (PDP) have been received from Marshall Space Flight Center. These comments, together with the changes resulting from the reprogramming outlined above, will be used to modify, update, and ready the PDP for final publication.

A. Systems

1. Operational Support Equipment

A plan to improve the documentation for the *Mariner* B operational support equipment (OSE) has been conceived and put into effect during the reporting period. Essentially, the improvement consists of the creation of a specification book which will serve as a single source of OSE information, as a valuable design tool, and an aid in the planning and coordination of spacecraft system testing, launch operations and spaceflight operations.

The OSE specification book will consist of four sections: (1) introduction; (2) spacecraft system design verification and operational support equipment; (3) design characteristics and restraints for system test complex, launch complex, and power and grounding systems; (4) functional specifications.

Section 2 will establish the general philosophy for spacecraft design verification, and flight readiness determination. Design verification and flight readiness are

UNCLASSIFIED

achieved by evaluation of data resulting from the performance of a prescribed list of tests which will be defined and described in this section.

Section 3 will describe the general requirements and characteristics of the test equipment required to perform the tests established as requirements in Section 2. The equipment is divided essentially into two groupings: (1) the system test complex (STC) and (2) the launch complex (LC). The STC is comprised of an integrated arrangement of subsystem test sets which have the capability of stimulating the spacecraft and measuring the corresponding response. In addition, spacecraft internal functions are monitored and recorded by direct access lines to the spacecraft. All subsystems of the spacecraft are exercised through their entire dynamic ranges for the purpose of evaluating their performance under influences produced by the presence of the complete spacecraft. The LC provides external power to the spacecraft and switches the spacecraft to internal power; it inserts flight parameters into the spacecraft and verifies their receipt. It monitors the operation of the spacecraft to verify that all subsystems are operating in a normal manner.

Section 4 will contain the functional specifications for the subsystem test sets, as well as functional descriptions of related systems, such as the ground radio and instrumentation systems, and data processing, handling and display systems.

B. Spacecraft Design

The preliminary design of *Mariner* B has been completed with the submission of all functional specifications and the issuance of the launch vehicle interface control drawing, the spacecraft dimensional control drawing and the configuration drawing. Detail layout and hardware drawings are now in process. Some prototype hardware fabrication is underway and the mockup is being updated as the design progresses.

1. Structures

a. Basic spaceframe. The structural configuration of the basic spaceframe is unchanged from the last reporting. Detail structural design layouts are being made.

The cable trough ring structure at the middle of the spaceframe will not be removable. Rather, the cable and its framework support will be capable of being added and removed from the vehicle with a major disassembly of the structure. The ring structure forming the cable trough will also be used as a major attaching and aligning point for the propulsion system structure.

The top ring will be a one-piece ring with an ID large enough to permit lowering the cable and its framework into the spacecraft.

The bottom ring will be a minimum ring; its primary function is to support the electronic chassis. The fixed solar panels will be attached in such a manner as to form a deep ring at the bottom of the spacecraft.

A shear influence coefficient test has been conducted on a typical packaging chassis shear plate with a maximum number of connector holes in it. A typical chassis installation of the same configuration was also tested (Figs. 1 and 2). The values obtained from these tests have been used in the computer analysis of the spaceframe.

The computer analysis of the spaceframe has progressed to the point that sizing of structural members can begin. A basic criterion requiring the overall first resonant frequency to be at least 25 cps is being used. At present, dynamic loads similar to those used for *Mariner* A are being used. However, efforts to obtain better load criteria are being pursued by JPL, MSFC and General Dynamics Astronautics.

Interface investigations required to firm the configuration drawing have been completed. Detailed structural design layouts are continuing and only minor changes to the configuration drawing are expected.

b. Solar panels.

Foldouts. A structural test module consisting of the first module of the typical panel and its two support beams has been fabricated by Ryan Aeronautical Co. The module consists of 0.008-in. aluminum corrugations spot-welded to 0.012-in. aluminum facing. At beam attachment, a technique using truss core and an edge member transfers beam bending shear to the module surface skin, thus making a width of module effective with the beam.

This module was static tested to verify that beam, and surface corrugation stiffnesses were met (Figs. 3 and 4). Some delamination of the truss core over the beam occurred before the maximum loading was reached.

The module was then placed on the low-frequency shaker and subjected to a sweep at component level input. At resonance of about 32 cps, the 0.008-in. corrugation

UNCLASSIFIED

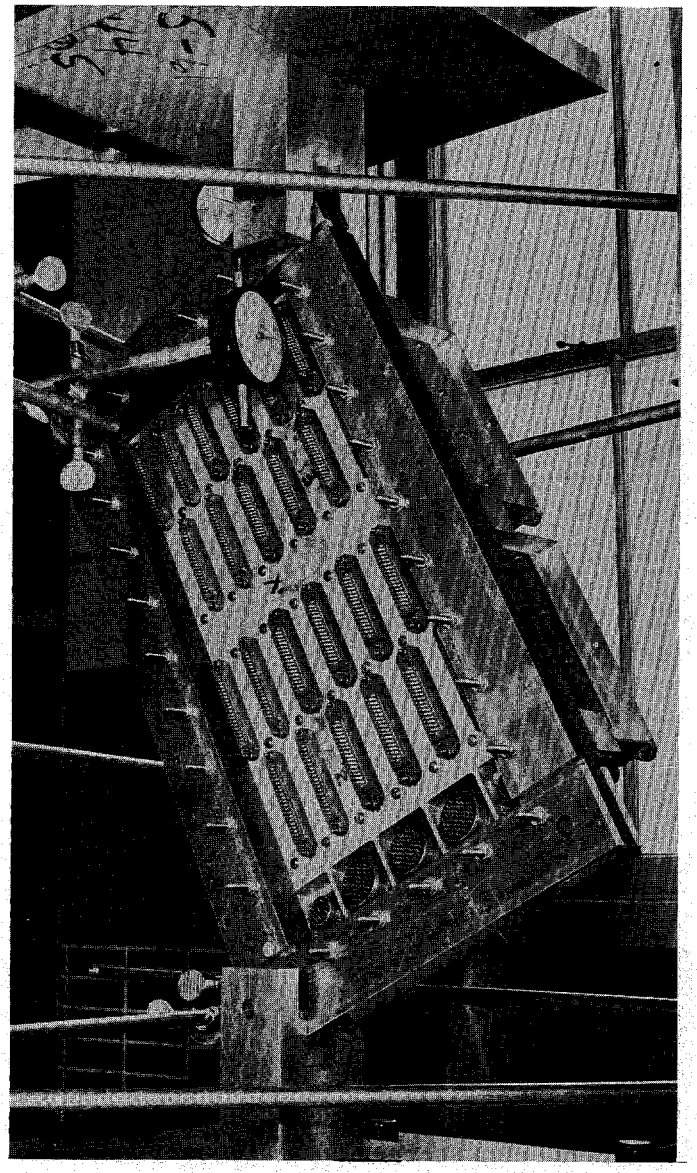

Fig. 1. Shear plate influence coefficient test, bottom view

buckled in the center of the span. The beams were effectively simply supported for this test, a condition more severe than that existing in the full panel configuration.

A redesigned module is being fabricated and will be tested in May. The redesign consists of bonding 0.008-in. strips to the inside of the corrugation caps, thus increasing the moment of inertia, but more important, increasing the buckling load of the corrugation (Figs. 5 and 6).

The delamination which occurred during static test will be corrected by better degreasing operations and a different approach to painting which may have affected the bond joint.

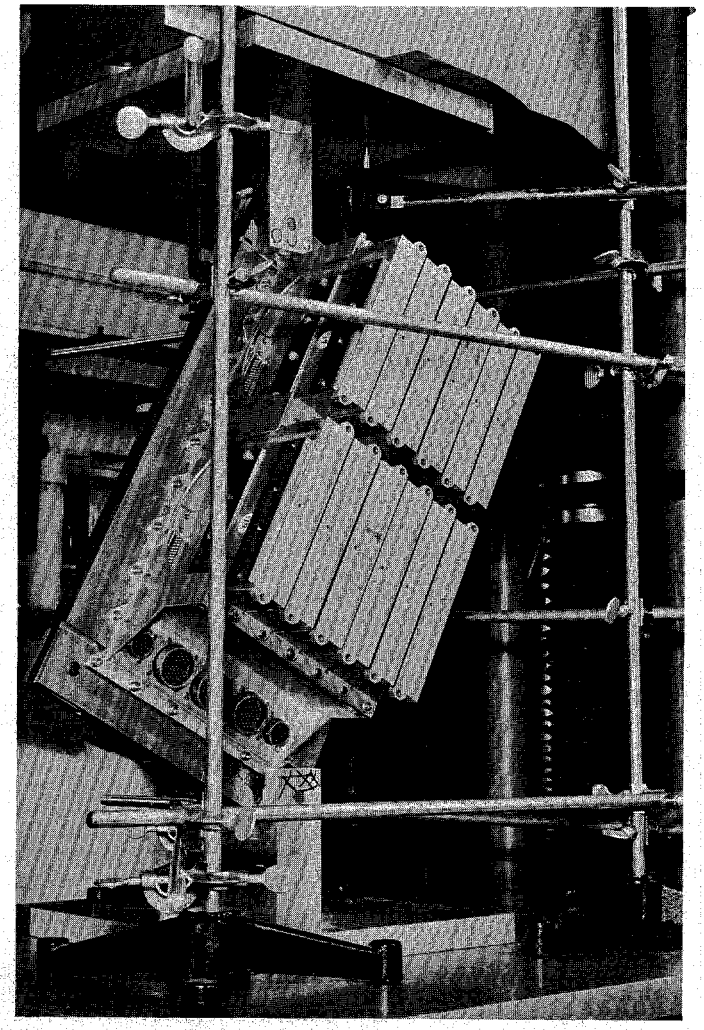

Fig. 2. Shear plate influence coefficient test

Fixed. The fixed solar panel will be designed in six segments. The edges will be attached to the spaceframe spokes and an attaching angle across the panel will pick up the lower ring of the spaceframe. The spoke and the panel will operate at the same temperature, thus eliminating a radial thermal problem. The panel and spokes will be thermally isolated from the spaceframe and the panel must withstand the resulting thermal loads.

It is planned that a double faced corrugation will be used for the panel. This gives the required shear rigidity to the overall spaceframe in this plane.

Cutouts will be available for instruments in two bays. Details of the splice to a removable piece containing these cutouts is being developed to give a maximum hole size and yet delete a minimum of useful solar panel area.

c. Antenna. The antenna reflector will be designed and fabricated by a vendor. Five companies have submitted

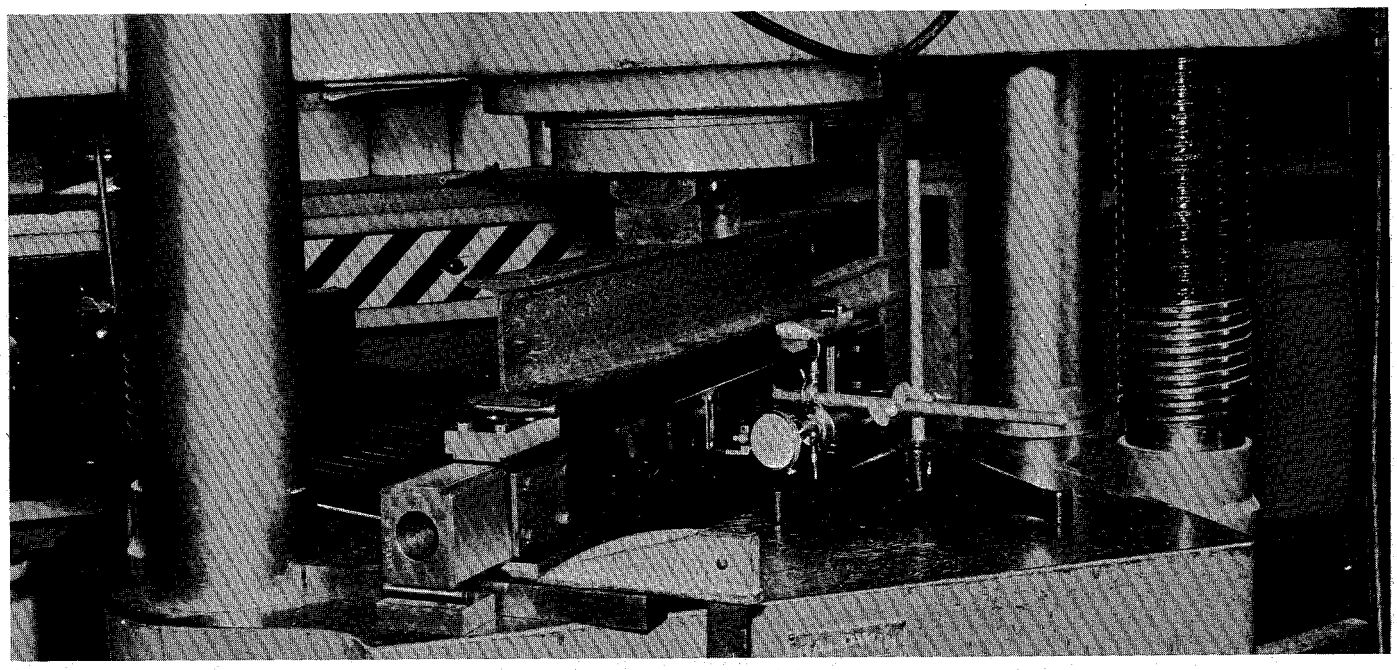

Fig. 3. Solar panel beam static test

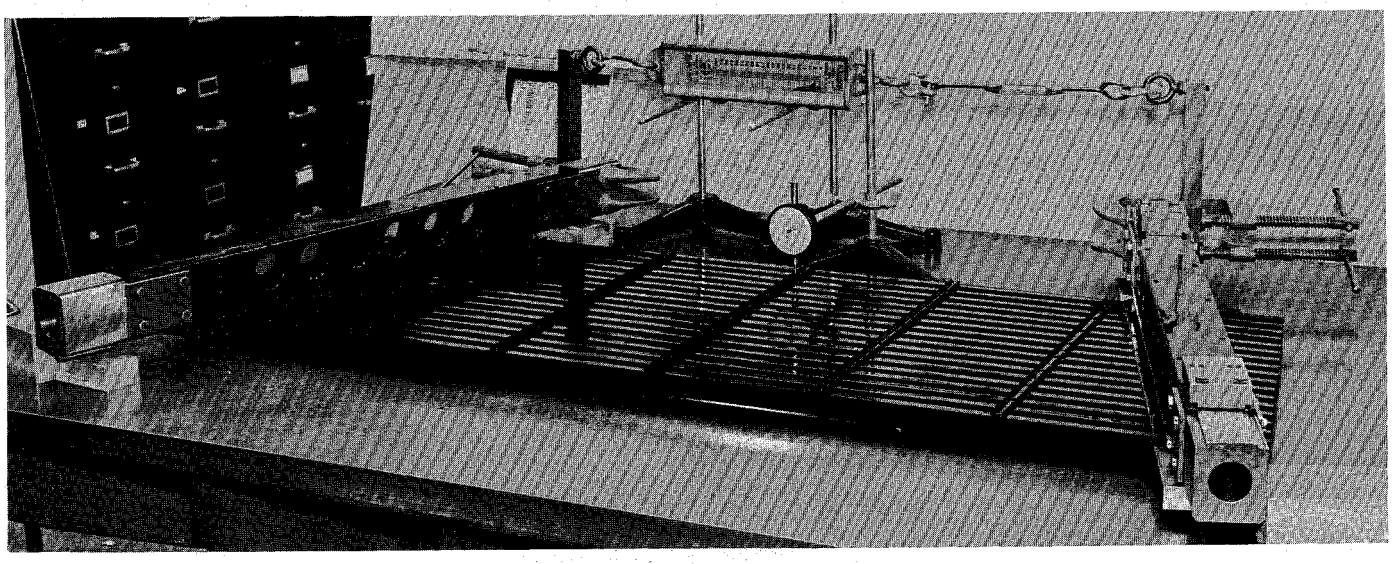

Fig. 4. Solar panel corrugation static test

proposals. Final evaluation will take place in early May with a test reflector delivered approximately 6 wk after receipt of the purchase order.

A basic shell approach to the reflector dish is being pursued by all vendors. Sandwich construction using an aluminum core with different approaches to obtaining the reflector surface predominates. Aluminum skins, vapor deposit on fiberglass and a thin skin bonded to fiberglass are the proposed methods for obtaining the reflector surface. Thermal treatment to diffuse solar spectral energy will be required on the surface fabricated by any of these approaches.

Much design layout effort has been placed on the antenna drive mechanism. The primary effect on the basic support frame is that the actuators are mounted closer to the hinge line to permit adequate clearance for the antenna dish.

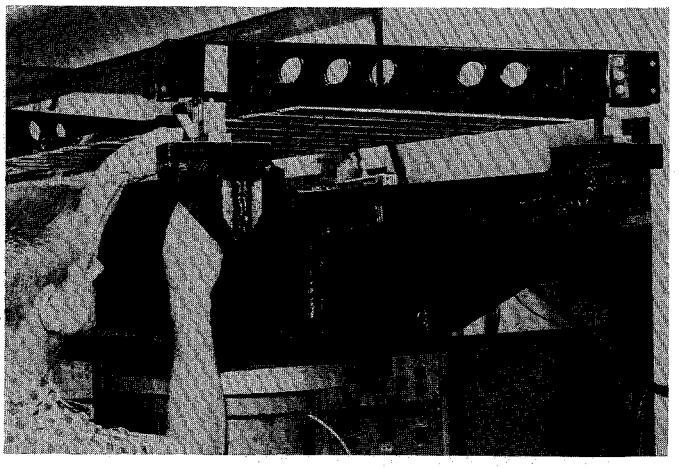

Fig. 5. Solar panel module low-frequency vibration test

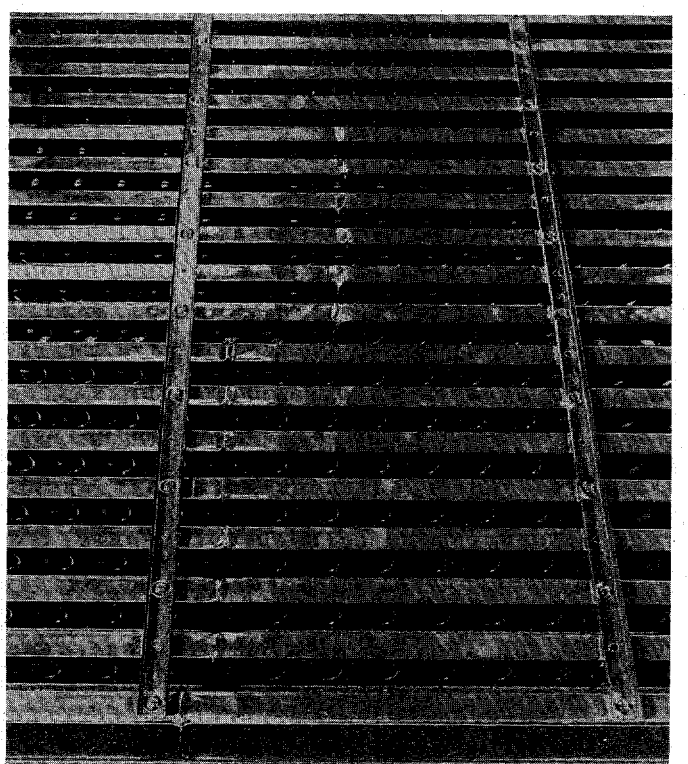

Fig. 6. Solar panel module failed corrugations

The latch support geometry has changed to minimize the excursion of the actuators caused by the vibration during boost. The main supports tie into the spaceframe approximately midway between the middle and lower rings. The dish is still supported back to the spaceframe by two members.

d. Mid-course propulsion package alignment. The interface for the propulsion system was raised from the lower ring to the middle ring. The propulsion package will be supported by brackets attaching to the middle ring and by tubes attaching to the columns near the lower ring. This structure will be designed to place the thrust vector of the propulsion system through the center of gravity of the spacecraft. Gross alignment is done on fabrication with a fine adjustment within a 1-in. diameter circle being done after the CG has been determined experimentally.

e. Adapter interface. The spacecraft will attach to the adapter at each of the six columns. Only three will carry tension loads. All will carry shear and compression loads.

Pre-load of the spacecraft will be employed, insuring that separation at the nontension columns does not occur.

Details of the attachment design are undefined at this time. The originally proposed latch mechanism which had undesirable backlash characteristics has been abandoned.

2. Mechanisms

Sufficient trajectory and planet pass information has become available so that the antenna cone and clock angles and the PHP planet encounter restraints have been defined up to planet encounter for all flights through 1967. The corresponding gimbal angles for the two antenna axes have been determined for the limits of the launch windows. These studies indicate that the following spacecraft roll orientations to Canopus will satisfy both antenna Earth tracking and adequate planet tracking (with one exception as noted):

Mars 1964 Type I trajectory, 40-deg roll

Mars 1967 Type I trajectory, 40-deg roll

Venus 1965 Type I trajectory, 160-deg roll

Venus 1967 Type I trajectory, 30-deg roll. (Approach asymptotes between 70 and 110 deg to the Sun will limit PHP planet tracking capability.)

An antenna gimbal system mechanical arrangement has been selected, from several considered, which satisfies the various geometric and mechanical restraints. It provides for a range of antenna gimbal angles of 150-deg (15 to 165 deg) elevation and 300-deg azimuth, adjustable in 15-deg increments, which gives a conservative margin over the presently known angle requirements.

An arrangement of antenna launch latching links has been developed which minimizes the forced angular displacements of the gimbal axes due to bus deflections. The predicted maximum pivot angular change is ± 0.3

deg at 30 cps. If the actuator can be designed to accept this deflection a pivot latch can be avoided.

Preliminary analysis of the PHP system indicates there will be displacements of the gimbal axes in the order of ±1 deg in the frequency range of 40 cps. If this deflection imposes an unacceptable torque on the actuators the gimbals will have to be latched during launch, or a torque relief device will have to be incorporated in the design.

The PHP configuration which was pursued for preliminary design was based on the Venus set of experiments. This configuration satisfied the science look requirements but required an extra foldout articulation of the planet seeker in order to come within the shroud envelope. The present PHP design effort is centered around developing a configuration for the Mars set of instruments. Due to the change from the Venus to the Mars configuration for the first flight this work is hampered by the lack of definition of the experiment envelopes.

Layouts of the solar panel and antenna deploying and latching mechanisms are in process.

3. Packaging

The general configuration having been established for the *Mariner* B spacecraft (*SPS 37-14*), the development of standard chassis and subchassis has proceeded and is described below.

The standard 6.5- × 6.3-in. and 14.0- × 6.3-in. subchassis which have been developed are shown in Figs. 7 and 8. These subchassis are designed for use as plug-in subassemblies using the Cannon Golden D non-magnetic connectors. The 6.5- × 6.3-in. subassembly can have one or two connectors. The 14.0- × 6.3-in. subassembly can have from one to four connectors. Figure 7 shows the machining detail for the connectors.

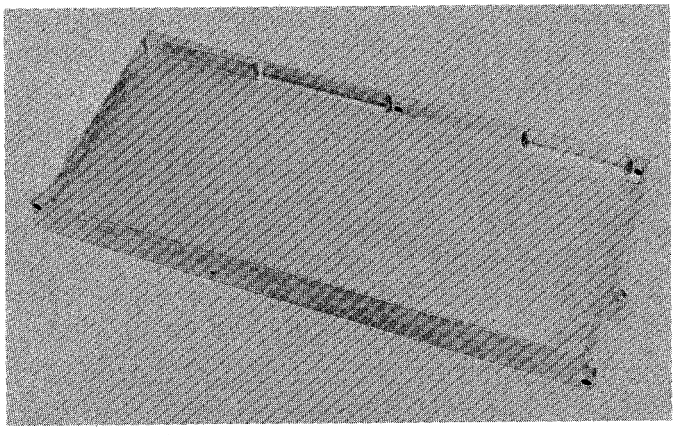

Fig. 7. Standard 6.3- × 14-in. subchassis

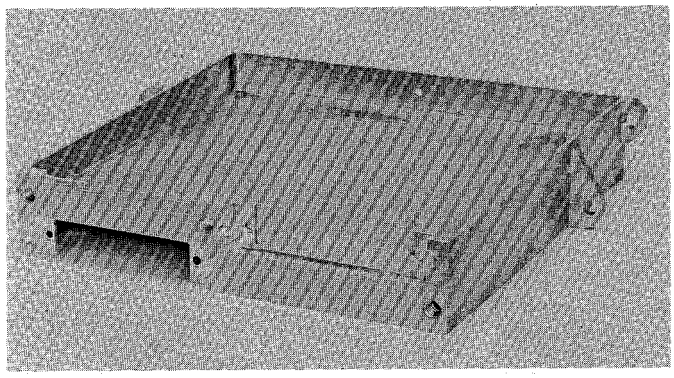

Fig. 8. Standard 6.3- × 6.5-in. subchassis

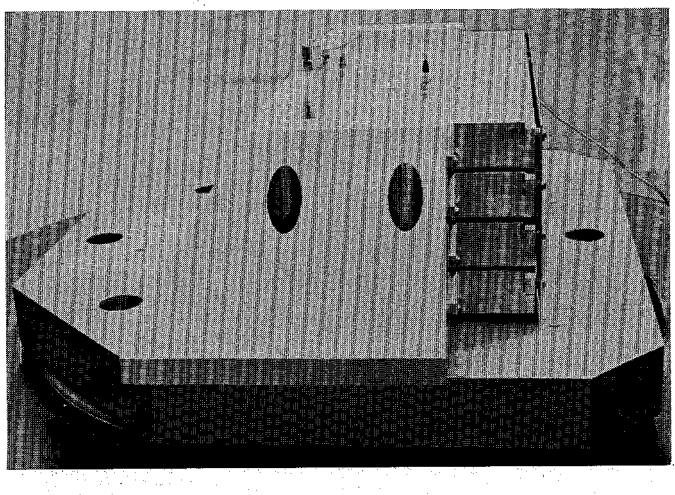

Fig. 9. 14-in. subchassis in shake fixture

A tie-plate for the tops of the 14.0- × 6.3-in. subassemblies has been determined to be necessary to raise the fundamental resonance to the 400-cps design goal. It is presently envisioned that the thermal shield will be used to satisfy this requirement. Figure 9 shows a tie-plate spaced ⅛ in. off the tops of the subassemblies and insulated thermally from the subassemblies. Figure 10 shows the proposed chassis for use on the transponder subassembly and is representative of the techniques used to accommodate special requirements within this envelope.

In the cabling area some mockup work was done to verify that the present configuration will work. A mockup (Fig. 11) of the system-ring-harness and assembly interconnect area was made and a tool developed for connecting and disconnecting the PT series connector. Use of the tool will allow the mounting of the 22-shell Pygmy connectors on 1¾-in. centers.

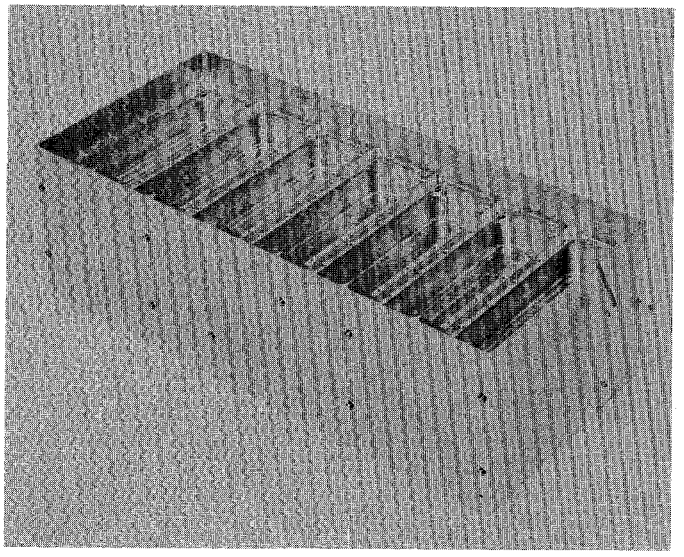

Fig. 10. Transponder subassembly chassis

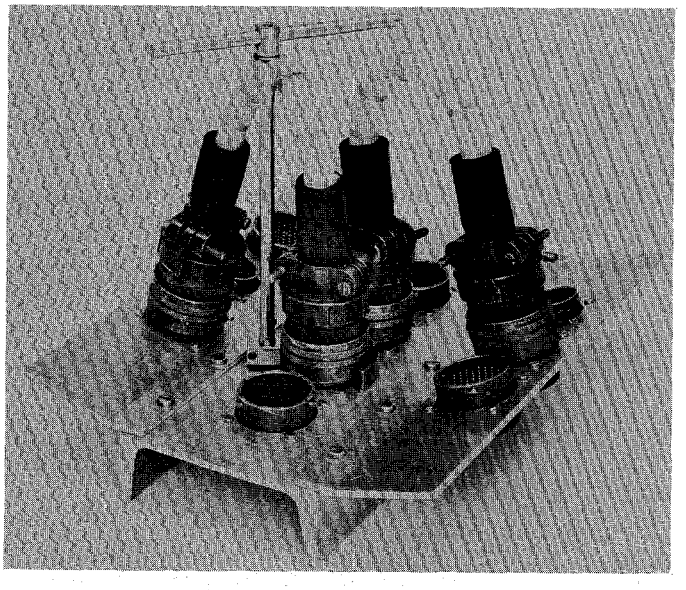

Fig. 11. Cable mockup with installation tool

A mockup (Fig. 12) was made of a "worst case" connector density configuration of the assembly cabling to show: (1) a means of adequately supporting the cable such that the connectors could remain unpotted, and (2) that sufficient dimensional float was available to allow proper engagement of the connectors when subassemblies are plugged in.

Several sizes of the assembly chassis (Figs. 13, 14, 15) have been procured for test and evaluation. The test assemblies for general usage are being evaluated based on the assumption that they would utilize the maximum number of connectors. Figure 16 shows one type of

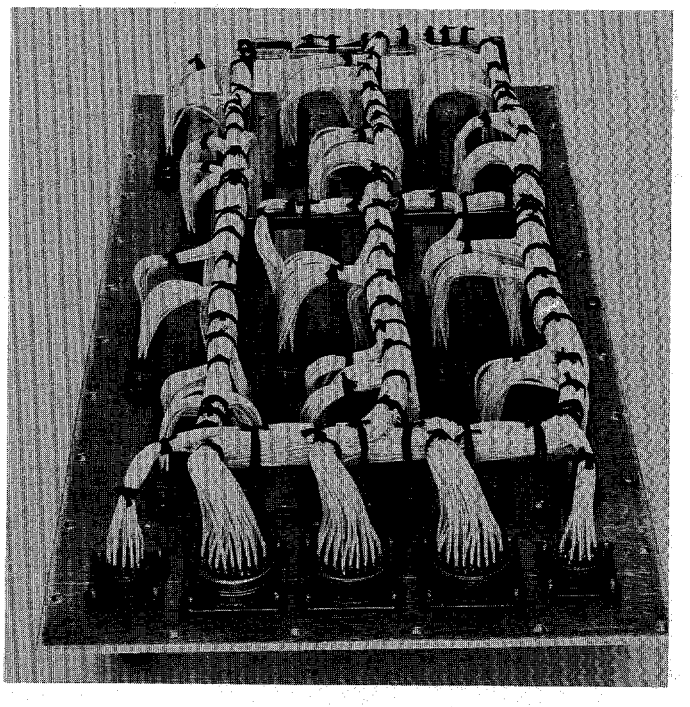

Fig. 12. Cable mockup

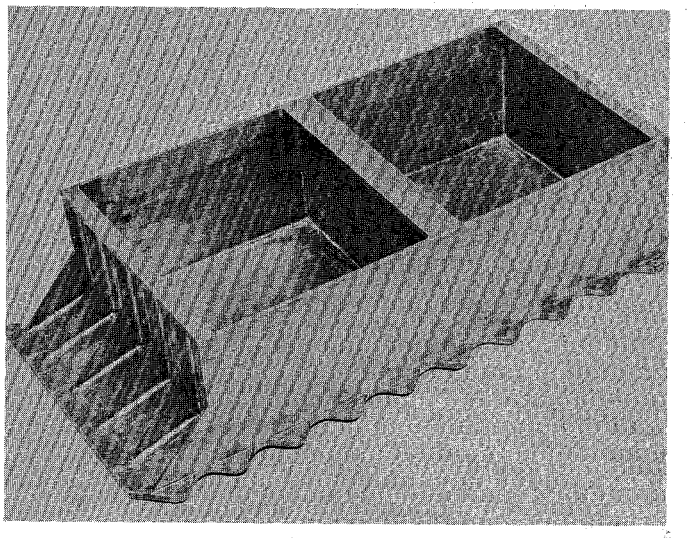

Fig. 13. Standard 17.5- × 8.75-in. chassis

chassis machined for 6.5-in. subassemblies. Figure 17 shows the dummy-loaded subassembly in the configuration used for dynamic testing. Figure 18 shows the subchassis for the command output CC&S.

4. Temperature Control

a. Bus. Analytical studies have been made on a representative bus structure during a maneuver. A 15-min pitch turn was considered, giving a 90-deg rotation rela-

UNCLASSIFIED

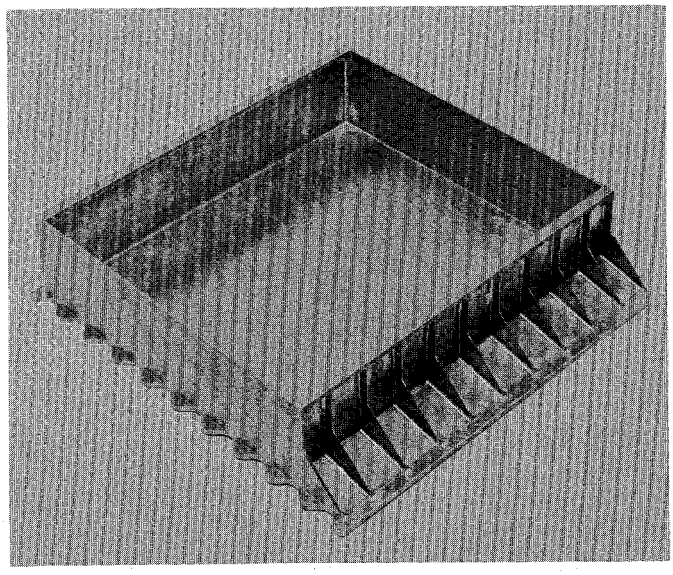

Fig. 14. Standard 17.5- × 17.5-in. chassis

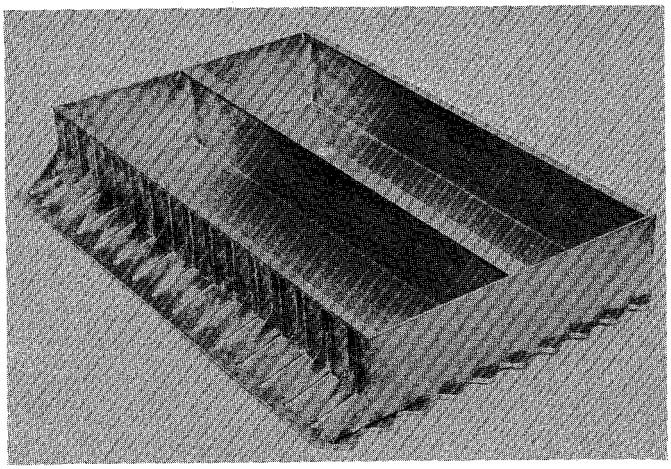

Fig. 15. Standard 17.5- × 26.25-in. chassis

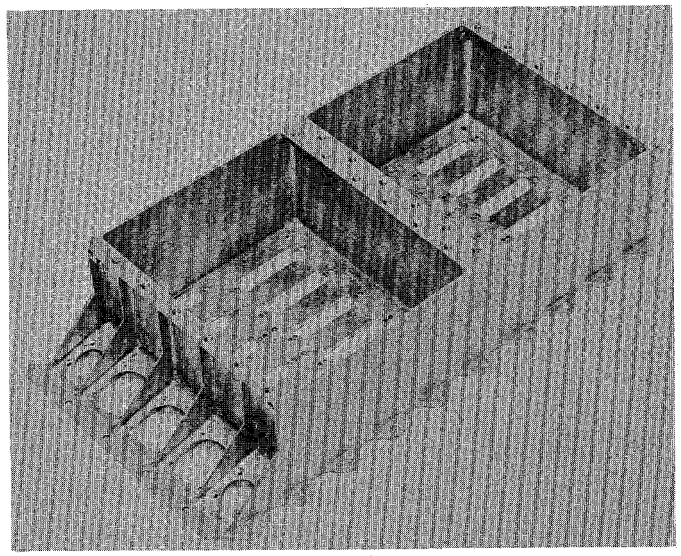

Fig. 16. Machined chassis

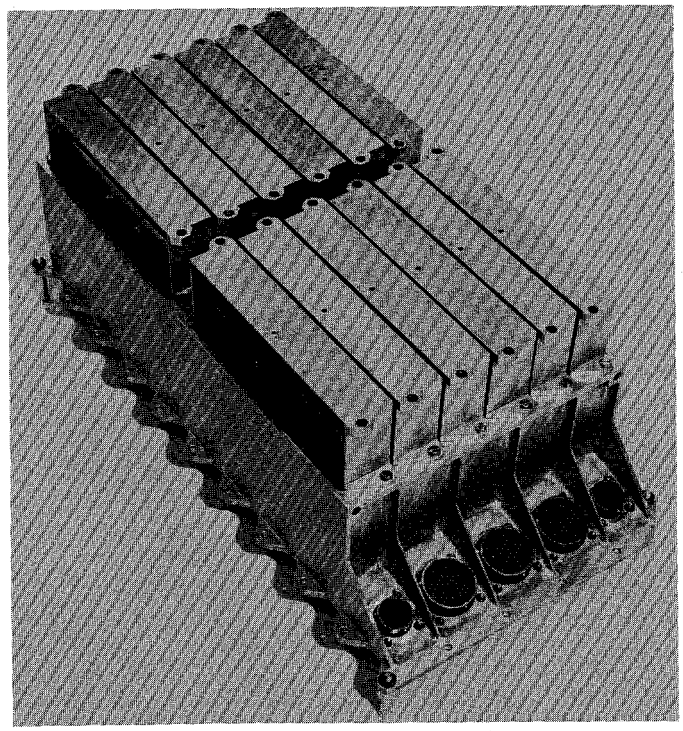

Fig. 17. Standard assembly dynamic mockup

tive to the Sun at Venus. The bus was held in this orientation for ½ hr, then turned back to normal orientation at the same rate. In the 90-deg position, one bay was considered normal to the Sun's rays, with an insulated PHP bay being on the dark side as shown in Fig. 19. No transverse conduction was assumed. This configuration gives the worst possible heating condition.

Starting at 540°R (80°F), the bays reached the following temperatures at the time the turn back was started: Bay A, 562°R; Bay B, 585°R; Bay C, 562°R; Bay D, 545°R; Bay E, 545°R; Bay F, 560°R (average of all other temperatures).

Using the results of the above analysis and estimates of the uncertainties in overall bus temperature due to variations in surface properties, it was determined that the servo heater control capability of the gyros is inadequate to accommodate the temperature variation in the bay facing the Sun, but that it would be adequate in the shade. Consequently, the bay containing the guidance package will be kept on the dark side during all maneuvers. Since this can be accomplished by a pitch turn

UNCLASSIFIED

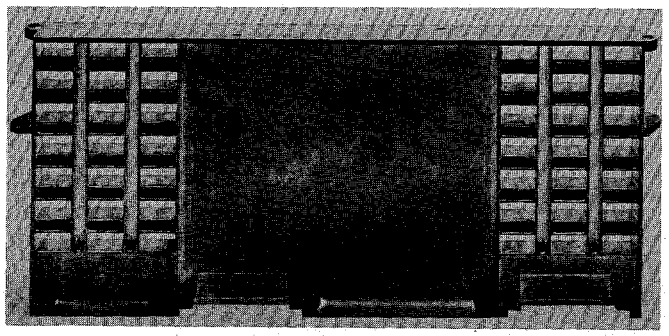

Fig. 18. Command output CC&S subchassis

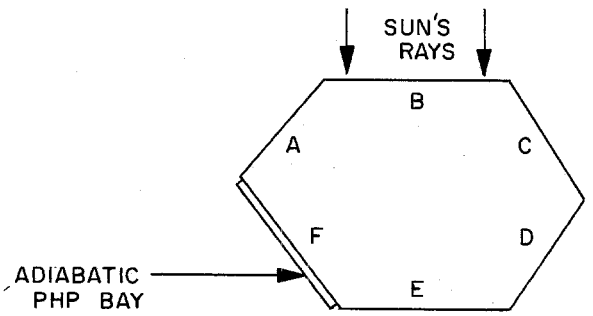

Fig. 19. Extreme heating condition of bus

or a yaw turn, the choice of type of turn will be made on the basis of providing the maximum thermal protection for critical components. It is presently felt that no other subsystems of the spacecraft will experience any difficulties due to the maximum temperatures indicated, but detailed analysis is underway to make sure.

The problem of aerodynamic heating is currently being investigated, both in relation to shroud ejection and parking orbit altitude. The significant parameter is $A/(W\,cp)$; where A = area normal to velocity vector in ft², W = weight of component in lb, cp = specific heat of component in Btu/lb °F. In general, if the value of this parameter is below 1 there is no problem with current trajectories. To date, only one component appears to have a higher value: space science Unit 29, which has a detector with $A/(W\,cp) = 9.26$. Efforts are being made to lower the value of the parameter for this detector.

b. PHP. The Venus 1964 mission has been cancelled. Consequently, the temperature control work to date on the Venus PHP is being summarized. Two configurations have been considered: Configuration 1 is the *Mariner* A configuration; Configuration 2 is new. The major problem in both configurations is overheating of the horizon scanner. In general, the horizon scanner should be on the shady side of the PHP. Configuration 2 is better because it provides more shade. However, in any configuration, the Sun shines on the germanium window of the horizon scanner at planet acquisition. This causes the window to exceed the 50°C limit for the instrument. This is an unresolved problem. The UV spectrometer temperature requirements have been relaxed. Thus, it might now be possible to control it passively. The microwave radiometer would be controlled passively.

For the Mars mission, some analysis has been done on the high-resolution vidicon and on the infra-red spectrometer. The vidicon as a whole cannot be kept warm, so the approach will be to keep only the electronics warm, allowing the optics to be colder. The infra-red spectrometer is a difficult temperature control problem because the minimum allowable temperature for some components is above the maximum allowable temperature for nearby components within the instrument. Temperature control inputs are influencing the internal design of the instrument. For the cruise mode on the Mars mission, some sort of cover over the PHP, electric power, or some method of controlled heat inputs to the instruments is required.

A tentative list of desired temperature limits has been acquired and is included as Table 1.

5. Materials

a. 4-ft high-gain antenna. Since the last reporting period, the resin bonded honeycomb sandwich approach has been further examined because of its attractiveness from the fabrication and weight standpoints. Brazed honeycomb sandwich fabrication for either all or part of the dish has been eliminated because of the extreme difficulty involved which is inconsistent with existing fabrication schedules. The explosive-formed chem-milled sheet approach for the dish looks less attractive at the present time because of unknown fabrication distortions.

Considering the resin bonded honeycomb sandwich construction, some of the fabrication techniques being evaluated are:

Front face

(1) 0.001-in. continuous sheet aluminum foil reflector bonded to 0.005-in. fiberglass.

(2) 0.002- to 0.004-in. continuous sheet aluminum foil reflector.

(3) Aluminum vapor plated reflector deposited on 0.005-in. fiberglass.

Table 1. Desired temperature limits

Component	Minimum temperature, °C	Maximum temperature, °C	Notes	Component	Minimum temperature, °C	Maximum temperature, °C	Notes
Data encoder	−10	75		Unit 21	−40	50	
RF system	−10	75		Unit 24	−40	90	
Command system	−10	75		Unit 25	−20	100	
Ranging	−10	75		Unit 26	−65	200	
Power conversion system	−10	75		Unit 27	−20	55	
				Unit 28	−30	65	
Battery	4	48		Unit 29	−30	65	
CC&S	−10	75		Unit 30	−30	65	
Control gyros	Indeterminate		Held ±0.7°C during maneuvers	Unit 32	−30	85	
				Unit 33	−73	85	
Planet approach scanner	Indeterminate		Held uniform within 7°C during guidance observation	Unit 36	0	50	Mars PHP
				Unit 37		−70	
Star tracker	Indeterminate		Held uniform within 7°C during cruise	Unit 41	−20	55	
				Actuators (antenna and PHP)	0	70	
Attitude control	−10	75					
Attitude control gas jets	−45	70		Mid-course motor	−18	74 (Catalyst bed)	
Solar panels	−100	230		Mid-course fuel tank	2	74	
Horizon scanner	−40	50					

Core

(1) Hexcel type.

(2) Multiwave type (consists of alternate strips of straight and sine wave ribbons).

Back face

(1) 0.002-in. aluminum foil.

(2) 0.005-in. fiberglass.

6. Mariner *B* Capsule

The study contract which has been let to the General Electric Company, Missile and Space Vehicle Division, is essentially complete. The final report is forthcoming and will be discussed in the next *SPS*. During the study period it became apparent that the *Nerv* vehicle was far enough below the desired performance level to discontinue any major efforts in that area. In the light of increasing performance, General Electric was asked to include in their study a brief investigation of two 37.5-in. D capsules. One of these maintained the standard *Discoverer* shape and the other was for an optimized shape.

To better understand the problems involved with parachute systems, an independent investigation separate from the above will be performed. It will concentrate on the optimization of a parachute system considering descent time, deployment altitude, parachute oscillation, weight, and impact velocity.

C. Guidance and Control

1. Power Subsystem Analysis

Basic aspects of the power subsystem operation have been previously described in *SPS 37-14*. A new power subsystem computer simulation program has been developed that is an improvement of the simulation programs described in that article.

The improved simulation program is designed to study the operation and interaction of the power subsystem elements. At present, it can be used for subsystems powered by photovoltaic solar-cell panels and batteries. With modifications, other power sources, such as fuel cells or thermionic diodes, can be studied.

Major uses of the simulation program include determination of and confirmation of the adequacy of solar panel, battery, and battery charger parameters, study of the effects of changes in the power distribution and regulation elements to improve overall efficiency, and

study of changes in control logic to improve efficiency and operation in abnormal modes. Inputs to the simulation program are:

(1) Time histories of the individual load demands (called power profiles).

(2) A description of the configuration and parameters of the power distribution and regulation elements.

(3) A description of the power switching and control logic.

(4) Solar panel parameters.

(5) Battery charger parameters.

(6) Battery parameters.

Outputs (as functions of time) include:

(1) Solar panel power output.

(2) Total raw power.

(3) Battery charger level.

(4) Solar panel voltage.

(5) Battery voltage.

The program divides the power subsystem into functional blocks that can be independently changed or modified. The block diagram is shown in Fig. 20; the blocks are described in the following paragraphs.

a. Solar radiation. The solar spectrum is constant. The radiation intensity L is given by

$$L = L_o (R_o^2/R^2)$$

where R is the Sun–probe distance and L_o is the radiation intensity at a distance R_o from the Sun.

b. Damage and degradation. Degradation is currently assumed to occur at a constant rate in time.

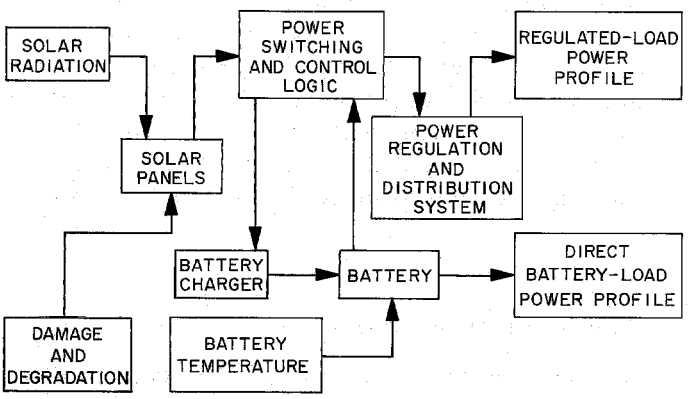

Fig. 20. Power subsystem simulation block diagram

c. Solar panels. Subsystems with 1 to 20 solar panels can be studied. The voltage–current relation for each solar panel has the functional form

$$E_p = A + B \log_e (I_s - I_p - YE_p) - rI_p$$

where E_p is the solar panel voltage, I_p is the solar panel current, Y and r are constants, A and B are functions of temperature, and I_s varies with degradation and radiation intensity. Figure 21 is typical of the voltage–current curve for a solar panel.

The solar panel temperature is related to the solar radiation intensity by the grey-body relation

$$T = (L/\sigma)^{1/4}$$

where T is the solar panel temperature in degrees Kelvin, L is the solar radiation intensity, and σ is a constant for a given solar panel.

d. Battery charger. The charger is considered to be a current limiter in series with a voltage regulator. This configuration prevents the battery from being charged too rapidly and prevents further charging when the battery voltage rises above a nominal maximum-charge value. The charger current is a function of the battery voltage and the charger input voltage (which is presently the solar panel voltage). Figure 22 illustrates the functional relation between charger current and battery voltage for two different input voltages: E_1 and E_2, where $E_1 > E_2$.

e. Battery. Charge and discharge voltage characteristics, internal discharge, and charge and discharge efficiencies are considered. The charge voltage characteristic depends on the charge level and maximum capacity of the battery. The discharge voltage characteristic depends on these factors and also on the discharge rate. Inter-

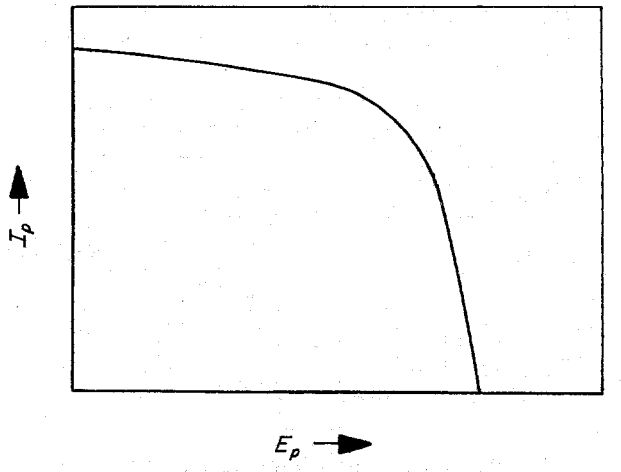

Fig. 21. Typical solar panel voltage curve

UNCLASSIFIED

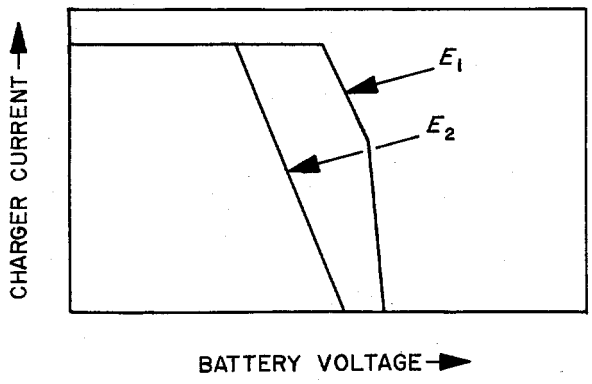

Fig. 22. Functional relation between charger current and battery voltage

nal discharge depends on the battery temperature. Charge and discharge efficiencies depend on the battery temperature and rate of charge or discharge. The maximum capacity of the battery depends on the battery temperature.

f. Battery temperature. The battery temperature depends on the solar radiation characteristics and power dissipation in electronic assemblies directly connected to the battery to provide a thermal balance among elements of the power subsystem.

g. Power switching and control logic. The logic determines the interaction of, and switching conditions for, the solar panels, battery charger, battery, and the power regulation and distribution elements. *SPS 37-14* describes the source and battery charger logic; load-control logic is still being designed.

h. Power regulation and distribution. The distribution is divided into blocks corresponding to functional units such as booster–regulators, inverters and transformers-rectifier (T-R) units. These blocks are connected together in a tree arrangement, such as the one shown in Fig. 23. The details of the arrangement are determined by input

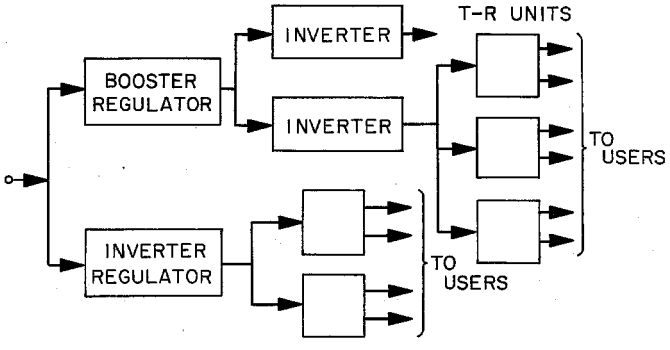

Fig. 23. Power regulation and distribution system block diagram

to the simulation program. The efficiency and voltage–power characteristics of these blocks are also described by input parameters.

i. Regulated-load and direct battery-load power profiles. Power profiles are determined from needs of the users. Although the profiles describe the outputs of the actual power system, the profiles serve as inputs for the simulation program.

The program computes the power at each branch of the tree, proceeding from the users to the power switching and control logic block. At this point, a computation is made of the coefficients of a quadratic relationship between input power and input voltage to the regulation and distribution elements. The exact values of input voltage and power are then determined from the voltage vs output-power relationship of the power source and the just-computed quadratic voltage vs input-power relation.

2. Planet Tracker Precision Actuator

In the *Mariner* B approach guidance sequence, it is required that angles between the target planet and two other celestial references be measured. This is accomplished by moving the optical axis of a sensor until a null is reached and then measuring the position of the actuator output shaft. Inside the actuator, an angle transducer is connected to the output shaft by means of a precision mechanical transmission.

A contract has been let to the United Shoe Machinery Corporation for the development of this precision actuator employing the harmonic drive concept.

The prime mover to be used in the actuator is a stepper motor, and the angle transducer is a digital shaft encoder. The stepper drives through a conventional spur gear train in series with the harmonic drive which gives the final reduction. The total reduction between the motor and output shaft is 12,960:1 with the harmonic drive being 180:1. The ratio between the encoder and output shaft is 675:1. For torque loads on the output shaft of ± 0.25 ft-lb, the maximum allowable error over a 40-deg range is ± 1 min of arc. For this same loading over any 5-deg range, the error cannot change more than 40 sec of arc.

3. Stepper Motor Evaluation

Each actuator for the antenna and PHP servos contains a stepper motor as prime mover, a gear train to increase its resolution and torque, and a readout device. A

UNCLASSIFIED

stepper motor evaluation program has been undertaken to select a suitable motor for the actuator.

Two types of steppers have been considered in this evaluation: variable reluctance and permanent magnet. In the variable reluctance motors, a rotor of soft magnetic material moves to reduce the reluctance of the magnetic circuit to a minimum. In order to make the rotor move to a new position, the magnetic field must be changed to a new orientation. The electronics containing the necessary logic circuitry rotate the field in such a manner as to impart an incremental rotation in a particular direction. In the variable reluctance steppers, there is a detent torque resisting motion away from the equilibrium position only when the meter is energized. When the meter is nonenergized, the rotor is free to turn and can stop in any position.

In contrast to the variable reluctance steppers, a permanent magnet motor contains a rotor made of a hard magnetic material. After the motor is assembled, the unit is magnetized and the rotor becomes a permanent magnet. Thus, whenever the stator is energized, the permanent magnet rotor aligns itself with the magnetic field produced. The electronic circuitry necessary to drive this type of motor is similar to that of the variable reluctance unit. By rotating the magnetic field in an incremental manner, the rotor will move in a corresponding manner. Because of the permanent magnet rotor, this motor has a detent torque in both the energized and nonenergized states. For the motors tested, the nonenergized detent torque is approximately 10% of that in the energized state. Because of this detent torque in the nonenergized mode, it was decided to use the permanent magnet type of motor in the actuators.

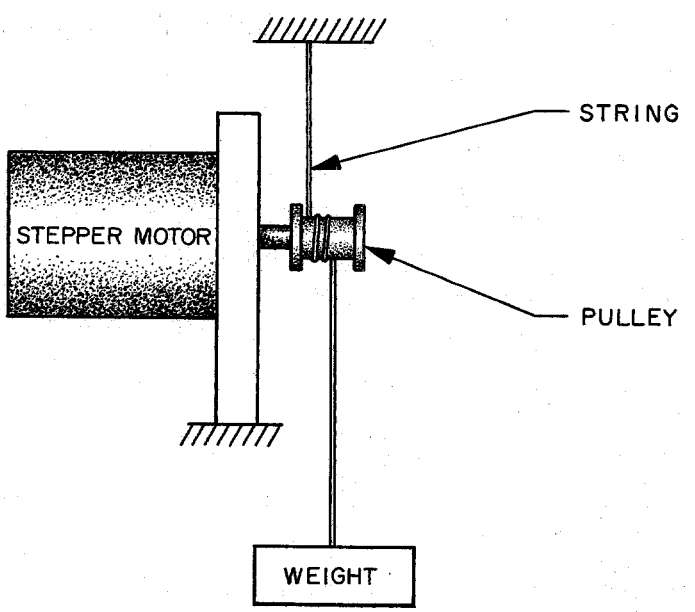

Fig. 24. Test setup for speed-torque tests

Most of the testing done, thus far, has been to determine the torque-stepping rate characteristic. A schematic of the test setup used is shown in Fig. 24. A string is wrapped around a pulley of known diameter. Weights are attached to one end of the string and the other end is held. When the friction of the pulley acting on the string is sufficient to support the weights without a force being required on the held end, the torque output of the motor can be determined. A typical plot of the test results for a Size 11 permanent magnet stepper is shown in Fig. 25. The running torque curve is obtained by slowly adding to the load with the motor running until it stalls. The starting torque is that load under which the motor is capable of starting from rest.

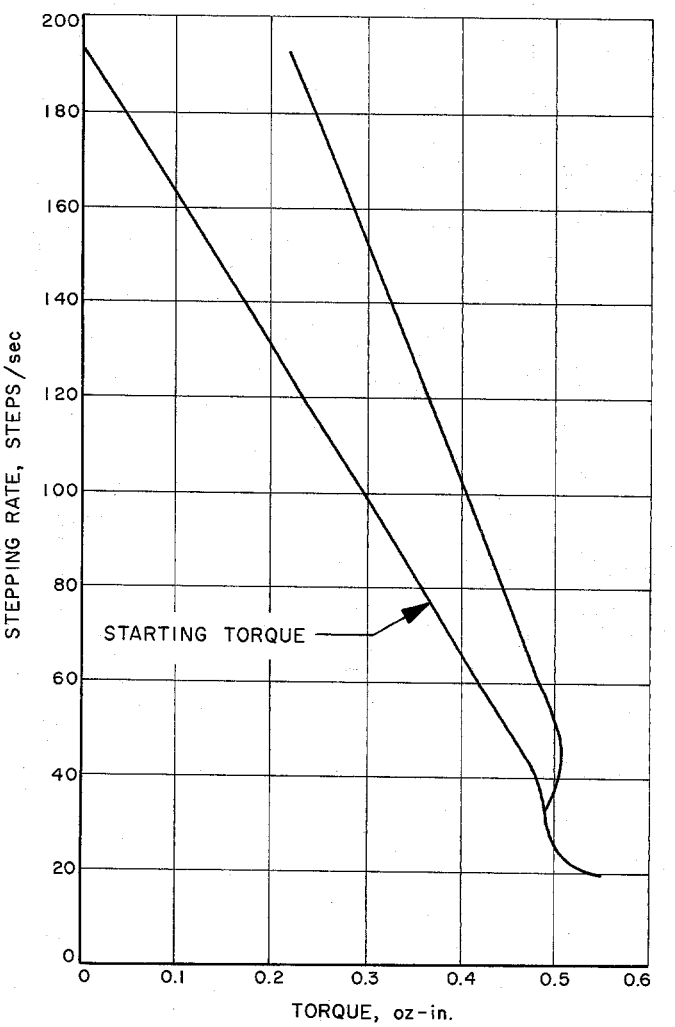

Fig. 25. Speed-torque curve for Size 11 permanent magnet stepper

UNCLASSIFIED

4. Central Computer and Sequencer (CC&S)

The *Mariner* B CC&S was designed to provide the type of timing and sequencing required by the *Mariner* A missions with an increase of storage and output capacity by 50% over the *Mariner* A CC&S and position programs for two antenna angles and the star sensor cone angle. The CC&S system, as mechanized, may be divided into six functional subsystems: (1) central clock; (2) memory; (3) input decoder; (4) actuator address decoder; (5) command output; (6) T-R and power logic. Fig. 26 is a block diagram of the CC&S system. The subsystem mechanization description follows.

a. Central clock subsystem. This CC&S subsystem consists of an oscillator with semiconductor and magnetic frequency dividers which provide precision timing refer-

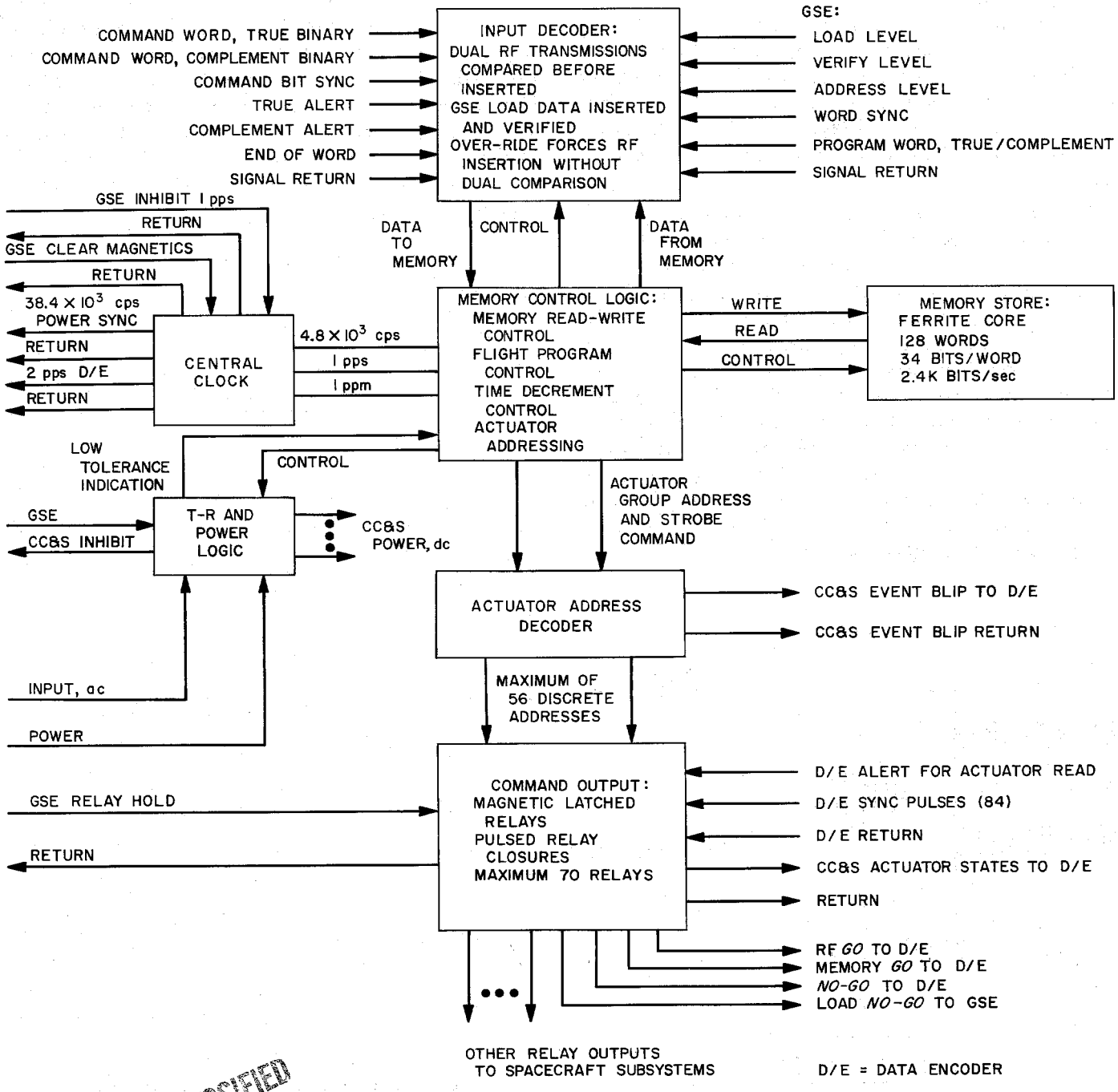

Fig. 26. *Mariner* B CC&S block diagram

UNCLASSIFIED

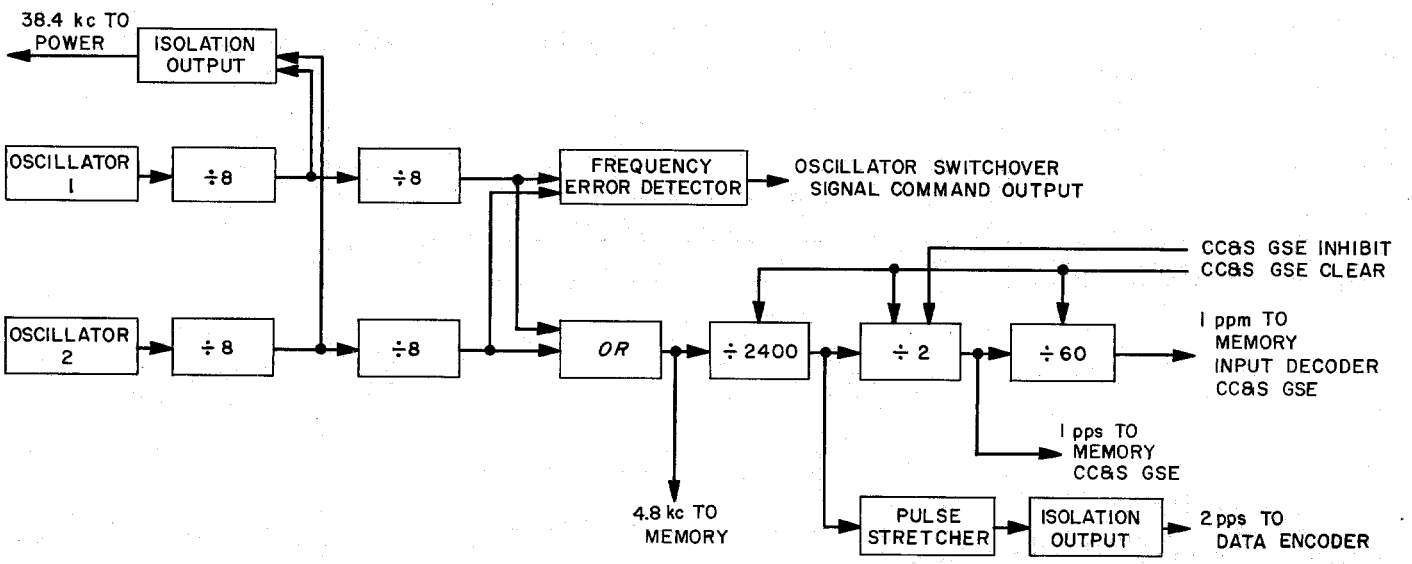

Fig. 27. Central clock system

ences to other spacecraft systems as well as CC&S subsystems. The oscillator and semiconductor frequency dividers are redundant. Figure 27 is a block diagram of the central clock.

The crystal-controlled oscillator, which is the heart of the central clock subsystem, has a nominal frequency of 307.200 kc +0.001% at 25°C. The frequency with temperature deviations from nominal are within the ranges of −0.012% at −10°C, +0.005% at +35°C, and −0.01% at +85°C. References of 38.4 kc and 2 pps are provided to other spacecraft subsystems while references of 4.8 kc, 1 pps, and 1 ppm are used by CC&S subsystems.

b. Memory subsystem. This CC&S subsystem consists of a ferrite-core memory store and semiconductor control logic. The memory store was designed to contain 128 words of 34 bits each. The store has random word selection with bit sequential readout of each word. The bit cycle rate is 2400 bits/sec. The design and fabrication of the memory store is subcontracted to Electronic Memories, Inc., Los Angeles. Figure 28 is a block diagram of the entire memory subsystem.

The CC&S control logic normally scans the memory at 1-min intervals. In general, the time portion of a word is decremented by one count during each of these 1-min scan intervals. By special programming, however, decrement intervals of 1 sec and longer than 1 min, such as 1 day, are made possible. If, during any scan, the portion of a word is decremented to zero remainder, the actuators associated with that particular word are initiated. The program portion of each word determines the decrement interval and the effects that actuation of a word has on other words, such as generation of cyclics and initiation of sequences. The memory word program and times will be loaded into the CC&S just prior to launch. The event time portion and some program portions of each word will be available for RF modification in flight.

Figures 29, 30, and 31 illustrate the type of event timing and sequencing that the memory subsystem is capable of providing. The memory subsystem also furnishes the position programs for the antenna and the star sensor. These position programs are designed to provide a linear approximation of the positions of two antenna axes and one star sensor axis. The CC&S memory capacity has been designed to provide no more than a total of 30 linear slope segments. The CC&S controls the direction of motion and the rate of decremental change of each axis as an open loop system. A typical single-axis program is illustrated in Fig. 32.

c. Input decoder. This CC&S subsystem consists of semiconductor logic whose function is to receive both the ground loaded CC&S flight sequence and any inflight RF modification for insertion into the CC&S memory. Figure 33 is a block diagram of the input decoder.

The CC&S ground support equipment (GSE) inserts the CC&S flight sequence just prior to launch. This program consists of 256 words of 34 bits each which are loaded at a nominal 300 bit/sec rate. Each word consists of a true and a complement binary section. The input decoder inserts the true binary word in the memory and then takes the complement binary word, inverts this word,

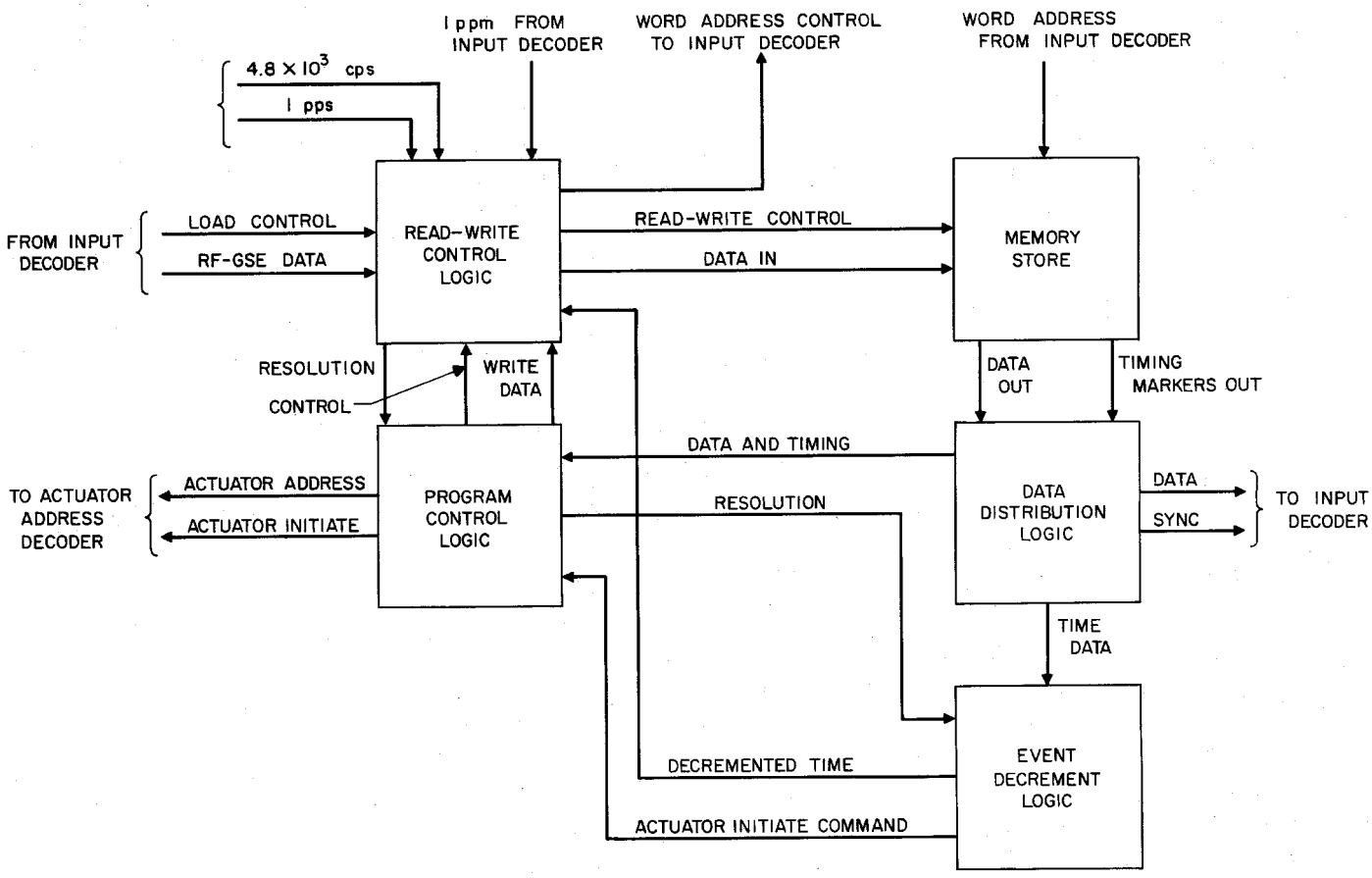

Fig. 28. Memory subsystem

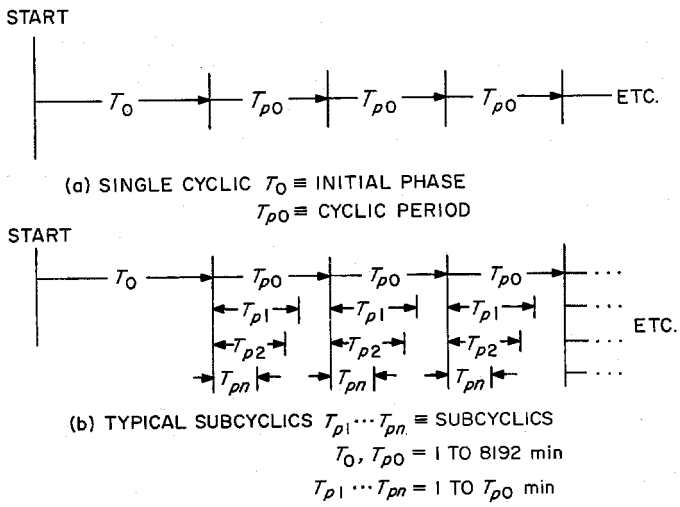

Fig. 29. Memory subsystem event timing and sequencing

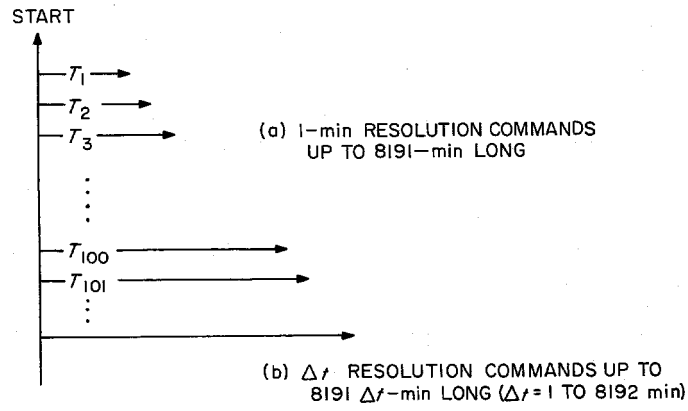

Fig. 30. Memory subsystem event timing and sequencing

and compares it with the stored true binary equivalent. The input decoder provides a *go* or *no-go* signal to the GSE to verify that any individual program word has been properly stored.

The input decoder receives from the spacecraft command decoder (C/D) any required inflight modifications to the CC&S flight sequence. Each C/D word to the input decoder consists of a true binary and a complement binary section. The input decoder receives the true binary word and compares this with the inverted complement word before insertion into the memory. If the comparison

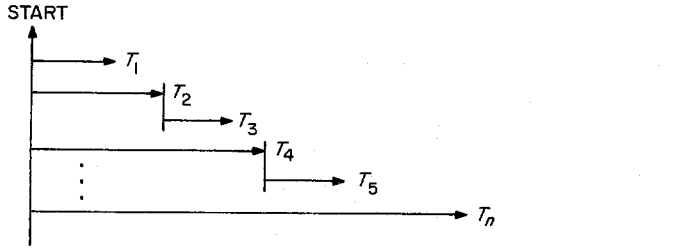

(a) SEQUENCE UP TO 8191-min LONG WITH 1-min RESOLUTION COMMANDS EXCEPT FOR T_3 AND T_5 WHICH HAVE 1-sec RESOLUTION AND UP TO 8191-sec DURATION

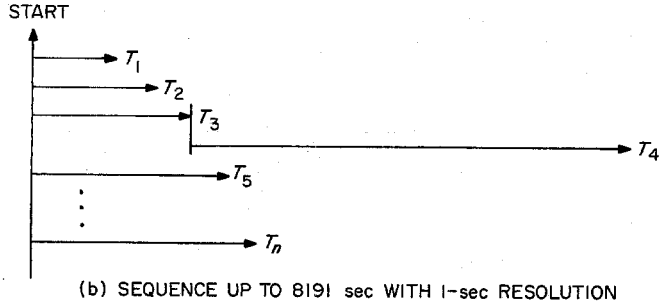

(b) SEQUENCE UP TO 8191 sec WITH 1-sec RESOLUTION COMMANDS EXCEPT FOR T_4 WHICH HAS 1-min RESOLUTION AND UP TO 8191-min DURATION

Fig. 31. Memory subsystem event timing and sequencing

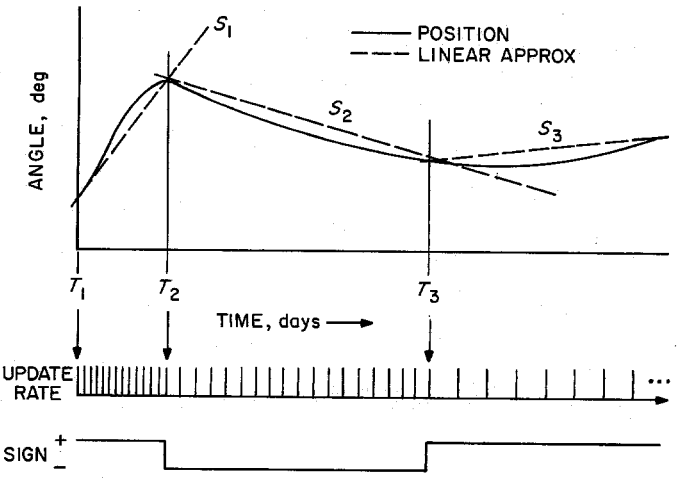

SLOPE BREAKPOINT TIMES $T_1 \cdots T_n$ MAY HAVE Δt RESOLUTION AND UP TO 512 Δt-min DURATION
UPDATE CYCLIC RATES MAY VARY FROM 1 TO 2048 Δt min ($\Delta t = 1, 2, \cdots 8192$ min)

Fig. 32. Typical single-axis program

is satisfactory, the input decoder waits until the memory has completed any existing operations (a maximum time of 1 min) and then inserts the word. The inserted word is then immediately compared with the true binary word still stored by the input decoder to verify proper memory storage. *Nothing* is inserted if the original comparison fails. The input decoder provides signals of *no-go*, RF-*go*, or memory-*go* to telemetry to indicate the insertion or transfer status of each RF command to the CC&S. For back-up, a special over-ride command exists from the C/D which forces the input decoder to store without verification either the true binary word directly, or the complement binary word after an interval inversion.

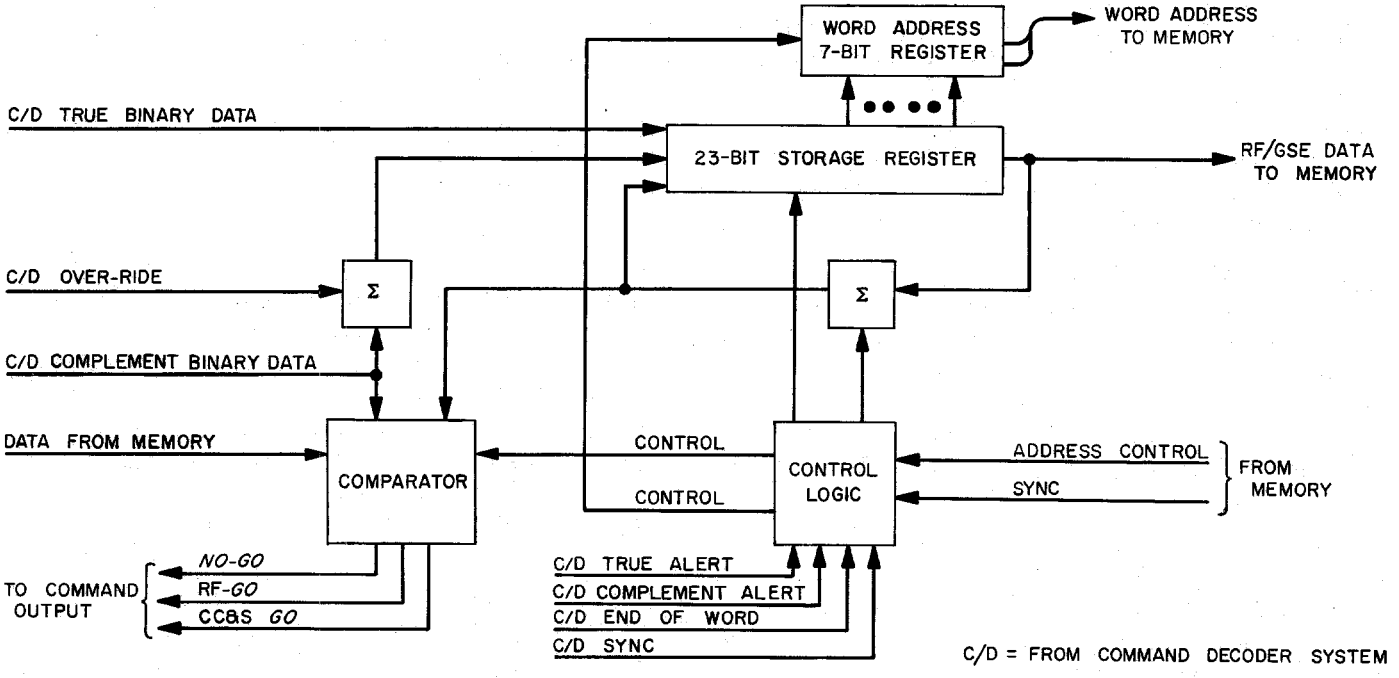

Fig. 33. Input decoder subsystem

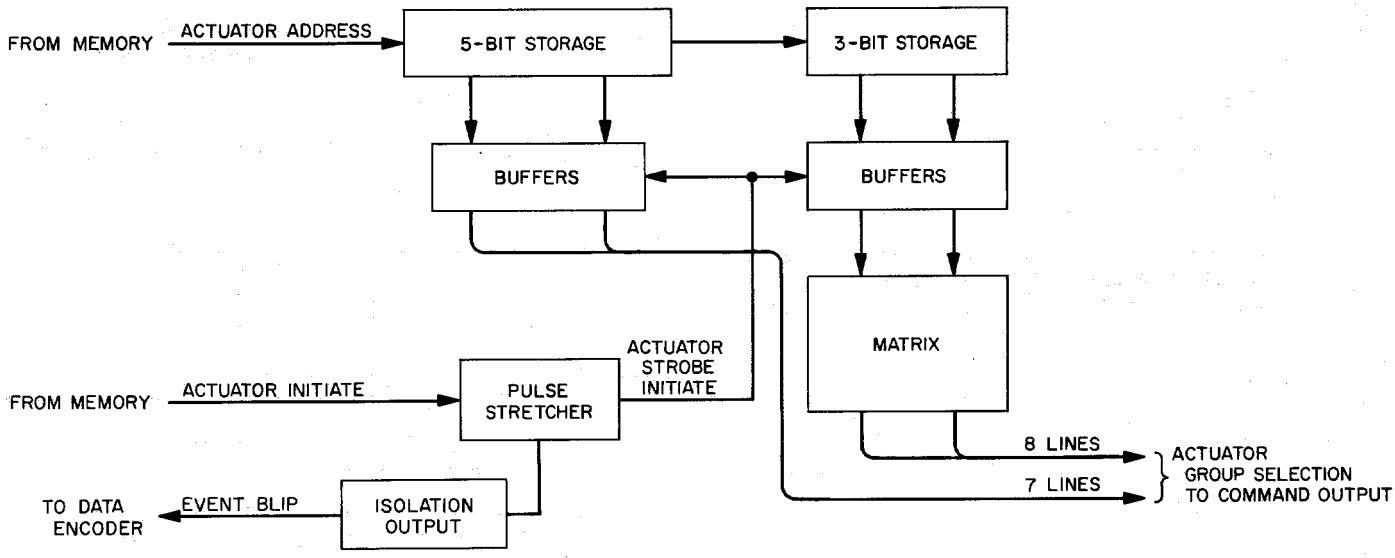

Fig. 34. Actuator address decoder subsystem

d. Actuator address decoder. This CC&S subsystem consists of semiconductor decoding circuitry which, when addressed and commanded by the memory subsystem, selects and actuates a fixed group of actuators in the command output subsystem. Figure 34 is a block diagram of the actuator address decoder.

The actuator address decoder can decode a maximum of 56 separate fixed groups of actuators. Any single actuator which appears for two or more CC&S event commands requires a separate address. Since a number of multiple event actuators are anticipated, CC&S personnel have restricted the number of CC&S event time and cyclic commands to a maximum of 40, so that as many as 16 addresses will remain available for multi-event actuators. The only spacecraft output of this subsystem is the CC&S event blip to the data encoder for event telemetry each time the CC&S issues an event command.

e. Command output. This CC&S subsystem consists of relay output actuators and their associated drivers which are controlled by the actuator address decoder subsystem. In addition, this subsystem also contains an actuator state monitor which, upon command from the data encoder, provides the state of all CC&S relay actuators for telemetry. Figure 35 is a block diagram of the command output subsystem.

A maximum of 70 relay actuator outputs is provided by the command output subsystem. These actuations are of two types: (1) pulsed contact closures for a duration of 30±15 ms, and (2) latched contact closures reset only by a later event command. A maximum of five relays may be energized at any event command. The grouping of relays to be energized at any event command is wired and not variable by program.

The actuator monitor portion of the command output subsystem consists of an 80-position magnetic stepping switch and 80 bits of core storage. Each of 70 bits of core storage is controlled by the contact position of its associated relay. Ten bits of storage are utilized as frame markers. When an alert or read command and a serial pulse train is received from the spacecraft data encoder system, the magnetic stepping switch sequentially samples each of the 80 storage cores which provide a "1" or "0" output indicating the state of the associated actuator. The data encoder readout interval must be smaller than the cyclic rate of any actuator or data will be lost, since a single storage core will only record one switching between readout intervals.

f. T-R and power logic. This CC&S subsystem contains the transformers, rectifiers, filters, power storage, and tolerance monitoring circuitry necessary to supply dc power to CC&S subsystems and to protect these subsystems from primary power dropouts. Approximately 15 w for 1 ms of capacitive storage is provided. This storage enables the memory subsystem to complete any single bit storage cycle after the voltage tolerance detector indicates a 20% (or higher) reduction of primary power voltage. The tolerance monitor logic then holds inhibited all CC&S subsystems until primary power again reaches the safe operating level. Figure 36 is a block diagram of the T-R and power logic.

The T-R and power logic subsystem receives 2.4-kc square wave power of 50 v rms from the spacecraft

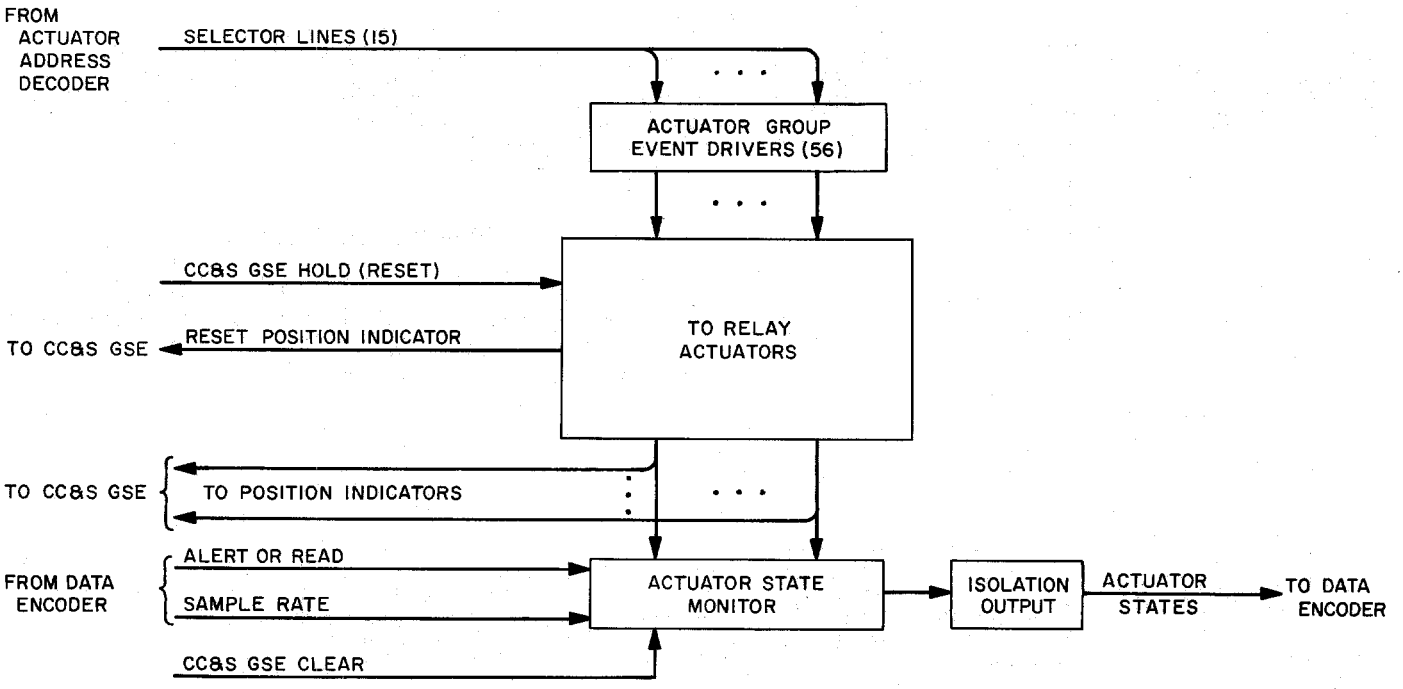

Fig. 35. Command output subsystem

power system. Estimated as of April 9, 1962, the total CC&S input power will be 20.6 w ±10% distributed as follows:

Subsystem	3 v dc	−3 v dc	15 v dc	28 v dc	Conversion loss
Central clock	—	0.006 w	0.275 w	0.46 w	—
Memory	5.25 w	0.1 w	3.1 w	0.4 w	—
Input decoder	1.64 w	0.06 w	2.26 w	—	—
Actuator address	—	0.1 w	0.945 w	0.095 w	—
Command output	—	—	—	—	—
T-R power logic	—	—	0.39 w	0.06 w	5.5 w

The actuator address decoder and command output subsystems require strobed power turn-on when a fixed group of relay actuators are being energized. This power is taken from separate 15 v dc and 28 v dc sources for 30 ms and requires 1.2 w plus 0.7 w per relay energized. No storage for this strobed energy is provided by the CC&S so that the load will be reflected back into the spacecraft power source.

g. Components. With the exception of a few specialized component types, the components used in the CC&S system are qualified either to *Minuteman* reliability specifications or to other high-reliability requirements specified by JPL. The memory and input decoder subsystems consist mainly of Fairchild micrologic elements designed for direct-coupled transistor logic applications. Each micrologic element contains multiple transistors and resistors diffused in a single silicon chip placed in an eight-lead TO-5 transistor can. The Fairchild manufacturing processes are very similar to the high-reliability planar transistor series. CC&S personnel have also written high-reliability specifications for each of the micrologic elements utilized. The component requirements for the CC&S per system are approximately 1400 resistors, 1000 logic diodes, 400 micrologic elements, 200 dual transistor elements, 200 glass capacitors, 100 transistors, 100 tantalum capacitors, and 5000 magnetic cores. Also, present plans are to substitute Elco Varicon hermaphroditic connectors for the Cannon D connectors.

h. Packaging. A subassembly chassis of the approximate envelope 1 × 6 × 14 in. is the foundation on which the CC&S volume allocations and packaging studies have been based.

The current best estimate is that the CC&S will comprise seven subassembly chassis as follows:

(1) Central clock and memory store.

(2) Memory control 1.

(3) Memory control 2.

(4) Input decoder.

(5) Command output 1.

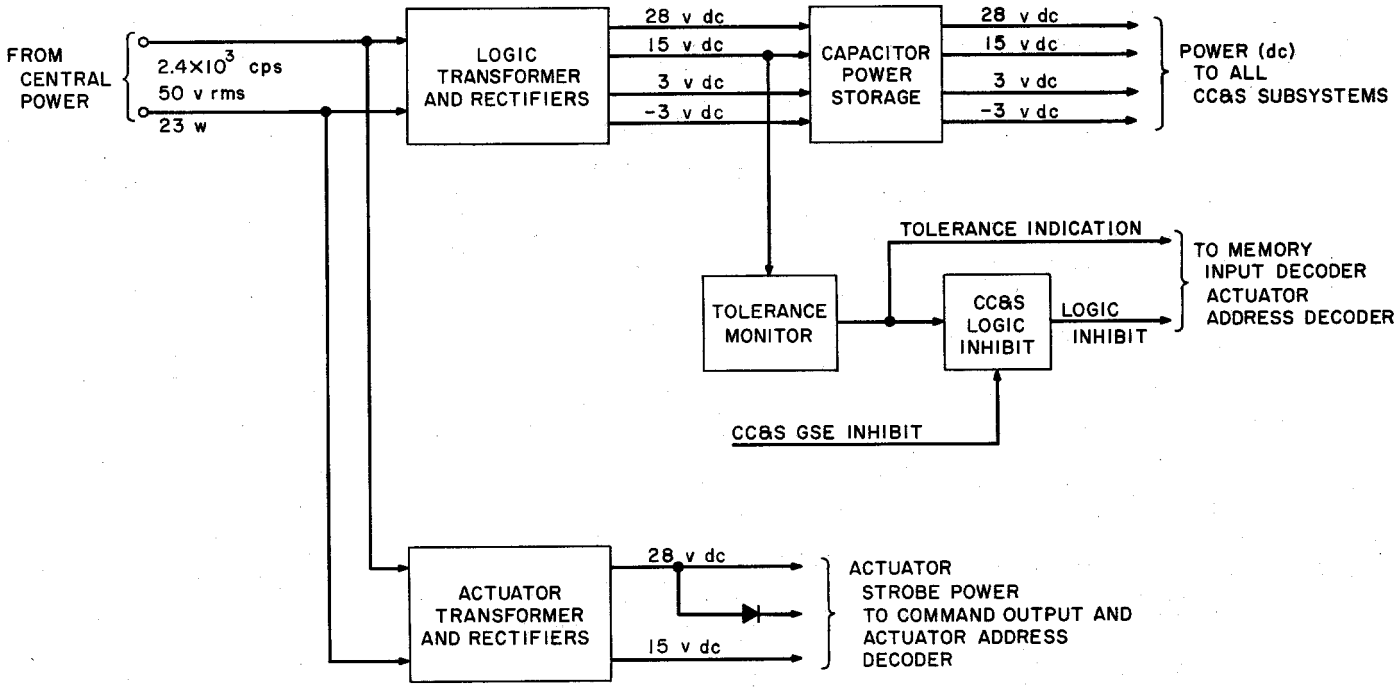

Fig. 36. T-R and power logic

(6) Command output 2.

(7) T-R, power logic and actuator address decoder.

i. Weight. As of April 9, 1962 the CC&S weight estimate is 30 lb ±10%.

j. Ground support equipment (GSE). The CC&S GSE provides the support equipment required to control CC&S pre-launch operations as well as all system test and laboratory test operations. The pre-launch or blockhouse GSE contains photoreader insertion equipment to load the CC&S flight sequence as described under the input decoder subsystem. The blockhouse GSE also contains the necessary pre-launch inhibit and operational controls required by the CC&S. The system test GSE contains the blockhouse functions but is expanded to include: (1) actuator state display; (2) time display; (3) manual control of CC&S actuators in event command groups; (4) manual access to and from the CC&S memory store.

The CC&S laboratory test GSE contains the system test functions expanded into a data processing system which includes Astrodata Corp. buffer equipment and a 160A computer from Control Data Corp. The 160A computer will be programmed to provide all diagnostic programs for CC&S test operations. In addition, the 160A will, when combined with the Astrodata buffers and the system test GSE, provide automatic sequencing and diagnostic monitoring of the entire CC&S system through simulated missions. Failure of the CC&S to perform any required flight sequence operation will result in typewriter printout of the failure at time of occurrence.

k. Present status. CC&S subsystem breadboard fabrication is complete, with the exception of actuator and harness wiring. Fabrication of subsystem test equipment is also complete. Functional and temperature tests on the subsystem level are progressing satisfactorily to meet the scheduled CC&S system integration on July 1, 1962. The CC&S memory subsystem control logic is shown in the photographs of Figs. 37 and 38. Figure 38 is a close-up of a section of the Fairchild micrologic utilized in the control logic. The memory subsystem tester is shown in the photograph of Fig. 39. This test equipment will also test the input decoder–memory combination.

An evaluation program for the 1 × 6-× 14-in. subassembly chassis is presently underway. Indications are that structural resonances at low vibration frequencies may possibly cause some problems. A command output chassis has been fabricated containing 36 relays and is presently being evaluated under the required shake and shock environments. In addition, a thermal test module representing the high density micrologic packaging is being fabricated to determine temperature conditions that will exist in the proposed flight package.

The design of the blockhouse GSE is nearing completion and design of the system test GSE is in process. The first 160A computer has been received, and program-

ming of the GSE data processing system has commenced. Integration of the CC&S with the GSE data processing system is scheduled for July 15, 1962.

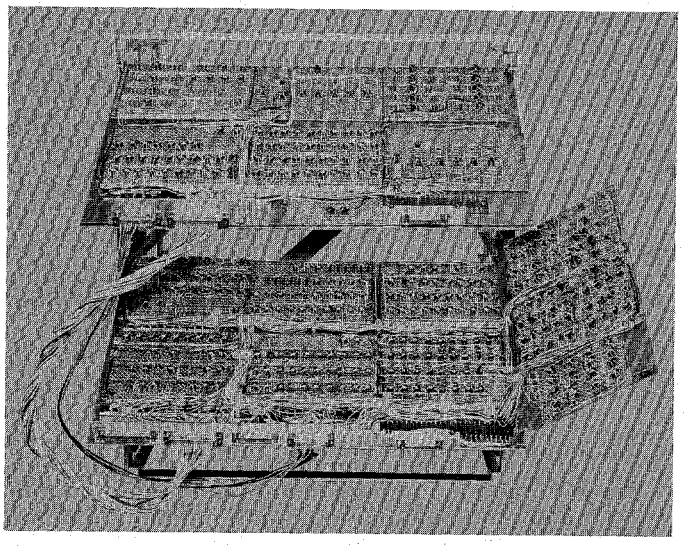

Fig. 37. Memory subsystem control logic

The first CC&S ferrite core memory is slightly ahead of schedule and is due for delivery to JPL on April 27, 1962.

5. Spacecraft Electrical Power

a. Subsystem design. The *Mariner* B power subsystem design has been revised somewhat from the description presented in *SPS 37-14*. The block diagram (Fig. 40) has been revised to incorporate the following additional items:

(1) A second booster–regulator and 2400-cps inverter.

(2) A separate 400-cps inverter to provide single-phase output.

(3) A separate energy source to operate the pyrotechnic subsystem.

(4) Capsule power system.

The estimated power requirements for the *Mariner* B system have also been revised from those described in

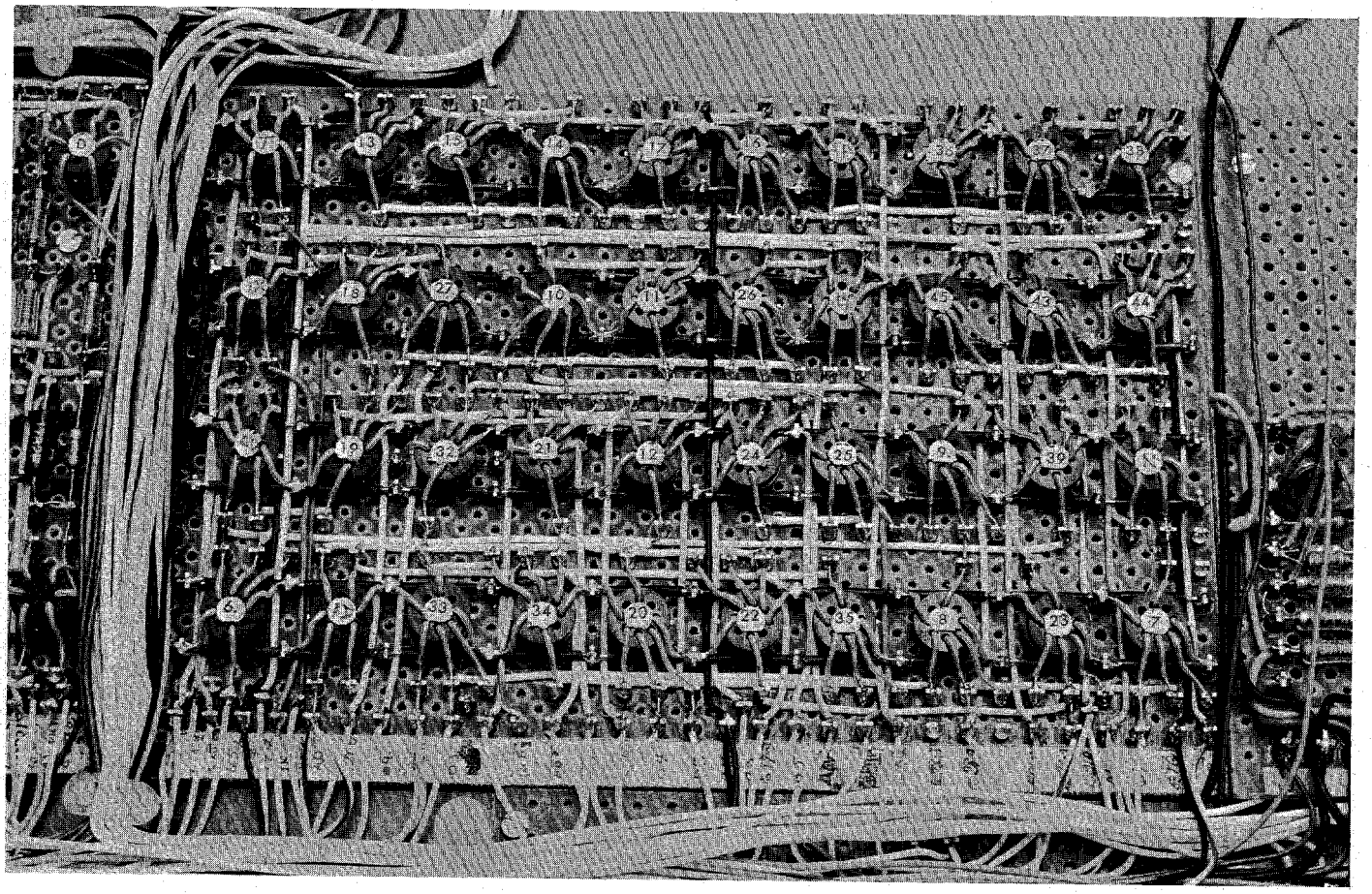

Fig. 38. Memory subsystem control logic detail

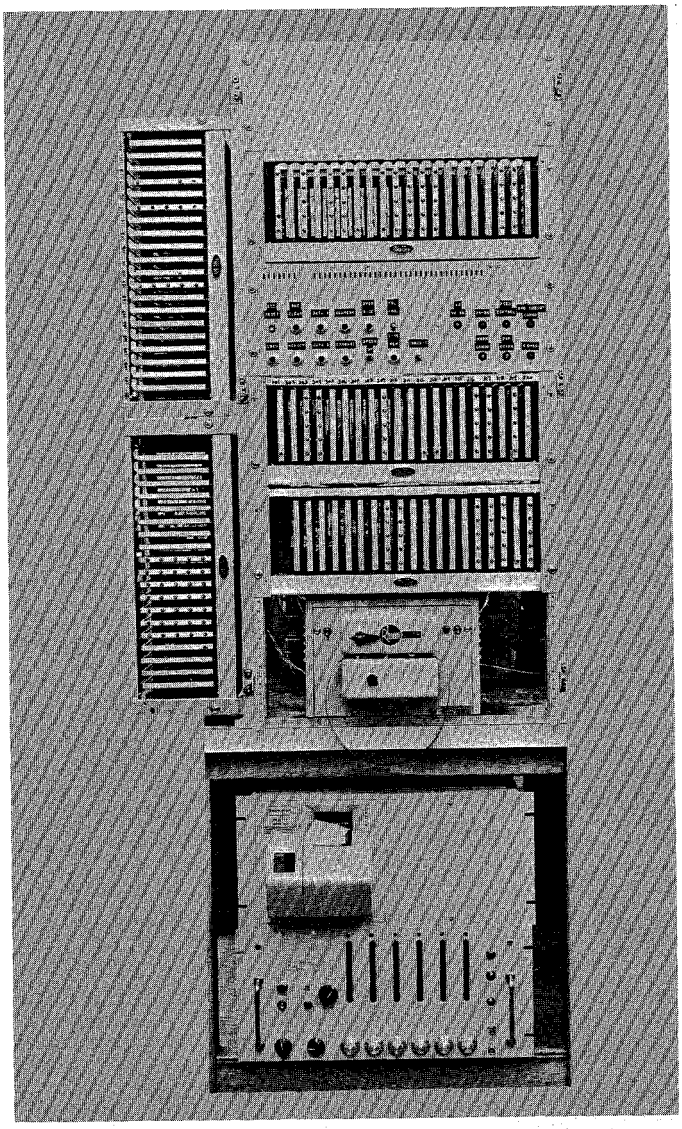

Fig. 39. Memory subsystem tester

SPS 37-14 and are presented in a condensed form in Table 2. These values can not be considered final, since they exceed the power capability of the solar panels. The 2400-cps power required dictates the use of two booster–regulator/inverter sets rather than one large unit with the associated large heat dissipation. The single-phase 400-cps load requirement is large enough to require a separate supply rather than providing one 400-cps unit with both three-phase and single-phase modes of operation. A separate energy device to supply the pyrotechnic system is presently planned as a result of the following two requirements. The peak current required to support the capsule release pyrotechnic event is presently estimated to range from approximately 70 to 100 amp. This peak current capability would be an excessive requirement from the standpoint of efficient design for the main spacecraft battery. Ground currents can result from a short between a squib current and the metal housing (spacecraft frame). To prevent this ground loop current from affecting spacecraft electrical operation the pyrotechnic system will be electrically isolated from the bus electrical power system by the use of a separate energy source. The capsule power system has been added in order to effect better control of the design interface problems.

b. Power conversion equipment. The *Mariner* B electrical conversion equipment (Table 3) will consist of 11 modules. These will be divided between two cases for mounting in the spacecraft. The following list and estimated sizes are based on the following assumptions:

Table 3. Electrical conversion equipment

Module	Estimated weight, lb
PS&L	6.0
Booster–regulator 1	3.8
Booster–regulator 2	3.8
2400-cps Inverter 1	1.8
2400-cps Inverter 2	1.8
Power sync supply	1.7
400-cps (3-phase) inverter	5.0
400-cps (single-phase) inverter	4.0
Communications regulator converter	9.0
Battery charger	2.0
Power monitor logic	2.0
Est. totals	40.9

Table 2. *Mariner* B estimated power requirements (watts)

Power subsystem	Flight phase					
	Launch	Acquisition	Cruise	Maneuver	Guidance observation	Encounter
2400-cps output power	129.2	181.2	165.2	201.2	166.2	207.2
400-cps output power (single-phase)	12.0	7.0	8.0	7.0	8.0	18.5
400-cps output power (3-phase)	28.0	28.0	—	28.0	—	—
Communications regulator–converter output power	50	50	50	50	—	50

UNCLASSIFIED [redacted]

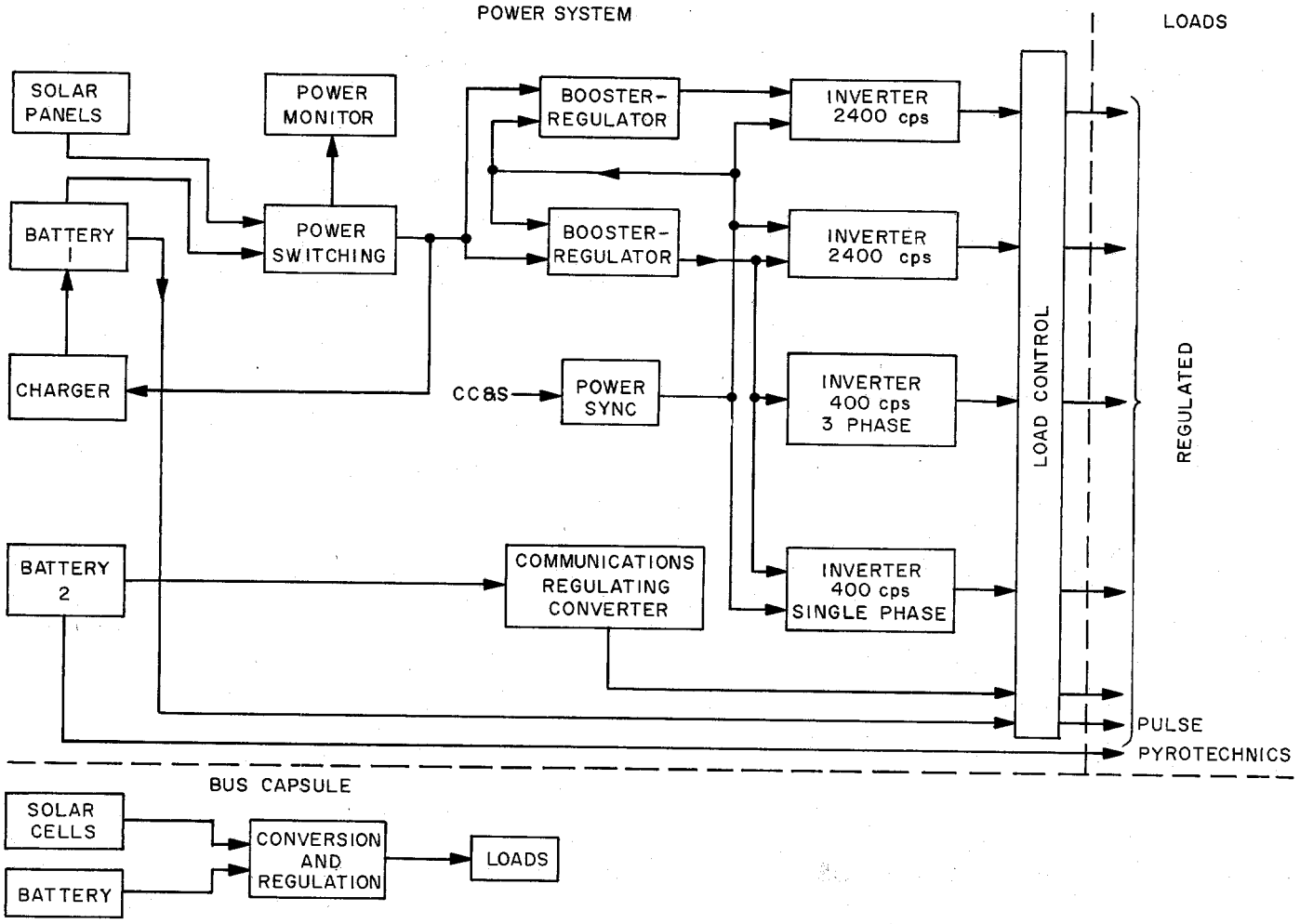

Fig. 40. *Mariner* B power subsystem block diagram

(1) The use of a stepped square wave for the 3-phase, 400-cps output.

(2) A dc to dc regulating converter for the communications transponder system.

(3) Pyrotechnics control to be handled by another division.

(4) The use of *Mariner* A and R designs, with minor revisions, for the first six items.

These estimated figures will change if any of these assumptions are revised.

A breadboard model of the 400-cps, 3-phase power amplifier has been completed and partially tested using resistive load simulation. Experimental data has been obtained showing output voltage regulation and efficiency vs output power at various output levels and with resistive loads (Table 4).

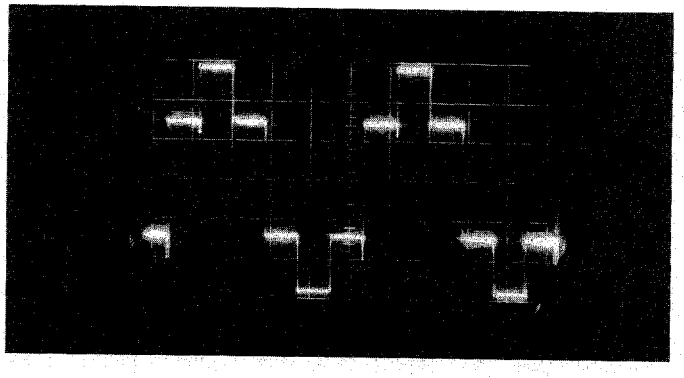

Fig. 41. Voltage waveforms at the output

The 400-cps power amplifier was designed with the intent to supply the gyro and motor loads with 3-phase and single-phase ac power, respectively. The power amplifier provides this ac output power in the form of a "Quasi" or "Stepped" square wave voltage to approximate that of a sinusoidal voltage waveform (Fig. 41).

UNCLASSIFIED

UNCLASSIFIED [redacted]

Table 4. Test results showing efficiency and regulation

E_{cc}, v dc	I_{in}, amp (avg.)	E_{out}, v rms			I_{out}, amp rms			R_L[a], ohms	P_{in}[a], w	P_{out}[a], w	Efficiency[a], %
		Phase A	Phase B	Phase C	Phase A	Phase B	Phase C				
52	0.041	19.50	19.55	19.55	0	0	0	00	2.13	0	0
52	0.40	18.70	18.70	18.80	0.304	0.302	0.306	60	20.8	17.1	82.2
52	0.46	18.60	18.55	18.65	0.359	0.359	0.360	50	23.9	20.3	85.0
52	0.565	18.75	18.75	18.85	0.445	0.444	0.442	40	29.4	25.0	85.1
52	0.71	17.95	18.05	18.10	0.575	0.576	0.580	30	36.9	31.2	84.6
52	0.837	17.75	17.90	17.95	0.682	0.681	0.689	25	43.5	36.7	84.4
52	0.968	17.35	17.40	17.55	0.792	0.791	0.793	21	50.4	41.4	82.1

[a]Test conditions are for three-phase operation, load (R_L) connected in wye-formation.

In this approach, the even harmonics as well as the third, ninth, fifteenth, etc. are eliminated. Recent tests have indicated that the gyro motor loads can operate from such a waveform without difficulty. The advantages of using such an output are reduction in the unit size and weight resulting from the elimination of filter components.

D. Space Sciences

1. Television Subsystem Optics

There will be two cameras in the *Mariner* B television subsystem: one for the purpose of obtaining high-resolution photographs of the Martian surface (Camera A), and another having a wider field of view for obtaining colorimetric information from the planet and its atmosphere (Camera B). (A discussion of the intended use of the *Mariner* B television subsystem and some of the characteristics of the vidicon television pickup tube was presented in *SPS 37-14*.)

a. Optical systems. The optical system for Camera A will be of standard Cassegrain telescope design. It is planned that the equivalent focal length of this camera will be 100 cm with an effective focal ratio, after accounting for the secondary mirror occultation, of f 5.1. Because of the uncertainties in exposure levels that will be required by the vidicon tube (sensitivity of the tubes is not yet firmly established) as well as the amount of exposure time that can be tolerated due to vibrations of the planetary horizontal platform (PHP), two optional focal lengths, 65 and 200 cm, are being designed into the optical system. The optional focal lengths will be achieved by changing the secondary mirror and its support structure.

With the 100-cm focal length, a resolution[a] of 1 km on the surface of Mars should be possible at a distance of 10,000 km from the surface assuming a PHP vibration no greater than 5.6 min of arc per second of time. Should the sensitivity of the vidicon be greatly improved, which is doubtful, shorter exposure times could be used with this focal length to achieve twice this resolution. If the PHP vibration can be substantially reduced so that longer exposure times are feasible, the 200-cm focal length optics would be capable of yielding surface resolution approaching 0.3 km. The field of view of the 100-cm focal length system will be 0.9 deg across the diagonal of the square vidicon format.

A Schott Type GG-15 filter will be used with Camera A to filter any UV and deep-blue radiation below 0.42 μ. This will prevent the haze effects of the Martian atmosphere from deteriorating the contrast of surface markings as seen by the high-resolution camera.

The shutter will be of a rotary disc type. A single pulse fed to the shutter solenoid will open the shutter and simultaneously code the spring which closes the shutter when the solenoid is de-energized. Thus, it will be possible to control the shutter exposure time by controlling the solenoid pulse width. However, it is not intended to vary shutter speed on board the spacecraft. This feature will be used only in the laboratory for tuning the system to optimum performance. It is expected that the required shutter speed will be approximately 40 ms from considerations of f-ratio, vidicon sensitivity, and PHP vibration.

[a]Resolution is used here in the television sense. Multiply resolution figures by 2 for optical resolution.

UNCLASSIFIED [redacted]

Camera B will be fitted with a 7-in. focal length, f 3.5 air-spaced triplet lens giving a surface resolution of approximately 4.5 km and a field of view of 5.1 deg across the diagonal. Since this camera is to be used to obtain colorimetric information from the planet and its atmosphere, it will be equipped with blue, green, and red filters. It has not yet been fully determined whether or not these filters will be mounted in a rotary filter wheel or incorporated into a combination filter–shutter disc design. In either case, sequential exposures with Camera B will be made through different filters in the order blue, green, red, blue, etc. The probable exposure time for this camera will be in the order of 100 ms.

b. Thermal control. The temperature-critical circuits of the vidicon electronics will be located in the spacecraft hex where temperature control will be provided at 75 ±25°F. However, it will be necessary to raise the temperature of the vidicon face plate to 25 ±25°C during its operational use after being stored at approximately −40°C on the PHP for 9 mo during the cruise phase of the trajectory. Heat dissipated from the electronic components within Camera A will not be sufficient for bringing the vidicon faceplate up to operating temperature. Therefore, passive thermal control is being designed into the camera. This will result in thermal gradients within the optical system which would be disastrous in normal ground-based astronomical telescopes.

To minimize the thermal gradients within the optical mirrors of Camera A, serious thought is being given to the use of the high thermal conductivity of metal mirror systems. Along with the fused quartz mirror system being fabricated for Camera A, a set of aluminum mirrors and a set of beryllium mirrors are being fabricated for thermal tests in the prototype camera. From the view point of weight and strength, beryllium mirrors appear particularly attractive. The unresolved questions relating to the use of metal mirrors in the *Mariner* B telescope are:

(1) Is the long-term dimensional stability adequate in terms of optical tolerances and under the heat cycling conditions to be encountered?

(2) Will the high thermal conductivity offset the disadvantage that metals have higher thermal expansion than fused quartz?

2. Television Subsystem Electronics

Picture quality for the *Mariner* B television experiment will be determined ultimately by the optical–electrical transfer characteristics of the vidicon transducer. The transducer may be evaluated in terms of the ratio of the vidicon output signal to the background noise. Corresponding resolution and sensitivity are then expressed in terms of signal-to-noise ratios. This form of comparison is particularly applicable to space television systems since contamination by noise is a significant problem. Within this frame of reference, a high-quality picture is defined as that produced by a peak-to-peak video signal at least 30 db above an rms noise background. An acceptable picture has a 20-db signal-to-noise ratio.

a. Preamplifiers. Vidicon sensitivity at low levels of target illumination is almost completely determined by the preamplifier performance. Thermal noise at the preamplifier input terminals may be defined by the Nyquist equation, $\overline{e_n^2} = 4KTRB$ v rms, where K = Boltzmann's constant, R is the vidicon signal-output resistance, T its temperature, and B the noise bandwidth of the video amplifier.

The video bandwidth required for the *Mariner* slow-scan system

$$B = \frac{N}{2t} = \frac{400 \times 400}{2 \times 14.8} = 5.4\,\text{kc}$$

here, N = the number of picture elements and t = time of the vertical scan in seconds. This bandwidth is sufficiently low to make practical the beam-modulation system utilized in *Rangers* 3, 4, 5. In this system the scanning beam is chopped at a high frequency and the photoconductive target modulates the beam in accordance with the incident illumination. The resultant output signal takes the form of a modulated RF signal with the video spectrum now transferred from dc to RF and surrounding the carrier as shown in Fig. 42. The *Mariner* beam-chopping oscillator is a 125-kc stabilized free-running oscillator with a simple binary relationship, ×8, to the 1-mc clock frequency. Thus, four samples are provided per picture element of 72 μsec. The carrier frequency of 125 kc is sufficiently low to permit simple RC coupling networks for the transistor amplifiers and yet is high enough to allow adequate post-detection filtering of the carrier.

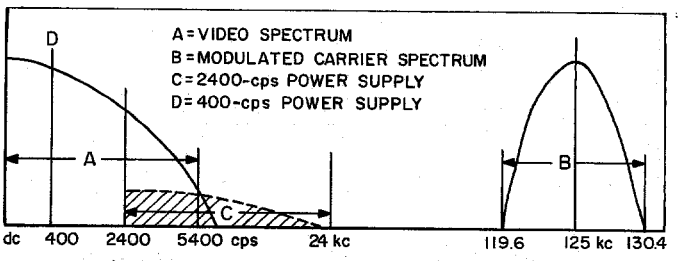

Fig. 42. Signal spectrums for *Mariner* B television

UNCLASSIFIED

The advantages of beam modulation for *Mariner* are: (1) Video information is in the form of an RF signal and may be amplified and transmitted as a high-level signal over a coaxial cable with a minimum of interference from the power supply and other noise producing sources (Fig. 42). This reduces weight on the planetary horizontal platform (PHP) as the camera and preamplifier only need be placed on the PHP with the major portion of the electronics back on the bus. (2) Grounding problems are greatly reduced as the vidicon output signal is now at RF, thus eliminating the need to transmit low video frequencies. (3) An isolation transformer may be used at the preamplifier input. This not only isolates vidicon operating potentials from the amplifier but permits accurate matching to the normally low-impedance input of a transistor preamplifier. RF beam modulation requires adequate shielding between the high-level chopping oscillator and the sensitive preamplifier. However, RF shielding techniques have been well developed for space vehicles and the weight requirements are considerably less than for the equivalent low-frequency shielding.

The usable output signal of the vidicon $I_o = I_s - I_d$ where I_s is the signal current and I_d the dark current. The present trend with the slow-scan mode is to operate with an extremely low I_d so that $I_s - I_d$ will produce the maximum output current. While this optimizes I_o for low values of target illumination, the low values of output current, possibly as low as 5 mμa, require an amplifier with a corresponding favorable signal-to-noise ratio. A completely transistorized system is greatly desired for *Mariner* B, particularly to secure the lowest possible primary power consumption. Fortunately the design of low-noise transistor amplifiers has been alleviated by the recent introduction of high-gain, passivated surface, low-noise transistors exemplified by the Fairchild 2N2049.

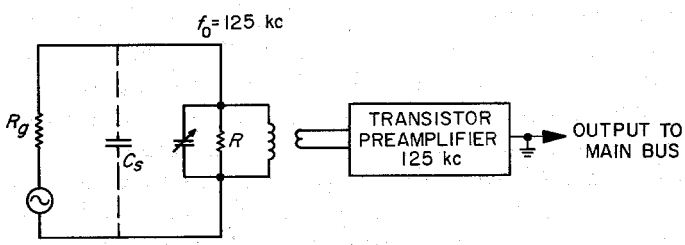

Fig. 43. Vidicon equivalent signal-output circuit for *Mariner* B television

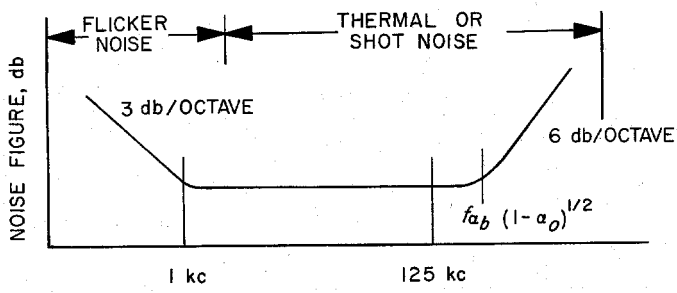

Fig. 44. Transistor noise spectrum related to *Mariner* B television amplifier

The vidicon signal-output circuit for the 125-kc carrier system is shown in Fig. 43. The photo-conductive target corresponds to an extremely high-impedance generator ($>>$ 10 megohms) so that the signal output for usable values of output impedance becomes a direct function of R. As thermal noise varies as $R^{1/2}$, the highest signal-to-noise ratio will be realized by maximizing R. The effective output load R equals $Q/\Omega C$. Therefore, R is maximized by minimizing C and operating with the highest possible Q for the tuned transformer. The capacity has been minimized by reducing all capacitances surrounding the target electrode to a minimum. The transformer Q has been optimized by compensating for the loss of response, due to a high Q, in the video amplifier. A resultant input resistance of 0.6 megohms has been achieved for the *Mariner* preamplifier using a powdered-iron toroidal coil. This compares quite favorably with input impedance values obtained with direct-coupled video vacuum tube amplifiers.

Figure 44 shows the noise spectrum for a typical transistor as related to the *Mariner* amplifier. Operation at 125 kc clearly obviates the flicker noise. However, $f\alpha_b$ must be considerably higher than 125 kc because of the term $(1 - \alpha_o)^{1/2}$. The 2N2049 has a specified $f\alpha_b = 800$ kc with I_c at 10 μa for which $f\alpha_b(1 - \alpha_o)^{1/2} = 112$ kc. However, for lowest noise the recommended collector current is in the 300-μa region for which $f\alpha_b$ is expected to be much higher than 800 kc. This would place the carrier frequency well within the lowest noise figure region. The optimum required source impedance for the transistor of between 500 to 1500 ohms is readily obtained by adjustment of the transformation ratio of the toroidal transformer.

Figure 45 illustrates a technique for evaluating the video amplifier using an amplitude modulated signal from an RF signal generator to simulate a 5-mμa vidicon highlight signal. Data so obtained is presented in Table 5 where it will be noted that a -40-db signal at the 5-mμa level has a signal-to-noise ratio of 15 db. A measured noise figure for this same amplifier indicated $NF = 3$ db which is close to the best obtainable with vacuum-tube devices. Transfer characteristic data presented for the

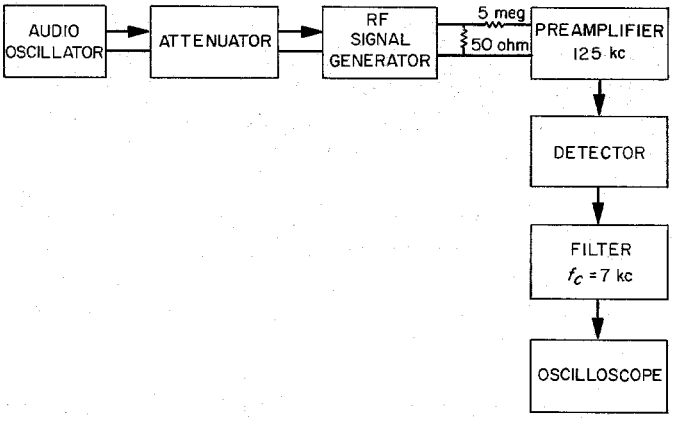

Fig. 45. Measurement of signal-to-noise ratios by simulating vidicon target signal characteristics

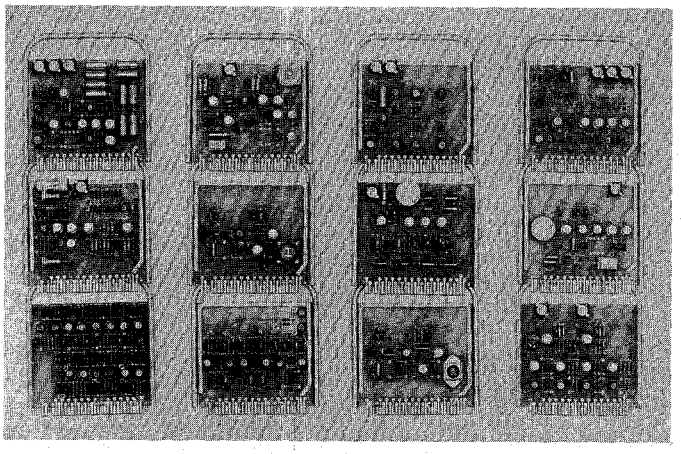

Fig. 46. Electronic modules for *Mariner* B television Camera A

vidicon in *SPS 37-14* was based on a 50-mμa maximum high-light signal. Thus the measured performance data indicates that the present transistorized amplifier system is unlikely to prove a limitation to picture quality with low dark-current operation.

b. Electronic modules and vidicon assembly. The electronic modules for processing the camera output signal and logical controlling of the input signals to the vidicon for slow-scan operation are shown in Fig. 46. Only one logical input signal is required to provide a continuous succession of pictures from Cameras A and B: a line synchronizing signal from the digital encoder. Output signals indicating the status of the television scans are available for the data automation system, (DAS). The modules are assembled in a container (Fig. 47) that simulates the shielding that would be provided in a payload configuration and yet gives desirable plug-in flexibility during the breadboard phase.

All modules have been thermally tested from −40 to +75°C and, with one exception, have operated completely satisfactorily. The performance of one unit, the output video amplifier, was found completely unacceptable. This amplifier is a relatively complex dc amplifier incorporating a dc black-level clamp and a synchronizing dc reference signal. The analog output from this amplifier is fed to the digital encoder, and hence must be completely stable. By changing to a differential amplifier configuration and thermally compensating the dc clamp and the associated impedance transforming circuits, the required stability has been achieved.

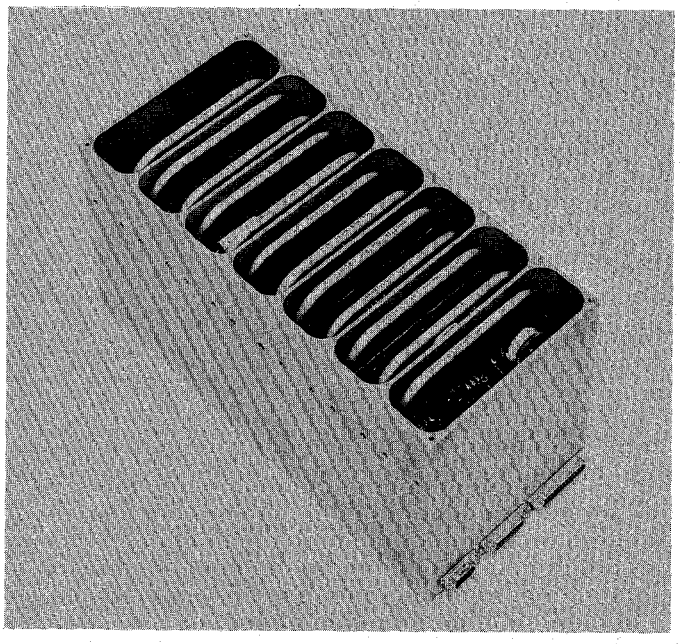

Fig. 47. Simulated payload configurations of *Mariner* B Camera A electronic packaging

Table 5. Measured video amplifier system performance data for a simulated 5-mμa vidicon signal

Modulation intensity, db 30% = 0 db	P-P video output signal, mv	RMS noise, mv	Signal-to-noise, db
0	1900	3.3	55
−10	600	3.3	45
−20	190	3.3	35
−30	60	3.3	25
−40	19	3.3	15
−50	6	3.3	5

Figure 48 shows the breadboard vidicon tube assembly which includes the preamplifier, erase lamps, and shutter. Considerable effort has been taken to ensure adequate

UNCLASSIFIED

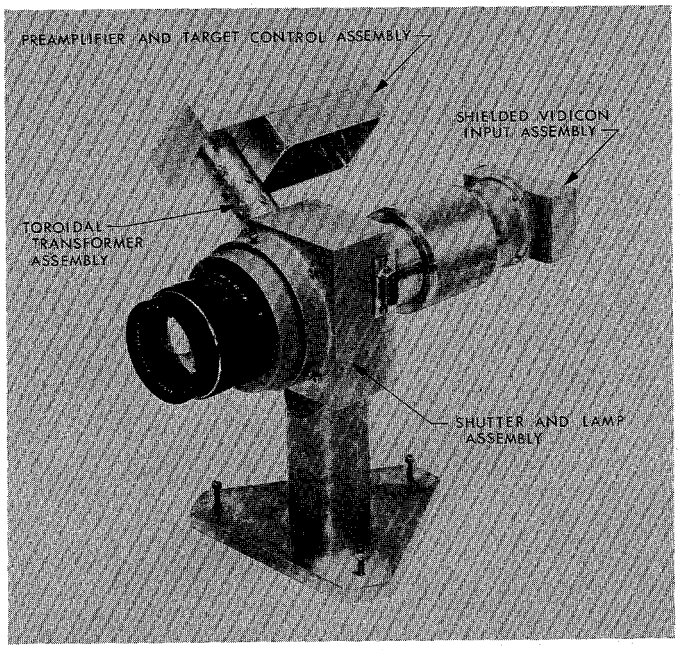
PREAMPLIFIER AND TARGET CONTROL ASSEMBLY
SHIELDED VIDICON INPUT ASSEMBLY
TOROIDAL TRANSFORMER ASSEMBLY
SHUTTER AND LAMP ASSEMBLY

Fig. 48. Experimental *Mariner* B television camera assembly

shielding of the camera tube to permit low-level I_o operation and to minimize the vidicon output capacitance. The assembly uses a *Ranger* shutter and a Takumar Asahi f 1.8 lens in a Pentacon mount complete with iris control and focusing adjustment.

During the next phase, overall television camera subsystem performance evaluation tests will be made using the present hardware which simulates the A camera operation but which also includes the logic control for the B camera. The B camera electronics will be fabricated during this period to permit television subsystem tests to be performed with both cameras operating. It is anticipated that the B camera will be assembled in a *Mariner* type housing with a *Mariner* shutter.

3. Ultraviolet Spectrometer

a. Comparison of* Mariner *A and B UV experiments. The *Mariner* B experimental objectives reflect recent development and availability of solar-blind photomultiplier tubes and the availability of lithium fluoride windows up to 2 in. in diameter. It is now feasible to measure radiation from 1200 to 3400 Å, in the presence of high-intensity visible radiation.

As a result, the instrument can look at the day side of the planet Venus, and detect UV aurora and day glow. The telescope will no longer be required to look at the night side while rejecting day side radiation from a source several degrees off axis. Instead, the optical imaging properties of the telescope will be adequate. The telescope walls will be needed mainly to keep out direct solar radiation and solar scatter from the spacecraft.

Within the *Mariner* A spectral range of 1200 to 4200 Å, radiation was expected to have a dynamic-intensity range of 10^6 or more. In the *Mariner* B experiment, the spectral range from 1200 to 3400 Å is expected to have a dynamic range of 10^4 or less.

A tungsten lamp will probably not be adequate for in-flight intensity calibration in a solar-blind spectrometer. For this reason, two new intensity sources are being investigated: a radioactive excited UV phosphor, and a frosted window to gather solar energy.

b. Test results of Model 9-15 UV spectrometer. Tests performed on the *Mariner* A Model 9-15 UV spectrometer during March and April 1962, may be divided into three groups: (1) optical tests, (2) electronic tests, and (3) magnetic field tests.

Optical tests. The Model 9-15 UV spectrometer flight instrument was tested to determine its absolute sensitivity in terms of a minimum detectable source brightness. The testing configuration is shown in Fig. 49.

A source monochromator was used to furnish spectral lines at 2537 and 3650 Å. An EMI 9526B reference photomultiplier tube with an S-13 response was calibrated against an Eppley Thermopile using a tungsten standard source. An Optics Technology Monopass filter was used in front of both the Eppley Thermopile and the reference photomultiplier to limit the radiation to the region of 5460 Å. Neutral density filters were then used to plot the reference-phototube gain vs voltage curve over seven decades.

Neutral density filters, consisting of metal plates with slot apertures, were used to attenuate the optical signal from the source monochromator in order to observe a minimum discernible level of excitation of the flight instrument.

Using these techniques, the closed loop minimum discernible brightness was 2×10^4 Rayleighs for $\lambda = 2537$ Å and 1.5×10^4 Rayleighs for $\lambda = 3650$ Å.

An electronic fault in the closed loop was found at the end of testing which may have been partially responsible for the low sensitivity of the instrument. The specification

UNCLASSIFIED

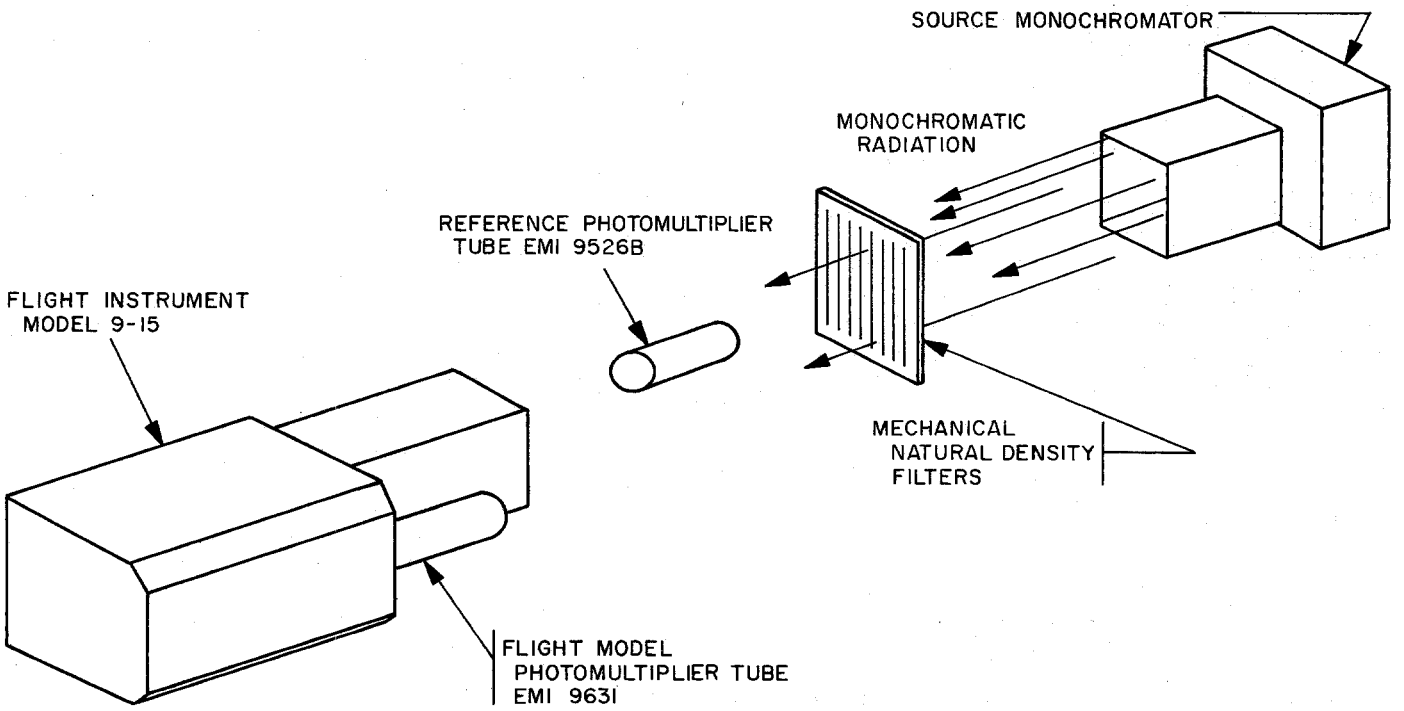

Fig. 49. Optical test for Model 9-15 UV spectrometer

calls for a minimum detectable brightness (MDB) of 100 Rayleighs. Open loop tests with a dc voltage on the phototube indicated less than 300 Rayleighs as the minimum detectible brightness.

Off-axis rejection characteristics of the telescope were tested in the celestial simulation laboratory. The test requires a laboratory with very dark walls and a collimated light source whose last scattering surfaces are distant from the detecting instrument. The spectrometer is tested with the grating in the zero-order position. The telescope is pointed in the direction of the collimated source to give a reference 0-deg output. The instrument axis is then inclined with respect to the collimated light source until it is looking only into the blackness of the laboratory walls. The bright source must still shine into the open entrance of the telescope, however. Figure 50 shows the rejection of the telescope as a function of angle for a point source at infinity.

Electronic tests. Electronic tests were performed on the system power supply, high-voltage power supply, servo loop, system operation, and band-pass amplifier.

(1) *System power supply.* The outputs of this supply were checked for ambient temperature characteristics and found to be substantially independent of temperature over the range −10 to +70°C.

(2) *High-voltage power supply.* This supply furnishes high voltage for the photomultiplier tube. It is in the closed servo loop and, therefore, is a critical circuit.

This supply exhibits as much as a 35% variation in output over the −10 to +70°C temperature range. The contractor has been apprised of this situation and is investigating the causes and solutions for this condition.

(3) *Servo loop.* This circuit is substantially independent of temperature.

(4) *System operation.* The analog output was recorded for a series of scans of the spectrum of a Mercury Pen Ray source over the temperature range of −10 to +70°C.

Figure 51 shows the output recordings for −10, +25 and 70°C and indicates a reasonable degree of independence from temperature effects. The high voltage was readjusted at each temperature during these runs in an attempt to correct the previously mentioned faults in this circuit.

(5) *Band-pass amplifier.* The band-pass amplifier was tested and found to be within specification limits except for the noise output (4.2 mv measured; 3 mv specified) and the gain (53 db measured; 64 db

UNCLASSIFIED

UNCLASSIFIED [redacted] UNCLASSIFIED

specified). These two areas are being investigated by the contractor. There does not seem to be any great problem involved in satisfying the specification limits.

Magnetic field tests. The Model 9-15 instrument was tested in accordance with the *Mariner* B specification which tentatively establishes 1 γ at 5 ft as the maximum allowable field strength. A maximum reading of 6.5 γ at 5 ft was measured. It was determined that the wavelength identification magnetic drum was responsible for the high field reading. It is expected that the magnetic drum will be replaced by an optical identification readout device which will remove this problem area.

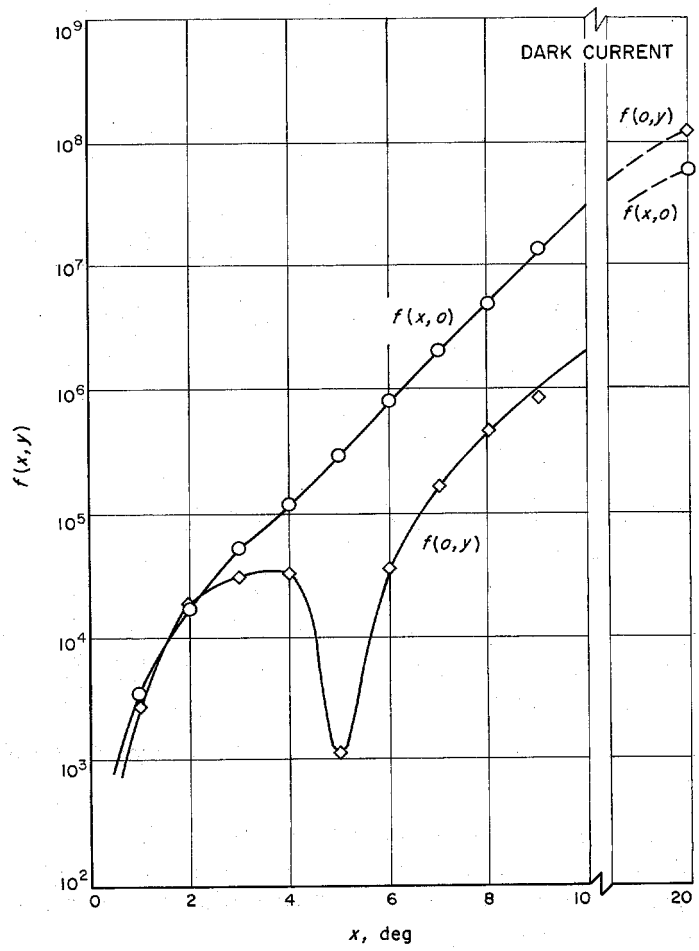

Fig. 50. Off-axis baffle tests of Model 9-15 UV spectrometer

E. Propulsion

The primary function of the *Mariner* B post-injection propulsion system is to remove or reduce injection dispersion errors so that planetary miss parameters on the order of 2000 km (1 σ) after mid-course corrections and 320 km (1 σ) after approach corrections can be realized. This function is performed during the four possible mid-course corrections and three possible approach corrections during which the spacecraft is directed to turn to a prescribed attitude in space and impart a corrective impulse via the post-injection propulsion system.

A secondary function of the post-injection propulsion system is to provide a post-separation adjustment of the spacecraft trajectory when an entry capsule without propulsion is carried and a bus deflection is desired.

1. System Description

A schematic of the propulsion system is shown in Fig. 52. The system utilizes a liquid monopropellant, anhydrous hydrazine, as the propellant. It is functionally a regulated-gas-pressure-fed, constant-thrust rocket. Principal system components consist of a high-pressure gas reservoir, a pneumatic pressure regulator, a propellant tank and propellant bladder, and a rocket engine. The rocket engine contains a quantity of catalyst to accelerate the decomposition of hydrazine.

The system concept shown in Fig. 52 is predicated on the basis that it satisfy the long-term space-storage (maximum of 250 days) and multiple start (maximum of 8) requirements imposed by the *Mariner* B missions. In order to fulfill better the long-term storage requirements, pressurization by gaseous nitrogen is used in lieu of gaseous helium, the latter being more prone to leakage. In a like manner, welded and brazed tubing and fittings are used wherever possible to minimize the number of potential leak sources. Also, metal seals are used (where welding and brazing are impracticable) in place of elastomeric seals to alleviate the effects of radiation, hard vacuum, and long-term storage on the critical system seals. Multiple start capability is realized by the inclusion of a solenoid control valve in the pneumatic circuit; also, a self-ratcheting oxidizer (N_2O_4) start slug piston, which is an integral part of the pneumatically operated propellant valve, provides repeated injection of the 13 cc of oxidizer required for each engine start. The propellant valve–start slug combination is pneumatically opened with regulated nitrogen pressure and closed by mechanical spring force when opening pressure is vented. The system, as shown in Fig. 52, provides multiple start capability limited only by the capacity of the oxidizer–start slug system.

UNCLASSIFIED [redacted]

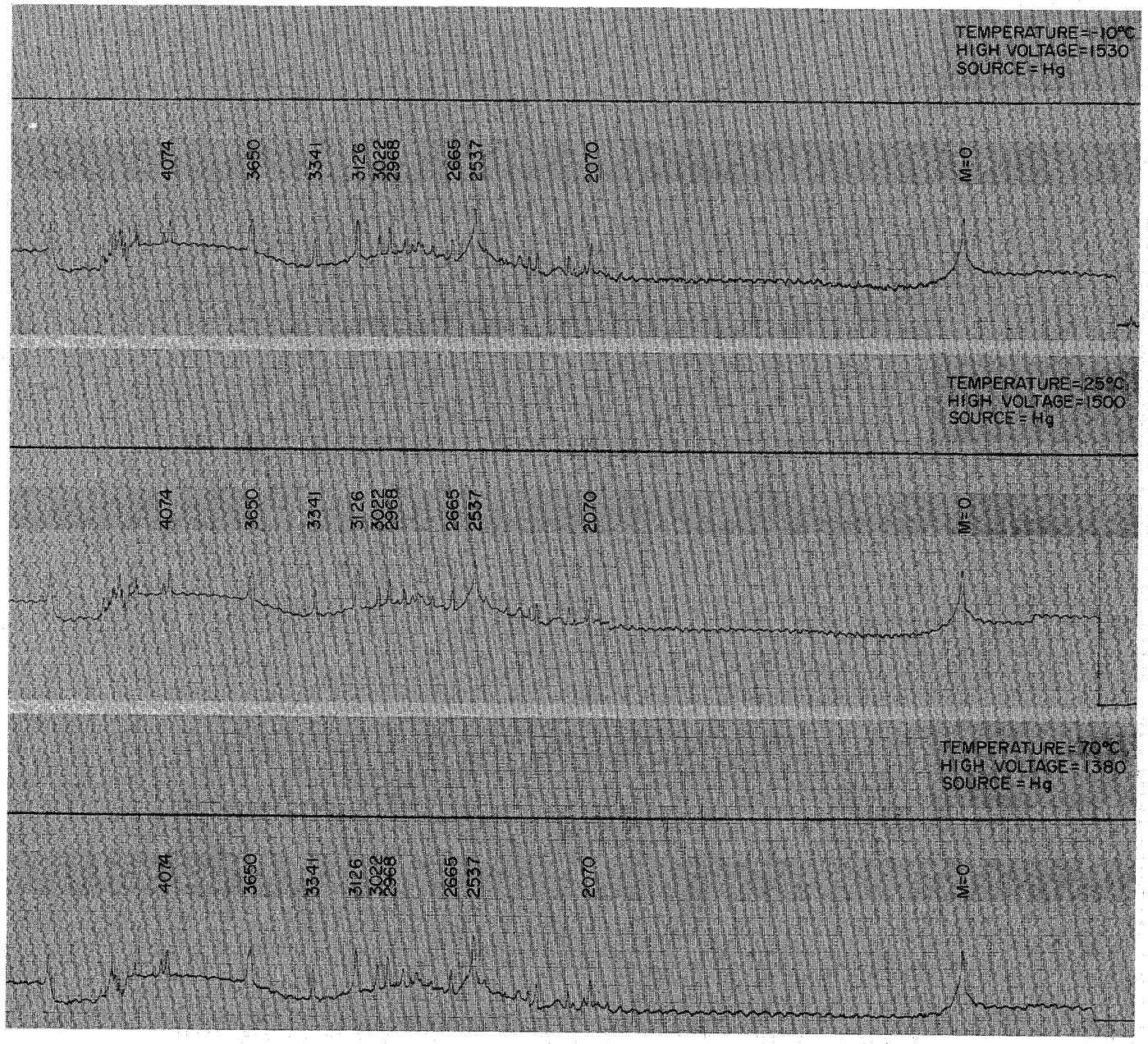

Fig. 51. Temperature dependence of hydrogen spectrum

The design and operational philosophy of the system (Fig. 52) is directed toward maximizing system reliability and reproducibility, minimizing pre-flight handling and spacecraft interactions, minimizing in-flight electrical signals and sequencing, and minimizing the number of system components.

The propulsion system can be fueled, pressurized, and monitored for several weeks prior to emplacement within the spacecraft and actual launch. The system in the pressurized and fueled condition is safe for personnel to work around over the temperature extreme of 35 to 110°F. (Burst pressures of the pressure vessels are a factor of 2.2 greater than maximum working pressures at 110°F.) No spacecraft umbilicals or hard lines are required to maintain the propulsion system in the ready condition.

A nominal engine performance summary is presented in Table 6, and nominal system pressures and temperatures are shown in Table 7.

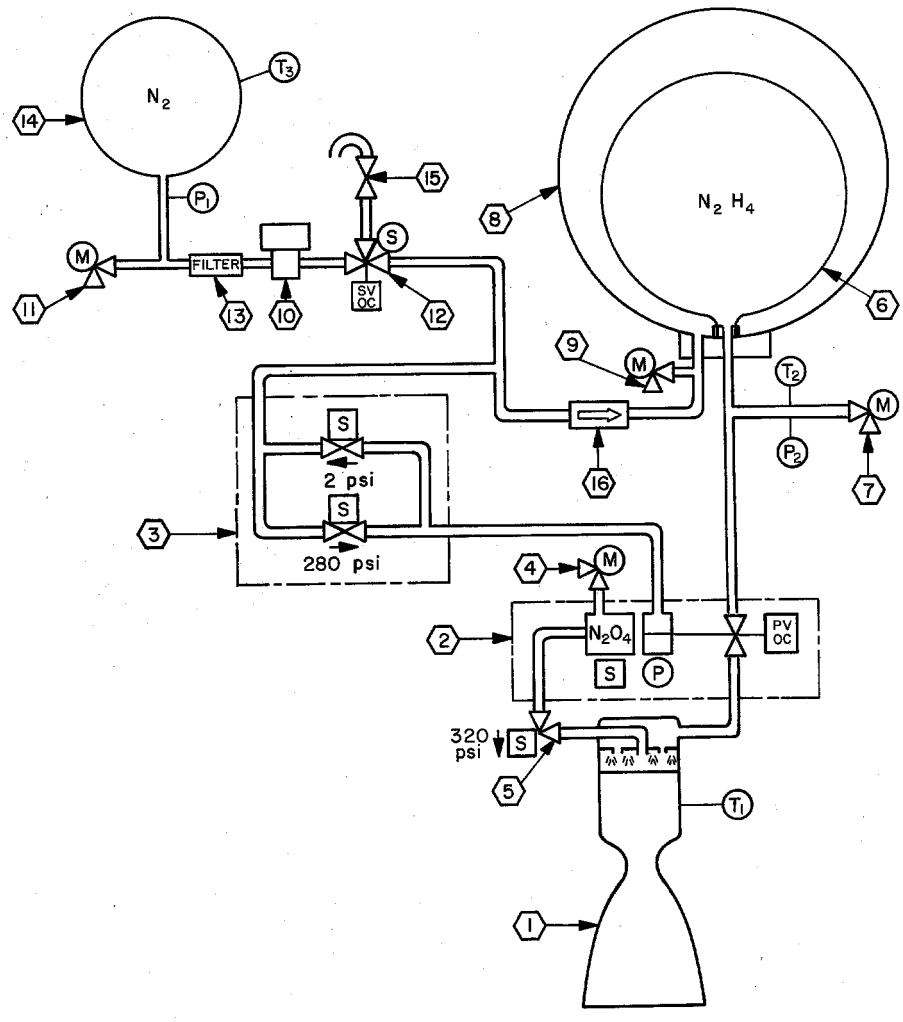

TWO-WAY ANGLE VALVE, MANUALLY OPERATED

TWO-WAY VALVE, WITH INTERNALLY VENTED CAVITY WHEN CLOSED, SOLENOID OPERATED

TWO-WAY SPRING RETURN VALVE, PNEUMATICALLY OPERATED

BACK-PRESSURE VALVE, SPRING RETURN, PRESSURE OPERATED WITH CRACKING PRESSURE AND FLOW DIRECTION INDICATED

RELIEF VALVE AND VENT

CHECK VALVE

FILTER

PRESET REGULATOR

COMPONENT NUMBERS

INSTRUMENTATION NUMBERS

INSTRUMENTATION

PRESSURE TRANSDUCERS

- (P1) NITROGEN TANK
- (P2) PROPELLANT TANK

TEMPERATURE TRANSDUCERS

- (T1) ROCKET ENGINE
- (T2) PROPELLANT
- (T3) NITROGEN TANK

VALVE POSITION INDICATORS

- PV OC — PROPELLANT VALVE MICROSWITCH, OPEN AND CLOSE
- SV OC — SOLENOID VALVE OPEN AND CLOSE SIGNAL GENERATOR

COMPONENTS

NO.	DESCRIPTION
1	ROCKET ENGINE
2	PROPELLANT VALVE, INCLUDING OXIDIZER RESERVOIR AND PUMP
3	DELAY VALVE, NITROGEN
4	FILL VALVE, OXIDIZER
5	BACK-PRESSURE VALVE, OXIDIZER
6	PROPELLANT BLADDER
7	FILL VALVE, PROPELLANT
8	PROPELLANT TANK
9	PREPRESSURIZATION VALVE, NITROGEN (PROPELLANT TANK)
10	PRESSURE REGULATOR, NITROGEN
11	FILL VALVE, NITROGEN TANK
12	CONTROL VALVE, SOLENOID
13	NITROGEN FILTER
14	NITROGEN TANK
15	RELIEF VALVE AND VENT
16	CHECK VALVE

Fig. 52. *Mariner* B post-injection propulsion system schematic

Table 6. Nominal engine performance summary (without jet vanes)

Characteristic	Value
Vacuum thrust, F_{vac}	52.5 lb_f
Vacuum specific impulse, $I_{s\ vac}$	242 lb_f-sec/lb_m
Vacuum thrust coefficient, $C_{F\ vac}$	1.808
Propellant flow rate, $\dot{w}$	0.217 lb_m/sec
Ambient throat area, A_t	0.15 in.
Hot throat area, A_t	0.1527 $in.^2$
Stagnation chamber pressure, p_c (based on hot throat area)	190.1 psia
Characteristic velocity, c^* (based on hot throat area)	4306 ft/sec
Engine expansion ratio, ε	103

Table 7. Nominal system pressures and temperatures

Component	Nominal pressure, psia	Nominal temperature, °F
Nitrogen reservoir, at first ignition	3,000	70
Propellant tank, operating	310	70
Thrust chamber, operating	190.1[a]	1700 to 1800

[a]Represents stagnation pressure at entrance to nozzle convergent section.

The firing of the post-injection propulsion system is controlled by the CC&S. For all mid-course maneuvers, the CC&S receives the time, direction, and magnitude of the mid-course firing through the ground-to-spacecraft communication link. In the case of the approach corrections, the CC&S can receive the commands from an onboard computer and/or through the ground-to-spacecraft communication link. After the spacecraft has assumed the correct firing attitude, the post-injection propulsion system is ignited (at the prescribed time) through an electrical signal which is originated at the CC&S. Thrust termination is controlled by the CC&S via an electrical signal once the specified velocity increment has been realized as computed by the spacecraft integrating accelerometer. A single electrical pulse is needed for each engine start and each shutoff. A single pair of wires carries all start and shutoff pulses. During the rocket engine firing, spacecraft attitude is maintained by the autopilot-controlled jet vane actuators. Referencing Fig. 52, the specific sequence of events for the propulsion system for each engine ignition and shutoff is as follows:

(1) At the command signal from the CC&S to ignite the engine, solenoid control valve ⟨12⟩ is actuated causing regulated pressurization of the propellant tank and pressurization of delay valve ⟨3⟩.

(2) Delay valve ⟨3⟩ opens (pressure open) when the propellant tank is up to pressure causing pressure actuation of propellant valve ⟨2⟩ and back-pressure valve ⟨5⟩, initiation of propellant flow (N_2H_4), and injection of a small quantity (13 cc) of oxidizer (N_2O_4) into the rocket engine.

(3) Hypergolic ignition ensues, followed by continuous catalytic monopropellant decomposition of the anhydrous hydrazine.

(4) At the command signal from the CC&S to terminate engine thrust, solenoid control valve ⟨12⟩ is actuated causing isolation of the remaining pressure in the nitrogen sphere and venting of the propellant valve ⟨2⟩ actuator pressure. (Pressure in the propellant tank is locked-off by check valve ⟨16⟩.)

(5) Propellant valve ⟨2⟩ closes (spring closure), terminating propellant flow and thrust.

2. Development Program

To date, the development program has been limited primarily to the generation of preliminary design layouts and a functional specification describing the design requirements for the propulsion system. A satisfactory spacecraft-propulsion system interface, permitting sufficient adjustment capability of the thrust vector through the spacecraft center of gravity has been achieved, and design layouts are proceeding on this basis.

Prototype regulators, check valves, and delay valves are currently being fabricated. These components will be tested on both the component and system levels in the ensuing months.

One welded and one riveted prototype aluminum structure are being fabricated to ascertain the relative structural, dimensional, and fabrication merits of the two fabrication techniques. Although the prototype structures under fabrication are not identical to the structure concepts shown in the current propulsion system layouts, the two fabrication techniques can be adequately compared and a selection made prior to initiation of flight design.

In addition to the above fabrication work, a component specification sheet describing the design requirements for the solenoid control valve has been released to prospective vendors, and design of the eight-start, propellant valve–oxidizer–start slug combination has been initiated.

IV. *Voyager* Project

Voyager missions are envisioned to evolve to sophisticated orbiters and landing experiments beginning in 1966 or 1967 using *Saturn* vehicles. Planetary orbiters are a necessary part of the evolution and are a logical step in the development of spacecraft technology. Orbiters are probably required to permit sufficient observation of the planet to know how to proceed with the landing missions. Furthermore, orbiters may well constitute an important step in the actual landing experiments. The emphasis on planetary orbiters, therefore, will be to contribute to the successful accomplishment of the landing objective.

The primary programming efforts conducted during this reporting period consisted of working with Marshall Space Flight Center in determining the feasibility, schedule, funding requirements, and mission suitability of a three-stage C-1 *Saturn* for use in the *Voyager* project. A vehicle concept has been generated by MSFC which could provide approximately 5500 lb of payload injected into Mars or Venus trajectories beginning in 1965 or 1966.

Specific efforts directed to accomplishment of the *Voyager* Project were initiated at the start of FY 62. A brief synopsis of these efforts is as follows:

The Systems Division is participating with the technical divisions and the Marshall Space Flight Center in the generation of mission objectives and the preparation of preliminary systems design specifications for interplanetary spacecraft to be used as planetary orbiters and landers and out-of-the-plane-of-the-ecliptic probes using the *Saturn* vehicle as the booster.

The Space Science Division is conducting *Voyager* scientific feasibility studies, establishing the feasibility of meteorological, biological, and certain adaptions of geological experiments for the *Voyager*, as well as refining knowledge of the Mars and Venus environments as they affect experiments and spacecraft for these flights.

The Guidance and Control Division is continuing its studies of guidance and control requirements, methods, and techniques for advanced planetary missions, both those currently planned and those that become necessary or desirable as a result of discoveries on early planetary exploration missions that require further exploratory operations. The methods to be used include study of possible mission requirements to deduce the general requirements for guidance and control subsystem performance, evolution of subsystem configurations to accomplish the required tasks, and parametric and error analyses of typical missions and operating situations to determine the ranges or parameters and tolerances required.

The Engineering Mechanics Division is performing *Voyager* spacecraft studies, including analytical investigations of configuration, thermal control, entry and landing dynamics, post-landing and roving techniques, booster compatibility, multiple mission or universal design concepts and compromises, and structural design problems.